June 2018

Dirty snow: The impact of urban particulates on a mid-latitude seasonal snowpack

David James Kelley
Syracuse University

Abstract

This thesis examines the spatial distribution of particulate matter in snow around a mid-size, midlatitude city. Particulates are small, light absorbing impurities that are produced from the incomplete combustion of carbon-based fuel. When deposited on the snowpack, these particles reduce snow albedo and accelerate melt. Two experiments were designed to explore the distribution and effect of urban particulate emissions on snow surrounding Syracuse, NY (43.049897, -76.149102, pop: 149,000). The "directional study" examined the relationship between distribution and cross-city prevailing wind, while, the "transect study" examined the variability of particulate concentration with distance from a busy interstate highway. Fifteen sites were sampled over two winter seasons (2016-2017 and 2017-2018). Eight sites were located in the suburbs roughly aligned to the cardinal directions with respect to the city, one site was located within the city boundaries and six sites were located on a transect across I-90. Snow temperature, air temperature, wind speed/direction and albedo were recorded at each site. A snow core was collected for laboratory analysis using the Light Meter Filter Analysis method and two photos were taken of the snow surface for a second albedo analysis using ImageJ. At the city-scale, trend analyses show that particulate concentration decreases from W to E across the urban center and albedo increases from NW to SE. The small westerly shift between albedo and particulate trend analysis may be explained by a slight difference in measurement parameters. Albedo analysis measures the effect of particulates on the snow surface since the end of snow accumulation. Particulate concentration, however, measures the total quantity of particulates in the entire snowpack. Both analyses align with the WSW to NW prevailing wind that is responsible for the formation of lake effect snow from Lake Ontario and

Lake Erie. That said, the observed distribution was found to be opposite expectations. This is likely a result of wind circulation patterns within the urban core. At the local-scale, high particulate concentration/low albedo was found adjacent to the interstate highway. Results show that the concentration does not necessarily decrease with distance from vehicle emissions. Instead, particulate distribution is altered by the presence of any obstacles within 600m of the highway. Snow surface photo analysis was able to determine the relative albedo of each site but not actual albedo value. Despite this, the photo analysis method looks promising for future citizen science based studies of particulate matter. Overall, findings suggest that urban particulate distribution in midlatitude snow is altered by city morphology and proximity to local emission sources. Future research is necessary to examine how this distribution affects climatic processes in the midlatitudes.

Dirty snow: The impact of urban particulates on a mid-latitude seasonal snowpack

by

David Kelley

B.A., University at Albany, State University of New York, 2013

Thesis
Submitted in partial fulfillment of the requirements for the degree of
Master of Arts in Geography

Syracuse University
June 2018

Preface and Acknowledgements

When I told my friends and coworkers about my idea for a snow study I would always hear the same thing: “You are crazy! Why would anyone want to stand out in the snow for hours on end?!” Of course, most people would not want to brave sub-zero temperatures just to examine snow properties, but, I may be a bit unusual. Instead of cold and tiresome, I see snow as fun and exciting. Throughout my childhood, snow was always associated with family. Almost every Saturday from age 2 to 15 my Dad and I would head up to Gore Mountain to ski in what must have been a consistent -20 degree wind chill. On Sundays (and really every other day I was off of school) I would spend the time outside sledding with friends, or even sometimes by myself. When I finally came back in my Mom would be there with hot cocoa and a hug.

While at the University at Albany, State University of New York, my undergraduate mentor, Dr. Andrei Lapenas, introduced me to the science behind the snow that I loved. Working with another research assistant, we tirelessly insulated small patches of snow (with bales of straw and a pitchfork!) to examine the effect of an elongated snow season on fine tree root growth. Here, I became interested in climate change and realized that I wanted to continue to study snow in graduate school. I found Syracuse University a few years later (after working an interesting job at the DEC sampling lakes from a canoe) and my advisor Dr. Susan Millar. Susan, a snow enthusiast herself, gave me the chance to develop my passion for snow into scientific scholarship. Over the last two years, she provided guidance and enthusiasm for my project. I owe her a debt of gratitude for this opportunity.

I would also like to thank, Jane Read and Jake Bendix. Thank you for supporting me in my studies and for providing advice throughout this project. Thank you to the Syracuse

University Geography Department, especially those who agreed to host a rain gauge in their yard when I needed a back-up plan as a result of low snowfall in the first season: Dr. Tod Rutherford, Heather Ipsen, Emily Bukowski, Pat Oberle, Katie MacDonald and Sohrob Aslamy.

Thank you to Heather, my partner in crime, for all the hikes, walks, sunsets, photos, happiness and adventures over the last two years. Thank you to my family: Mom, Dad, Matt, Megan, Aislynn, Teagan, Nolly, Riley, Wally and Poppy. Your love and support helped me throughout this process. Finally, thank you to Lake Ontario and the snow gods, I could not have done this without you – quite literally!

Table of Contents

List of Illustrative Materials

Figures

Tables

Equations

Chapter 1 – Introduction

The Importance of Particulate Matter in the Global Climate System

On the morning of March 23, 2018 alpine skiers in Russia, Ukraine, Bulgaria and Romania awoke to an interesting sight. Ski slopes, covered in white snow the night before, were now painted a dull orange-brown. Some patrons claimed it was the beginning of the snow-apocalypse, others chatted about traveling to Mars, however, those that mentioned skiing in the desert, were somewhat correct (Langone, 2018). The orange color was caused by small particles of mineral dust that were incorporated into the snowpack overnight. In this case, the dust was entrained into the atmosphere over the Sahara Desert and transported northeast across the Mediterranean Sea (Mauro et al., 2015).

Mineral dust is one of many types of snow impurities known as particulate matter. These particles including, black carbon, brown carbon, road debris, fly ash and soot, are implicated in a variety of human health problems and environmental issues (Bond et al., 2013; G. Wu et al., 2016). When particulate matter is deposited on snow it alters the reflective properties of the snow surface – a process known as snow surface darkening. Any decrease in reflectivity as a result of darkening can have a profound effect on the local and global climate systems. This thesis explores the impact of urban particulates emissions on seasonal snow surrounding a midlatitude city. By examining snow albedo, wind patterns and particulate concentration this study identifies patterns of particulate distribution and the potential impact on the city-scale climate system.

Particulate matter alters the energy balance of a snowpack by increasing absorption in the ultraviolet and visible light wavelengths. This process increases snow grain metamorphism and accelerates snowmelt during the late winter and spring (Bond et al., 2013). Given enough particulate deposition, this process can lead to snowpack thinning and an earlier melt-out date in the spring (Yasunari et al., 2015). In addition to disappointing skiers, this effect can substantially alter snow water equivalent, flood probability and vegetation distribution (Steltzer et al., 2009).

Particulates-snow interaction is a fast developing field of scientific study. Currently research focuses on the effect of particulates (especially black carbon) on high latitude or high elevation glaciers, sea ice and perennial snowfields (C. Gertler et al., 2016; Keegan et al., 2014; Hewen Niu et al., 2017a; Pedersen et al., 2015). Snow cover outside of these areas is often neglected. Doherty et al. (2014) and Wang, Doherty and Huang (2012) provide a good overview of regional patterns of black carbon concentration in the midlatitudes. However, there are few studies that explore midlatitude particulates at a smaller scale. This area is of particular importance as anthropogenic sources of particulate matter are prevalent in the midlatitudes.

Terminology

A number of different terms are used to describe light absorbing particles. In the literature the most common usage is “black carbon”. Technically, this term refers to a single form of carbon that strongly absorbs solar radiation at the 0.5 μm wavelength (Bond et al., 2013). It is distinct from other forms of carbon as well as other light absorbing particles. Despite this distinction, “black carbon” is often used as an all-encompassing phrase to describe any light absorbing particle (Bond et al., 2013; Pedersen et al., 2015). Some authors use the phrase

"elemental carbon" to differentiate between true black carbon and other particulate matter. Others use the term "refractory black carbon" as suggested by Bond et al. (2013). However, since the use of "black carbon" in the broad sense is inherently incorrect, Gul et al. (2018), Hewen Niu et al. (2017a), Hewen Niu et al. (2017b), and Yasunari et al. (2015) use "light absorbing impurities" or "light absorbing aerosols" to identify a subset of all light absorbing particles. Even so, this terminology can become confusing as each author individually defines which particles are included in the term.

For this thesis, the term "particulate matter" is used to describe all light absorbing particles, in accordance with Cereceda-Balic et al. (2017) and Grenfell et al. (2011). Further, this term is commonly used in air quality research and by the United States Environmental Protection Agency (EPA). Its usage encompasses any foreign particle that is incorporated into the snowpack and alters the snow absorption properties. In this study, when referring to an individual type of particulate, the specific type will be specified.

The Origin of Particulate Matter

Particulate matter originates from a large variety of natural and anthropogenic sources. The mineral dust discovered on the ski slopes of Eastern Europe for example, originated in the Sahara Desert where it was aerosolized into the atmosphere. Road debris, another type of particulate, is created whenever a vehicle slows down and releases brake dust (Heal & Hammonds, 2014). Most authors, however, explore the creation and effect of carbonaceous particulate matter. This sub-set includes black carbon, brown carbon, fly ash and soot all of which are created as a byproduct of incomplete combustion.

Incomplete combustion is a common process that occurs when carbon-based fuel burns in an oxygen-poor environment (Bond et al, 2013). Fuel type, reaction temperature and availability of oxygen all influence the quality and quantity of particulates that form (Ni et al, 2014). Significant attention is focused on the creation of particulates from the burning of fossil fuels. Bond et al. (2013) note that these particulates are subjected to a coagulation process where combustion products clump together to form dense particles. Once created, particulates are extremely stable and are only removed from the atmosphere by deposition.

The quantity of new particulate matter emitted into the atmosphere varies substantially each year. Bond et al. (2013) estimate that 7,500 Gg are emitted by known sources each year. However, they suggest that this number may be inaccurate as it is difficult to quantify sources in remote areas or in countries with limited research access. Briggs and Long (2016) attempted to quantify source emissions in the United States and Europe. To do this, sources were divided into eight categories: energy production, industry (including coal burning for industry), transportation (diesel and gasoline), residential/domestic, agricultural waste burning, waste, grassland fires and forest fires. Their results show that transportation, residential use and industry make up over 90% of particulate emissions.

About 75% of global particulate emissions are released in the Northern Hemisphere, with only 13% attributed to Europe, North America and the former USSR (Ni et al., 2014). That said, not all particulates are created equal. Despite producing fewer emissions by quantity, almost all emissions in these countries can be sourced to the burning of fossil fuels. Cui et al. (2016) and Lund et al. (2014) note that particulates released from fossil fuels have stronger absorption properties and a greater impact on the climate compared to those produced by

other sources. Interestingly, there is little emphasis on particulate pollution and its impact on snow at the local scale. A few studies focus specifically on air pollution within an urban area (Bowker et al., 2007; Yuan, Ng & Norford, 2013; A. Gertler, Gillies & Pierson, 2000) or the effect of particulates on arctic snow (Kahn et al., 2017; Kuliński et al., 2014) but not both. Considering the extensive burning of fossil fuels in the midlatitudes, the lack of research at this scale is surprising.

Dispersal of Particulate Matter

The concentration of particulate matter in a specific area can vary over space and time. Typically, the maximum concentration is observed in winter when surface temperature inversions stifle vertical air redistribution (Liu et al., 2011; Neff, 1997). Over time emissions build up in the lowermost atmosphere to create a concentrated layer of particulates. This happens somewhat frequently in Denver, CO where surface topography is favorable for inversion formation. Under normal atmospheric circulation, particulate matter is transported away from the source area. This is not possible within an inversion.

Particulates have a short residence time before they are deposited on the surface. Zhang et al. (2015) describe regional differences in particulate residence time. They note that emissions from East Asia remain suspended for only 2.2 days, while emissions from the Middle East are suspended almost 10 days; the global average is 4.9 days. Overall, particulates with a greater residence time show a more distant distribution (Zhang et al., 2015).

Local pollution levels can significantly affect residence time in the atmosphere. In areas with high levels of gaseous sulfuric acid, particulates are more likely to act as condensation nuclei and become incorporated into regional atmospheric circulation (Liu et al., 2011). When

this occurs, extended residence times and long range transport become likely. Therefore, regions with high general pollution levels tend to disproportionately contribute to the global background levels of particulate matter. Liu et al. (2011) note that these particulates are not usually a significant contributor to local concentration levels. Instead, local emission sources contribute the majority of measurable particulates (Liu et al., 2011; Wagstrom & Pandis, 2011).

The Importance of Particulates and their Interaction with Snow Cover

The impact of particulate pollution on the cryosphere can be explored across various geographic scales. Snow is highly sensitive to particulate deposition. On a global scale, particulates alter the albedo and melt rate of glaciers and snow fields. At the micro-scale, particulates change the physical snow structure. Most research focuses on one of these two areas.

Keegan et al. (2014) explore particulate-snow interactions on the Greenland Ice Sheet. This region, one of many climate research hot spots, is vulnerable to particulate-induced warming. Greenland imports most of its particulates from large-scale forest fires in North America or Siberia. Once arrived, these particles are deposited onto the snow surface through one of two deposition processes. Wet deposition occurs when particulates become condensation nuclei and are incorporated into snow or rain (Bond et al., 2013; Persad, Ming & Ramaswamy, 2012). These particles fall during precipitation and are found throughout the entire snowpack. Dry deposition takes place when particulates land directly on the snow surface. These particles accumulate on the surface and continue to darken it over time (Bond et al., 2013). Dry deposition varies spatially - local winds can redistribute surface particulates and obstacles may shield terrain from deposition (Bowker et al., 2007; Zhang et al., 2015).

The Greenland Ice Sheet can be divided into two distinct regions. The primary region spans over 600,000 km^2 across the center of the ice sheet. This region has a relatively high albedo and experiences little to no snow melt (Keegan et al., 2014). The secondary region includes the Greenland coastline and margin glaciers. This area is experiencing rapid snow melt in response to rising global temperatures and serves as a good example of the impact that particulates have on snow albedo (Hanna et al., 2008; Keegan et al., 2014).

Snow albedo is determined by calculating the ratio of reflected solar radiation to the total incoming radiation hitting the snow surface. Normally, clean, fresh snow reflects almost all radiation in the ultraviolet and visible spectrum (Dang et al., 2017; Gray and Male, 1981). The addition of any particulate matter increases absorption substantially. Keegan et al. (2014), found that a particulate concentration (their study examined black carbon) exceeding 0.01 µg altered albedo and caused widespread snowmelt in the center of the ice sheet.

Doherty et al. (2016) present one of the few studies to investigate particulate-snow interaction in the midlatitudes at a sub-regional scale. Here, snow samples were collected at three field sites in Idaho and Utah. Each sample was analyzed to determine the vertical distribution of particulates in the snow column as well as snow structural changes associated with snow metamorphism. Their results show that in addition to reducing albedo, particulate matter indirectly alters snow structure. This process begins when an increase in particulates reduces the snow surface albedo causing the snowpack to absorb additional energy and the top 10 cm of the snow surface to warm (Jacobi et al., 2015). Warming at the surface accelerates snow aging, a process where individual snow grains increases in diameter, and creates a positive feedback within the snowpack (Gray and Male, 1981). As the diameter of individual

snow grains increase, the overall albedo of the snowpack decreases. This leads to additional warming at the snow surface and another increase in grain size (Bohren & Barkstrom, 1974 as cited in Gray and Male, 1981). Over time this process can cause substantial melting within the snowpack. As meltwater percolates through the snow, particulate matter is washed into the snow column and accumulates in bands of elevated concentration (Doherty et al., 2016).

The effect of particulates on albedo (Keegan et al., 2014) and on snow structure (Doherty et al., 2016; Jacobi et al., 2015) substantially impacts the energy balance in the cryosphere. As a result, scientists examine these processes at the global, regional and micro-scales. However, few studies are performed at the local scale – especially in the midlatitudes or in urban areas. The lack of research is surprising as substantial particulates are produced in this region. Perhaps scientists believe that research in the arctic has a more immediate impact on the earth-environment system and it should take precedence over studies in the midlatitudes. Nevertheless, urban areas provide a significant, reliable source of particulate matter for deposition on snow. These particulates not only affect snow, but also environmental systems people rely on for everyday life. As such, research on the distribution of particulates in the midlatitudes is crucial. A well implemented particulate-snow study would help to address a number of environmental issues including: the urban heat island effect, soil moisture availability, local water contamination, winter flooding and drought.

Research Objectives

The overall purpose of this study is to understand the distribution of particulate matter at a city-wide scale. Specifically, this study aims to explore how particulates are distributed on snow across the urban landscape and the associated effect on albedo. This thesis expands upon

current particulate-snow research in the midlatitudes by mapping the spatial distribution of particulates with respect to wind direction in a mid-size city. Using these data, the impact of particulates on seasonal snow albedo is examined. Three specific research questions guide this study:

1. *How does a mid-size city and prevailing wind direction affect the spatial distribution of particulates in the surrounding snowpack?*

Particulate matter has a substantial impact on snow albedo and the amount of energy absorbed by the snowpack. Any decrease in albedo can reduce snowpack stability and lead to an earlier snowmelt – an effect that has been studied extensively at the global and regional scales (Bond et al., 2013). This question explores the particulate distribution and the resulting snow albedo reduction at the city-scale. The study examines particulate concentration upwind and downwind of the urban core. It was assumed that wind direction and particulate emissions from the city alters the geographic location of high and low concentrations that are observed in the surrounding snowpack.

2. *How is the distribution of particulate matter in snow altered by the proximity to vehicle emissions released on an interstate highway?*

The transportation sector is a substantial source of particulate emissions within the city. A number of studies explore the impact of high-traffic corridors on local air pollution levels, however, there is little research on the dispersal and effect of vehicle emissions on nearby snow (Bowker et al., 2007). This question examines particulate matter in an interstate highway corridor. The highway acts as a fixed, reliable source of particulates for deposition on the surrounding snowpack. It was assumed that the influence of highway particulates should

decrease with increasing distance from the source. Both albedo and particulate concentrations are assessed to identify spatial patterns within 120 m of the highway.

3. *Can digital photography be used as an accurate and cost-effective alternative to measure particulate concentration in snow?*

Current methods of particulate-snow research are expensive and time-consuming (Bond et al., 2013; Doherty et al., 2014). This question explores the use of digital photography as an alternative method to quantify particulates in snow. Increasingly, photo analysis is becoming integrated into snow research as an inexpensive and easily accessible means for quantitative and qualitative analysis (Bernard et al., 2013; Dong and Menzel, 2017). The use of photography to identify particulates could facilitate new particulate-snow research using citizen scientists. This study tests a method developed by Corripio (2004) and implemented by Gorsky (2018) and Gilchrist (2011) to calculate albedo from digital photographs.

This thesis is organized in a manner similar to that of a scientific journal article. The following chapter introduces the study area, Syracuse NY, and explores why it is an ideal location for research on particulates in the midlatitudes. Chapter three explains the experimental design for two different sampling strategies, the “Directional Study” and the “Transect Study”. This chapter details the methods used for sample collection and analysis and discusses how these techniques were designed to address each research question. Chapter four presents the results and discusses interactions between particulate matter and albedo. It elaborates on the spatial distribution of particulates in snow surrounding Syracuse and near I-90. This chapter also discusses the use of photography as a cost-effective technique for particulate measurement. Finally, chapter five examines the implications of this study and how

the results relate to the broader environmental system; thus, providing insight into the significance of particulate matter in a midlatitude urban climate system.

Chapter 2 – Study Area

Overview

Syracuse NY (43.049897, -76.149102), serves as an ideal location to explore particulate concentration and distribution in snow [Figure 2-1]. The city is situated in Onondaga County, approximately 300 km NW of New York City, 200 km WNW of Albany and 225 km ENE of Buffalo. Two major interstate highways (I-90 and I-81) pass through Syracuse and contribute to particulate emissions in the city. The urban center itself (2010 census population 149,000) is surrounded by suburbs on four sides. The north, east, and west suburbs extend 14 km from the city center, while the suburbs to the south extend only 8km before reaching the mostly rural Onondaga Nation territory. In total, 87.4% of the county lives within urbanized areas [Table 2-1] (United States Census Bureau [USCB], 2010). A number of industrial facilities are located in the urban center and surrounding suburbs – many release substantial emissions into the atmosphere (United States Environmental Protection Agency [EPA], 2015; United States Environmental Protection Agency [EPA], 2018a). In winter, particulates produced in Syracuse are deposited onto 300 cm of fresh snow that falls each year (Call, 2005; Midwestern Regional Climate Center [MRCC], 2018; Millar, 2017). The extensive accumulation often builds a snowpack that lasts through the winter season (MRCC, 2018). Regular access to a stable snowpack is essential for the success of an urban particulate sampling strategy - Syracuse meets this criterion with ease.

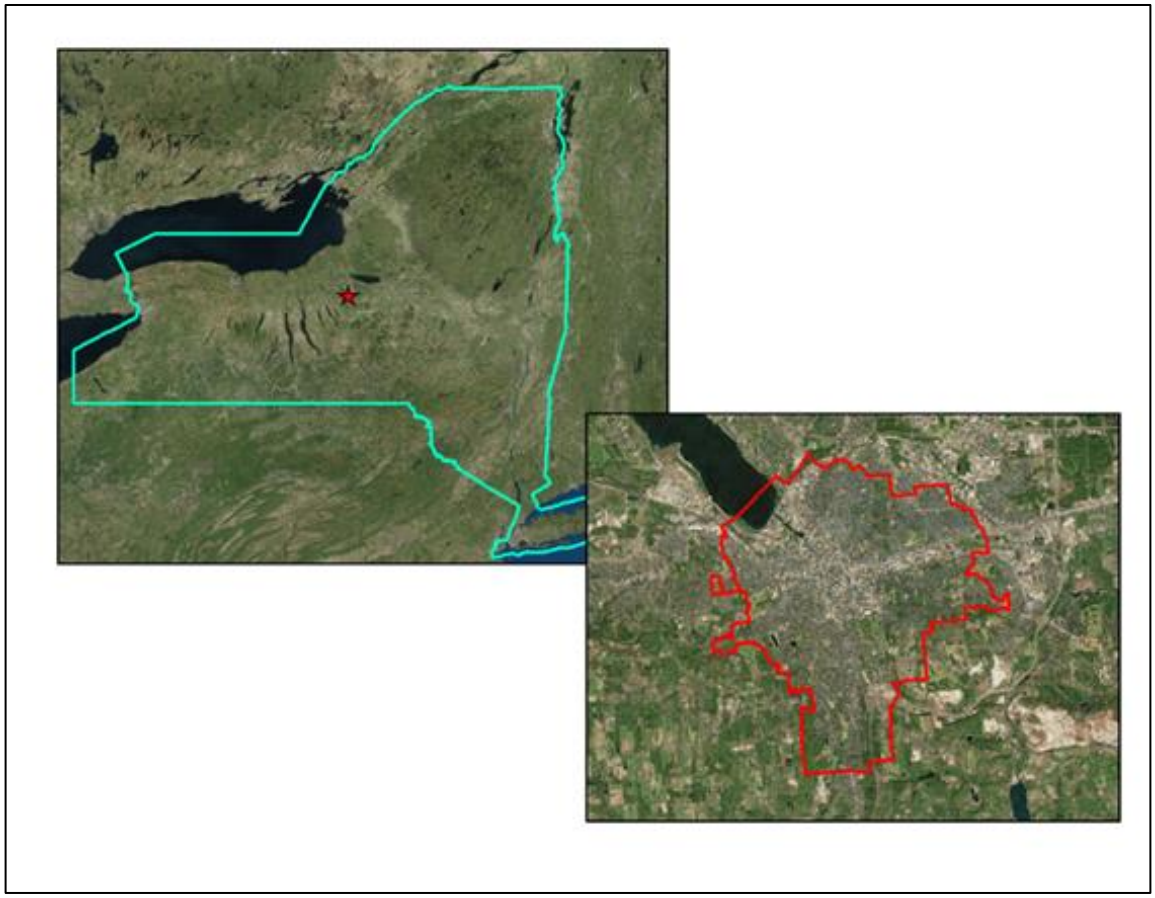

Figure 2-1: Map of Syracuse and its location in NY

Town or city	Total Population	Urban Population	Rural Population	Percentage of County Population
Camillus	24167	21520	2647	5.1
Cicero	31632	28740	2892	6.7
Clay	58206	55032	3174	12.4
DeWitt	25838	25203	635	5.5
Elbridge	5922	0	5922	1.2
Fabius	1964	0	1964	0.4
Geddes	17118	17118	0	3.6
LaFayette	4952	193	4759	1.0
Lysander	21759	16666	5093	4.6
Manlius	32370	28180	4190	6.9
Marcellus	6210	2898	3312	1.3
Onondaga	23101	18914	4187	4.9
Onondaga Nation	468	0	468	0.1
Otisco	2541	0	2541	0.5
Pompey	7080	1253	5827	1.5
Salina	33710	33710	0	7.2
Skaneateles	7209	3415	3794	1.5
Spafford	1686	109	1577	0.3
Syracuse	145170	145170	0	31.0
Tully	2738	0	2738	0.5
Van Buren	13185	10118	3067	2.8
Total	467026	408239	58787	
Percent of total	100	87.41	12.59	

Table 2-1: Total, urban and rural population distribution at the 2010 census in Onondaga County (USCB, 2010)

Pollution in Syracuse

Syracuse and much of Central NY was covered by the Laurentide ice sheet throughout the Pleistocene. This glacier began retreating around 17,000 years before present and left numerous lakes and drumlins throughout the Syracuse area (Kappel et al., 2007; Yager et al., 2007). Deglaciation contributed to the development of the extensive deposits of halite brine in the glacial valley immediately south of Syracuse (the Onondaga Trough). Beginning in 1787

these deposits were mined by local industry to produce salt and later soda ash – a water softener for industrial manufacturing (Allen, 1842; Effler, 1996). These efforts continued through the end of the 20th century and contributed to extensive pollution in the Onondaga Lake watershed. Research by Steven Effler and the Upstate Freshwater Institute led to the designation of Onondaga Lake as a superfund site in 1994 and its eventual remediation in the early 21st century (Urbina, 2004 as cited in Bergeron, 2017; Effler & Hennigan, 1996; Kirst, 2010).

Air pollution

In contrast to water pollution, air quality research in Syracuse is less developed and only focuses on air pollution from 1980 to the present. This relatively short timeframe is likely in response to the lack of monitoring prior to the implementation of the Clean Air Act (Public Law 88-206) in 1970. A number of new industrial manufactories were established throughout the 19th and 20th centuries. These include Crucible (1876), Bristol-Meyers Squibb (1943), Solvents & Petroleum Service (1946) and Anoplate (1960) (Anoplate, 2018; Bristol-Meyers Squibb, 2018; Crucible Industries, 2018; Solvents & Petroleum Service, 2018). These companies and others still release harmful pollutants into the air today [Table 2-3] (EPA, 2018a).

Company	Air emissions (kg)
Advanced Motors & Drives INC	0
Anaren Microwave INC	0.09
Anheuser-Busch LLC	2848.56
Anoplate Corp	907.18
Armstrong Mold Corp	0
Bodycote Syracuse Heat Treating Corp	194.14
Bristol-Myers Squibb Co	0
Byrne Dairy	0
Cargill Animal Nutrition	0
Chemtrade Solutions-Syracuse	5994.89
Cooper Crouse Hinds	0
Crucible Industries LLC	1254.18
Eagle Comtronics INC	0
Empire Vision	0.09
Feldmeier Equipment INC	7.26
ICM Controls Corp	1.81
Jamesville Mix Plant	1.34
Kilian Manufacturing	0
Liverpool BWE LLC	0
Lockheed Martin Corp	1.84
Meloon Foundreis LLC	170.55
Omega Wire INC - Jordan Plant	0
PPC A Belden Co	0.23
Safety-Kleen Systems Syracuse (Syr)	481.72
Solvents & Petroleum Service	15697.92
Strathmore Holdings LLC	209.11
Syracuse GH Berlin Windward	0
Ultra Dairy LLC	0
US Optical LLC	0
Welch Allyn INC	0
Westrock - Solvay LLC	6477.98
Total Air Emissions	**34248.89**

Table 2-3: EPA 2016 Toxic Release Inventory [TRI] air pollution releases for Syracuse area industries (EPA, 2018a)

The EPA monitors air pollution in Syracuse from a network of air quality monitoring stations operated by the New York State Department of Environmental Conservation [NYS DEC].

Historically, 15 stations operated in the Syracuse area to measure carbon monoxide (CO), sulfur dioxide (SO_2), nitrogen dioxide (NO_2), Ozone (O_3), particulate matter (PM_{10}, $PM_{2.5}$) and lead (Pb) (United States Environmental Protection Agency [EPA], 2018b). Only one site (with two active stations) remains operational today (43.05235, -76.05921) (Buckley & Mitchell, 2011; EPA, 2018b).

Long term trends show a statistically significant decline in the concentration of all six pollutants. On average the EPA Air Quality Index [AQI] for Syracuse has decreased from 71 in 1980 to 37 in 2017 [Figure 2-2] (EPA, 2018b). However, Buckley and Mitchell (2011) note that trends vary substantially by decade and pollutant (the AQI spike in the 1980's is a result of an increase in the concentration of CO), and may be influenced by the importation of pollutants from the Midwest or Canada (SO_2 and O_3, respectively). That said, it is possible that abrupt changes in the AQI could be explained by the relocation of monitoring stations from the suburbs to the urban core [Figure 2-3] (EPA, 2018b).

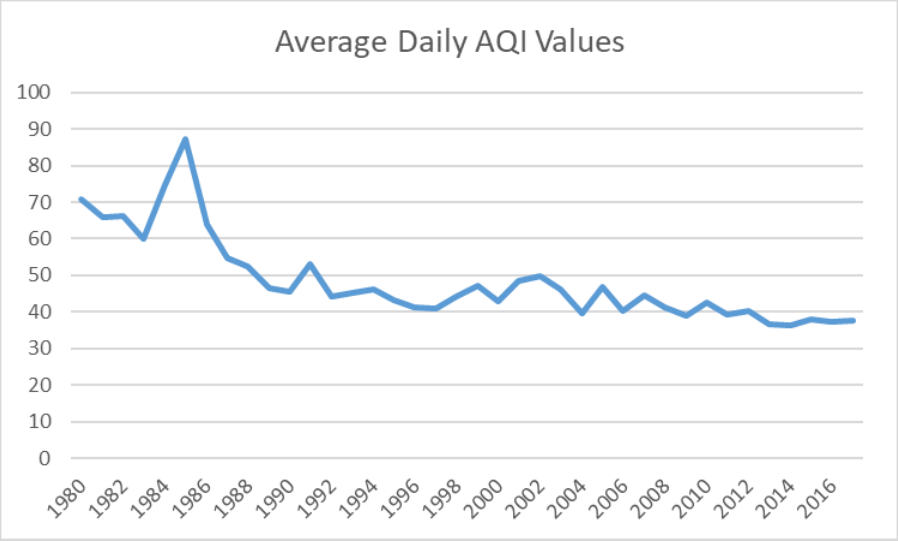

Figure 2-2: Average daily AQI value in Syracuse (1980-2017); reported values represent the highest value recorded each day by any measured pollutant (EPA, 2018b)

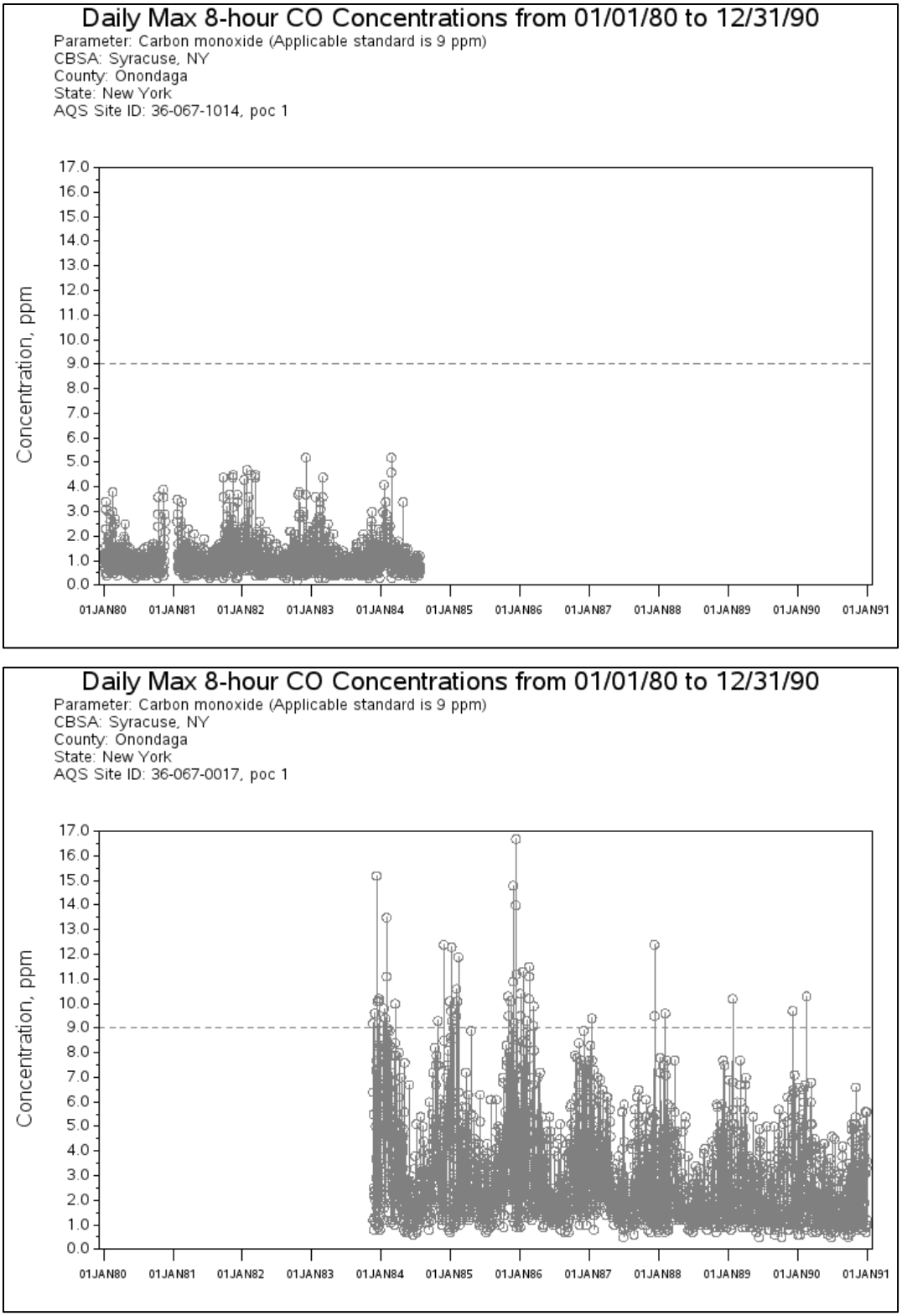

Figure 2-3: CO emissions at two monitoring stations in Syracuse; note the increase in recorded CO levels between the old station (top) and the new station (bottom) (EPA, 2018b)

Particulate monitoring

In 1989, the EPA began monitoring particulate matter at two stations in Syracuse. For ten years, daily measurements were recoded for particulates with a diameter less than 10 µm (PM_{10}). Beginning in 1999, ultra-fine particulates with a diameter less than 2.5 µm ($PM_{2.5}$) were recorded as well (EPA, 2018b). The majority of PM_{10} and $PM_{2.5}$ particles are linked to vehicle exhaust, tire and brake wear or the aerosolization of road debris – all sources that are prevalent in urban areas (A. Gertler, Gillies & Pierson, 2000). Buckley and Mitchell (2011), focused on $PM_{2.5}$ in their analysis of particulates in Syracuse. According to the study, $PM_{2.5}$ does not follow the same downward trend as the other pollutants. Instead, concentrations peak in 2002 and 2006, contrasting with a 19% nationwide decrease in $PM_{2.5}$ from 1990 to 2008 (United States Environmental Protection Agency [EPA], 2010). It is difficult to determine if the observed peaks are a result of increased pollution, abnormal precipitation or other external factors.

$PM_{2.5}$ measurements reported by the EPA include five types of particulates: sulfate, nitrate, elemental carbon (black carbon), organic carbon and crustal material (dust, aerosolized soil and rock particles). Sulfate and nitrate make up over 50% of particulates measured in the eastern US (EPA, 2010). While this is useful for examining air quality and shortwave radiation backscattering, sulfate and nitrate concentrations were not examined in this study. Furthermore, EPA $PM_{2.5}$ measurements at the East Syracuse station do not include quantification of brown carbon, fly ash, soot and other carbonaceous aerosols – all important light absorbing aerosols necessary for an accurate reflectivity analysis of the snow surface (Bond et al., 2013; G. Wu, et al., 2016). This study aims to address this limitation by assessing all particulates (including those not measured by the EPA) that are deposited on the snow surface.

Climate

Climate in Syracuse is influenced by its location in the midlatitudes and its proximity to Lake Ontario and Lake Erie. Much of central NY experiences a humid continental climate with warm summers and cold winters – Syracuse is no exception (National Centers for Environmental Information [NCEI], n.d.). Hourly temperature, precipitation and snowfall data are recorded at Syracuse Hancock International Airport, 6km NNE of the city (43.1111, -76.1038). Continuous records date back to 1949, when the station was moved from its original location (43.066667, -76.266667) (National Centers for Environmental Information [NCEI], 2018). Figure 2-4 shows the maximum, minimum and mean normal temperature values by month recorded at the weather station from 1981 to 2010. The mean high of 21.8˚C (July) and low of -4.7˚C (January) are consistent with observations reported by the NCEI (n.d.) and patterns observed in humid continental climate regions (MRCC, 2018).

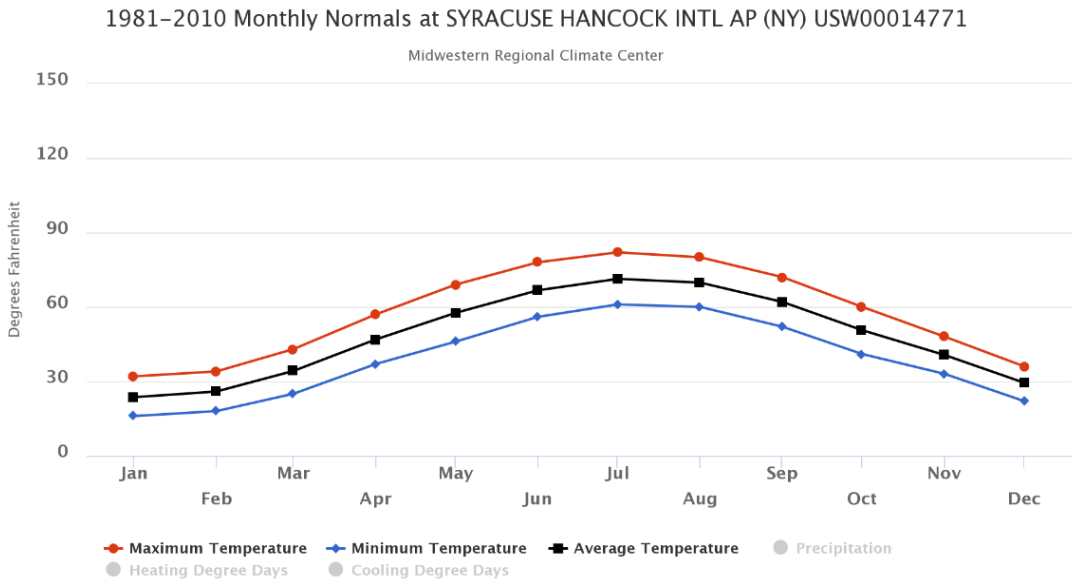

Figure 2-4: Minimum, maximum and mean temperature normal (1981-2010) at Syracuse Hancock Airport (MRCC, 2018)

Lake Ontario is situated 55 km NE of Syracuse, Lake Erie 220 km WSW. Both lakes, along with Superior, Huron and Michigan (collectively known as the Great Lakes), make up a series of large, well known, inland, freshwater lakes that substantially influence the climate and precipitation patterns of nearby states. This is especially true on the leeward side of the lakes where, under specific atmospheric conditions, lake effect precipitation tends to develop. These rain or snow events occur when cold air moves across the relatively warm lake. In a typical year, this occurs from late July until the end of January (or later if the lakes remain ice-free through the winter) (Miner & Fritsch, 1997).

The precipitation normal shows that Syracuse experiences substantial precipitation throughout the year, however, July through November are the wettest months [Figure 2-5] (MRCC, 2018). The wet fall is notable as most locations experience the highest quantity of precipitation in the summer when surface heating causes instability in the boundary layer. According to Miner and Fritsch (1997), the extra precipitation is likely a result of the proximity to Lake Ontario. To quantify this effect, their study, examined precipitation at weather stations directly located downwind of Lake Erie and Ontario. These measurements were compared to precipitation readings from stations at least 100 km away (these stations represent a similar climate with little to no lake influence). Results show an additional 8-28 mm of precipitation was recoded at the near-lake weather stations. Figure 2-6 compares the precipitation normal in Syracuse to Binghamton, Ithaca and Elmira. The comparison cities (150 km, 100 km and 130 km away from the Lake Ontario, respectively) show a decline in precipitation from September through January (MRCC, 2018). This downward trend is expected as temperatures decrease

through the fall. In contrast, precipitation in Syracuse remains relatively constant through December before it falls in January. This pattern is likely a result of lake effect rain.

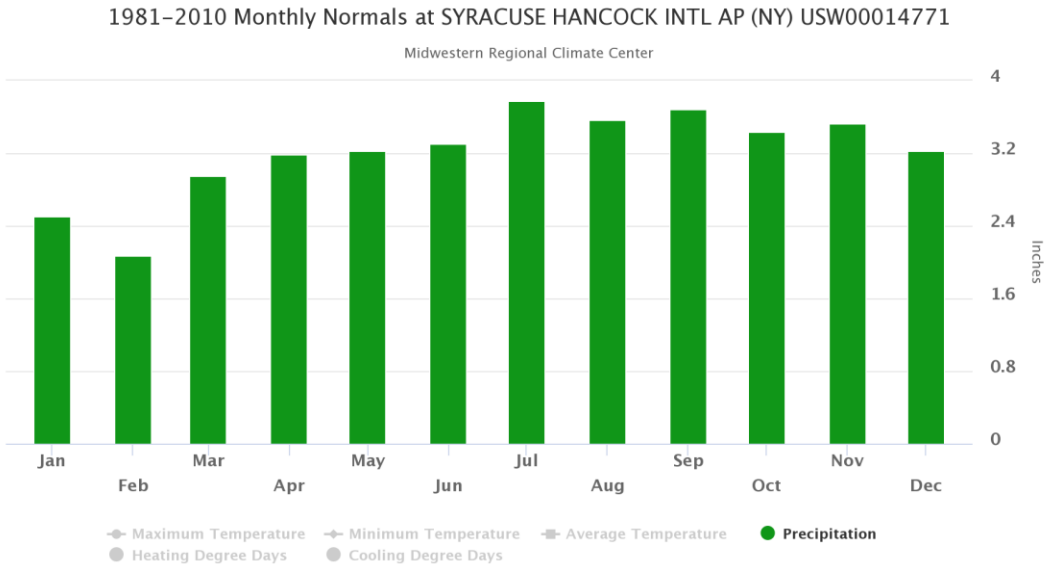

Figure 2-5: Precipitation normal for Syracuse Hancock International Airport (1981-2010) (MRCC, 2018)

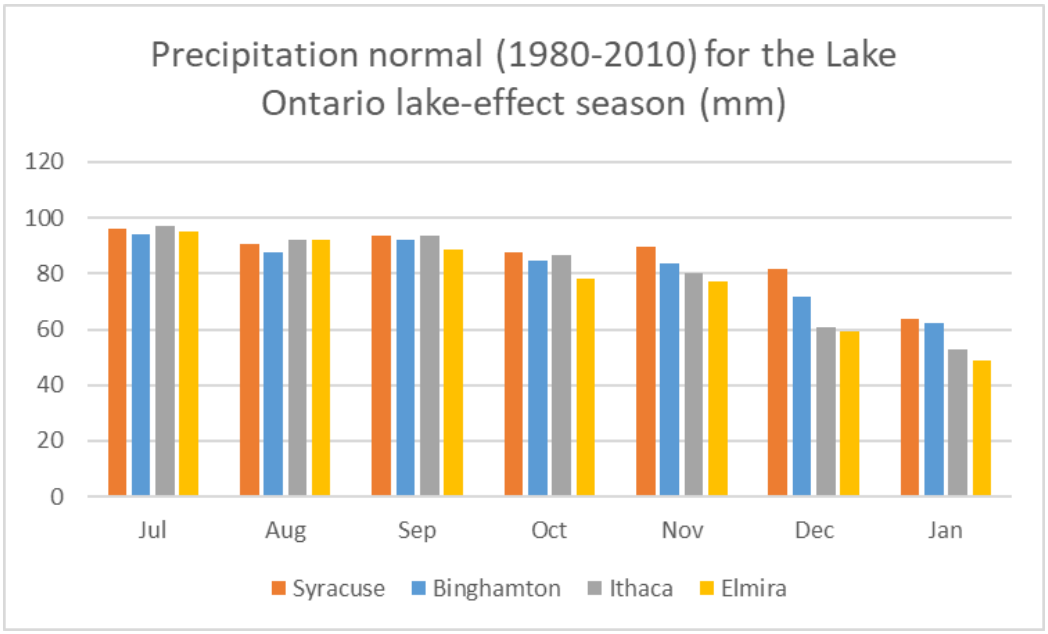

Figure 2-6: Precipitation normal for Syracuse, Binghamton, Ithaca, and Elmira from July to January (1981-2010) (MRCC, 2018)

Snow in Syracuse

Lake effect rain may soak Syracuse in the fall, however, lake effect snow is the city's true claim to fame. On average, about 300 cm of fluffy white snow falls on the city and surrounding area each year (Call, 2005; Millar, 2017; MRCC, 2018). In fact, Syracuse often wins the prestigious (to snowy cities, that is) "Golden Snowball" and "Golden Snow Globe" awards for the highest annual recorded snowfall in a city over population 100,000 in NY and the US respectively (Millar, 2017; Kirst, 2013). Even with this relatively high total, Val Eichenlaub (1970) excluded Syracuse in his delineation of the Lake Ontario Snow Belt. Instead he marked the boundary approximately 25 km north between Syracuse and Fulton, NY (as cited in Monmonier, 2012, p. 2). This demarcation makes sense as snowfall totals expand rapidly to 350 cm in Fulton (37 km NW) and explode to over 750 cm (record is 1077 cm) in the small town of Redfield, NY (60 km NNE) (Monmonier, 2012; Becker, 2018). Despite this, Syracuse has experienced a large number of medium to high impact snow events since record-keeping started (Call, 2004).

While there are many types of storms that affect Syracuse, five types stand out: Alberta Clipper, Colorado Low, Panhandle Low, Nor'easter and Lake Effect. Each storm brings substantially different snow conditions and impacts the area in a unique way. Cyclogenesis of the Alberta Clipper takes place on the leeward side of the Canadian Rockies, often in or near the province of Alberta. These fast-moving, low moisture (snow to liquid ratio of up to 20:1), cyclones move quickly to the southeast through central Canada and eventually to the north shore of the Great Lakes (Thomas & Martin, 2007). Clippers can bring light to moderate (8-15 cm) synoptic snow (widespread snow associated with frontal uplift) to the area north and south of the storm track (Call, 2004, Thomas & Martin, 2007). Forecasters in central NY often dismiss

the Alberta Clipper as insignificant because of its lack of moisture and intensity. However, if the storm passes over the Great Lakes, it can become enhanced with lake moisture, yielding (if conditions are right) a much more powerful storm. This was the case on January 11, 2004 when a clipper forecast to bring 5-10 cm, dumped over 27 cm on the greater Rochester area (Rochette, Market, Gravelle & Niziol, 2017).

Similar to the Alberta Clipper, the Colorado and the Panhandle Lows form on the leeward side of the Rocky Mountains. Cyclogenesis takes places in the south-central Rockies often near Colorado (Changnon, Merinsky & Lawson, 2008). While the two lows form in the same relative location, their path across the US defines how they affect Central NY. The Colorado Low tracks northeast across the Midwest and over the Great Lakes to arrive in Syracuse from the SW. Its proximity to the Great Lakes suggests that this storm can be enhanced with lake moisture similar to the Alberta Clipper. In contrast, the Panhandle Low, tracks southeast through Oklahoma and Arkansas before turning northeast to arrive in Syracuse from the SSW (Changnon, Merinsky & Lawson, 2008; Loveless, Godek & Blechman, 2014). Of the two storms, the Panhandle Low is often slightly more intense – likely a result of its southern track. As the storm moves across the south-central US, it picks up additional moisture from the Gulf of Mexico. The eventual turn to the northeast places the Panhandle Low on a path that is well east of the Colorado Low track. This increases the likelihood that Central NY will be located in the cold section of the storm (Loveless, Godek & Blechman, 2014). Despite these differences, both systems can produce significant, widespread synoptic snow in Central NY. Under the right circumstances, they can also intensify as the low interacts with coastal waters (Loveless, Godek & Blechman, 2014).

A Nor'easter is a powerful costal storm that can bring a large amount of precipitation and high winds to Syracuse. Like the Alberta Clipper, Colorado Low and Panhandle Low, the Nor'easter specializes in synoptic snow. It differs, however, in the moisture content of the storm. Snow associated with a Nor'easter is often heavy and wet as a result of access to oceanic moisture in the North Atlantic. At times the storm can boast a snow to liquid ratio of 10:1 or less (Call, 2004). A Nor'easter usually forms over the Gulf of Mexico or southeastern Atlantic and tracks up the east coast of the US. To affect Syracuse, it must follow a westerly track up the coast, which often leads to record breaking snow totals. The blizzard of 1993 followed this course and left a whopping 106 cm of snow at Syracuse Hancock Airport over two days. If it had remained further east, Syracuse would have been left with only sunny skies. (Call, 2004).

By far, the most common type of storm observed in Syracuse is Lake Effect. In order for lake effect snow to persist, certain conditions need to be met. Lake effect forms only when the air at the 850 mb level (about 1.6 km above the ground) above the lake is at least 13°C colder than the surface water (Call, 2004; Suriano & Leathers, 2017). In addition, air must move across the lake at a speed between 5m/s and 20m/s for a significant distance. When this happens, moisture transfers into the airmass from the relatively warm lake water and condenses to fall as snow (or rain if temperatures are above freezing) (Monmonier, 2012; Suriano & Leathers, 2017). Unlike synoptic snow, lake effect typically remains in localized bands aligned to the direction of wind (types 1, 2), however, it can form parallel to the shore (type 4) or in a small vortex (type 5). Bands range from 5-50 km wide and can reach up to 200 km away from the lake (Niziol, Snyder & Waldstreicher, 1995). Occasionally bands that form off of Lake Ontario and Lake Erie form a connection to moisture in upstream lakes including Lake Huron and the

Georgian Bay (type 3). When this occurs, lake effect snow can extend upwards of 375 km away from the lake (Niziol, Snyder & Waldstreicher, 1995; Villani, Jurewicz & Reinhold, 2017).

Lake effect bands change position as the direction of prevailing wind shifts. This results in an uneven snow distribution across the landscape. High snow accumulations are found where bands persist for an extended period. Figure 2-7 shows the frequency of the observed wind direction at Syracuse Hancock Airport from October 1 to March 31 (1981-2010). The highest frequencies of lake effect capable wind (5 m/s to 20 m/s) originated between the WSW and the NW. Assuming all other criteria are met, these winds should create snow bands downwind of Lake Ontario from the Tug Hill plateau (WSW wind) to Syracuse (NW wind). Bands that form off of Lake Erie should produce snow from Buffalo (WSW wind) to Erie, PA (NW wind). At 225 km ENE of Lake Erie, Syracuse is not affected by the majority of Lake Erie bands. However, it is possible for occasional bands to extend to Syracuse (and beyond) especially if there is a connection to upstream moisture (Niziol, Snyder & Waldstreicher, 1995; Villani, Jurewicz & Reinhold, 2017). This can occur when a WSW wind is observed in Syracuse.

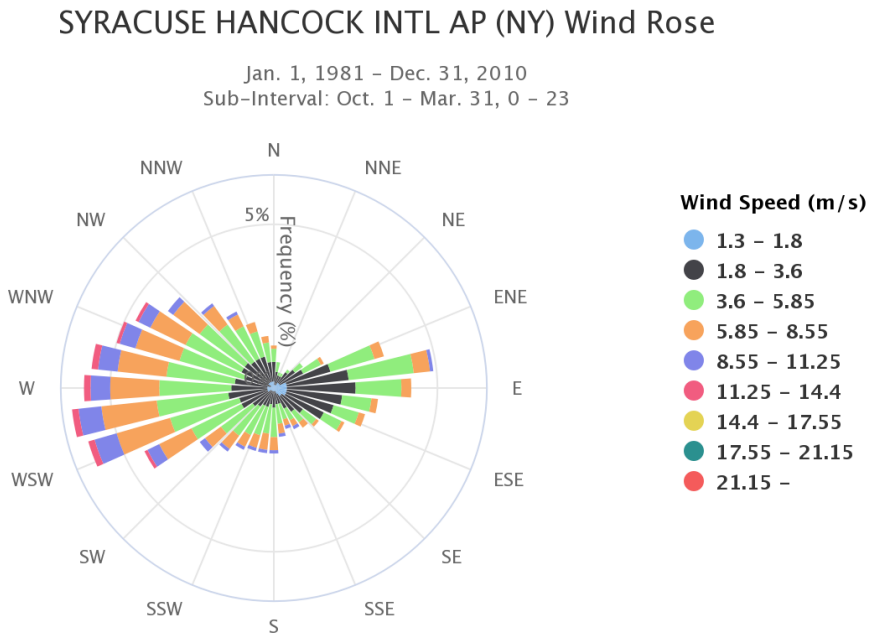

Figure 2-7: Frequency and intensity of observed hourly wind direction from October 1st to March 31st (1981-2010) at Syracuse Hancock International Airport (MRCC, 2018)

A Necessary Study

With a history of environmental degradation, access to a variety of pollution monitoring data and a location (almost) within the snow belt of Lake Ontario, Syracuse NY is the quintessential city for environmental pollution and snow research. Most studies, however, only focus on one area: pollution (specifically in Onondaga Lake) or snow (specifically lake effect snow). This study bridges both human and environmental processes. As of yet, there are few comprehensive studies on particulate pollution in the midlatitudes; Doherty et al., (2014) penned a notable exception. Of these, no studies explore the direct influence of urban particulates on the city-scale distribution of particulates in snow.

The location and climatology of Syracuse provide an opportunity to examine this influence. Reliable snowfall supports the development of an in depth study that requires

numerous individual snow events to examine the spatial patterns of particulate distribution. The consistent westerly wind during most winter storms makes it possible to assume that snow travels across the city from the W to the E. As the snow passes over the urban center it should incorporate particulates into the storm and impact the concentration downwind. Even the morphology of Syracuse is important – a smaller city may produce too few particulates to make a study worthwhile, whereas, a larger city would increase the distance between sample sites rendering fieldwork unfeasible. Syracuse provides access to multiple high traffic roadways for analysis of local-scale distribution – a smaller city may not provide the traffic density required to accurately access vehicle distribution. Perhaps the most important aspect, however, is the similarity of Syracuse to other midlatitude industrial cities across NY and the US. While Syracuse does sport uniqueness in its location and snowy climatic conditions, this study could be repeated in cities regardless of snow accumulation – a process that could be streamlined by the successful implementation of particulate analysis method utilizing digital photography. Nevertheless, increased study of particulate matter and its effect on midlatitude urban snow is needed to understand how a city affects its surroundings. Perhaps, the Golden Snowball/Globe competition list can serve as a starting point for a second particulate-snow case study location.

Chapter 3 – Methods

Experimental Design

Two strategies, termed the "directional study" and the "transect study, were applied to test the research questions outlined in the introduction. Table 3-1 details the specific question addressed by each strategy, as well as the general sampling design. Both studies incorporated the use of digital photography as a novel method to measure particulate concentration on the snow surface.

Experiment	**Directional Study**	**Transect Study**
Location	Syracuse suburbs and Skytop	Onondaga Lake County Park
Number of sites	9 experimental	6 experimental
Distance from the city center	Min: 6 km Max: 16.5 km Central site (Skytop): 5 km	11 km
What is it?	Each site location corresponds to a compass direction with respect to the city	The six sites form a transect across an interstate highway (I-90)
Research questions addressed	1. How does a mid-size city and prevailing wind direction affect the spatial distribution of particulates in the surrounding snowpack? 3. Is digital photography an accurate and cost-effective procedure for measuring particulate concentration in snow?	2. How is the distribution of particulate matter in snow altered by the proximity to vehicle emissions released on an interstate highway? 3. Is digital photography an accurate and cost-effective procedure for measuring particulate concentration in snow?

Table 3-1: Overview of the directional and transect studies

The directional study

Syracuse experiences a prevailing WSW to NW wind in winter that causes snow to travel from W to E across the general area (MRCC, 2018). If the city acts as a source of particulate pollution, the snow should pick up particulates as it passes over the urban core. This would result in a distribution where upwind sample sites measure fewer particulates than sites downwind. The directional study was designed to test this hypothesis. Nine sample sites were selected for measurement: eight in the suburbs surrounding the city and one central location. Sites were roughly aligned to the cardinal directions with respect to the city (N, NE, E, SE, S, SW, W and NW) and analyzed in pairs. The upwind sites (usually SW, W, NW or N) measured the concentration of particulates before the snow event reached the city center. Downwind sites (usually NE, E, SE or S) measured the concentration after the storm passed over the urban core. The eight suburb sites were located a minimum of 6 km and maximum of 17 km from the city center. This restriction helped to prevent contamination from city-produced particulate sources and avoid contamination from other urban areas [Figure 3-1]. The central location was sited 5 km from the city center.

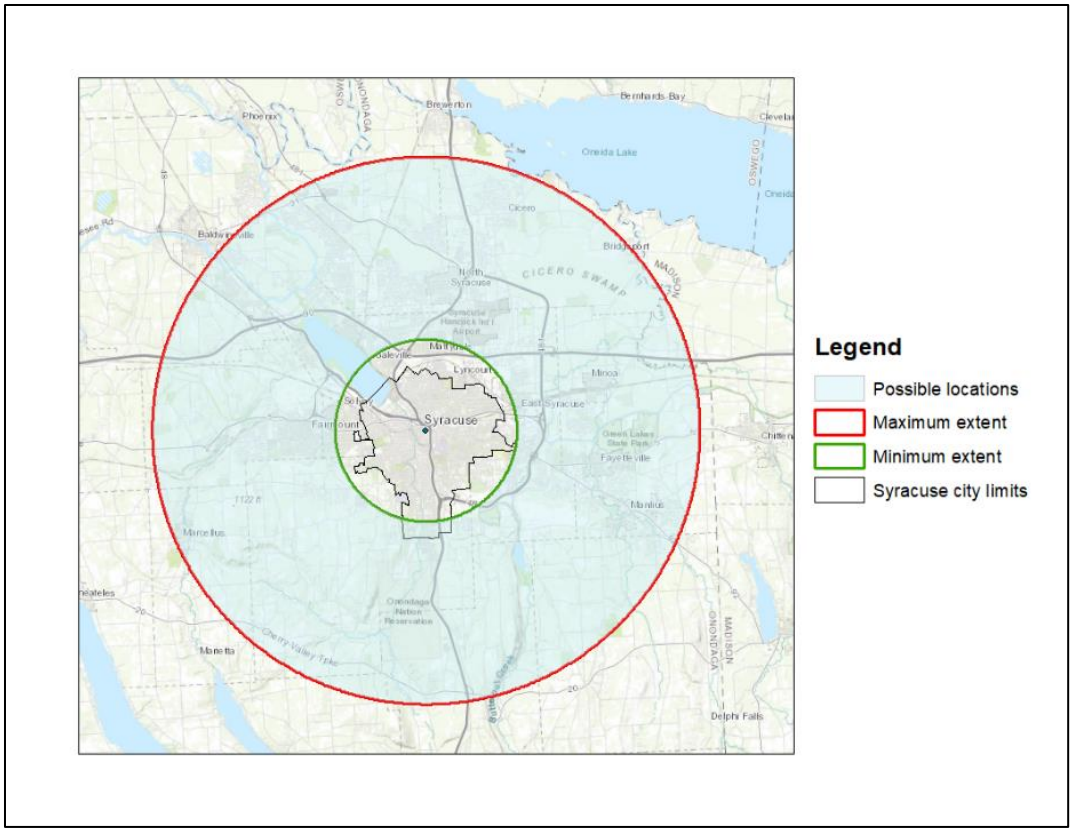

Figure 3-1: The area surrounding Syracuse considered for directional site selection

City-based studies of air pollution typically do not address the spatial variation of pollution within the surrounding area. Grimmond et al. (2002) and Lestari, Oskouie and Noll (2003) examine pollution (CO_2 and PM, respectively) in Chicago. Both experiments were designed to collect data from a single location within the city. This type of study ignores local scale sources that can substantially alter the pollution quantity. Researchers that do include a spatial component, examine particulates at a regional scale that can span hundreds of kilometers (Doherty et al., 2014; Li et al., 2014). In this case, samples are rarely collected from a seasonal snowpack (Bond et al., 2013). The directional study aims to address this deficiency with a rigorous examination of particulate distribution at the city-scale.

The transect study

Six additional sites were added as part of the transect study. These sites, running perpendicular to the interstate, were designed to examine the particulate distribution that results from intense vehicle emission at the local scale (Lund et al., 2014). Cereceda-Balic et al. (2018) observed a daily decrease in near-highway snow albedo after heavy traffic. The transect study explores this concept from a spatial perspective. As particulates are dispersed from the interstate, the highest rate of deposition should be observed nearest the pollution source. Transect studies are often used to examine spatial and or temporal variability in a snowpack. This technique can be used to explore snow properties including depth, density or snow water equivalent (SWE) (Kinar & Pomeroy, 2015; Neumann et al., 2006). For this study, the "transect" component explores the change in concentration of particulates with respect to the proximity to I-90.

Digital photo analysis

With the proliferation of high resolution cameras, the use of digital images for scientific analysis is expanding. Aerial photography and terrestrial photography have been used in research applications ranging from vegetation and leaf identification (Maloof et al., 2013) to the identification of glacier calving events (Medrzycka et al, 2016) to the mapping of periglacial geomorphology (Boike & Yoshikawa, 2003). An advantage of using this method in scientific research is the ability to greatly expand data collection through citizen science. For this study, a methodology is tested that uses digital photos of the snow surface to quantify particulates and streamline the fieldwork process.

Sampling Methodology

Sites were sampled for two winter seasons. The first season (2016-2017) provided few opportunities to collect snow. As a result, this season became a pilot study to improve sampling methodology. In addition, rain samples were collected weekly from August 3rd 2017 until November 6th 2017. The samples were used to test laboratory methodology before the second winter season. The gauges were purchased from weatheryourway.com and installed in the Westcott neighborhood (east of the Syracuse urban core). A "4 inch" (10.16cm diameter) gauge was mounted to a wooden post 122 cm above ground level [Figure 3-2]. The second season (2017-2018) provided ample snow for particulate analysis. Field and laboratory methods that were identified and refined in the first season and summer were implemented to streamline sample collection and analysis.

Figure 3-2: Rain gauge installed at the Skytop location

Site Selection

Location, access and local contamination all contributed to site selection. The directional sites were located as close as possible to their respective direction. Transect sites were located near I-90, a highly trafficked transportation and shipping corridor north of the city. Access was the most restricting factor that influenced selection. Directional sites were located in public parks (state, county and city), NYS DEC easements or on college campuses. Only one public space, Onondaga Lake County Park, provided uninterrupted access to I-90 – the transect was located there.

Local contamination played an important role in the final selection. In order to properly address the research questions, it was necessary to assume that Syracuse (the city) and I-90 were the only two sources of particulate pollution. Therefore, local sources of contamination were identified and avoided if possible. The EPA published a GIS database of air pollution permit holders across the US. These data were first accessed in fall 2016 in order to determine the location of all major sources of industrial air pollution in the Syracuse area [Figure 3-3]. Twenty locations were identified as emitting either “major” pollutants (often greenhouse gas emissions) or “hazardous” pollutants (these are not described in the metadata) (EPA, 2015). In order to reduce contamination, a 500 m buffer around each site was calculated. Potential sampling locations within this buffer were excluded from selection. At the time of writing (Spring 2018), the EPA air pollution permit data are no longer accessible – likely a result of the current US political climate.

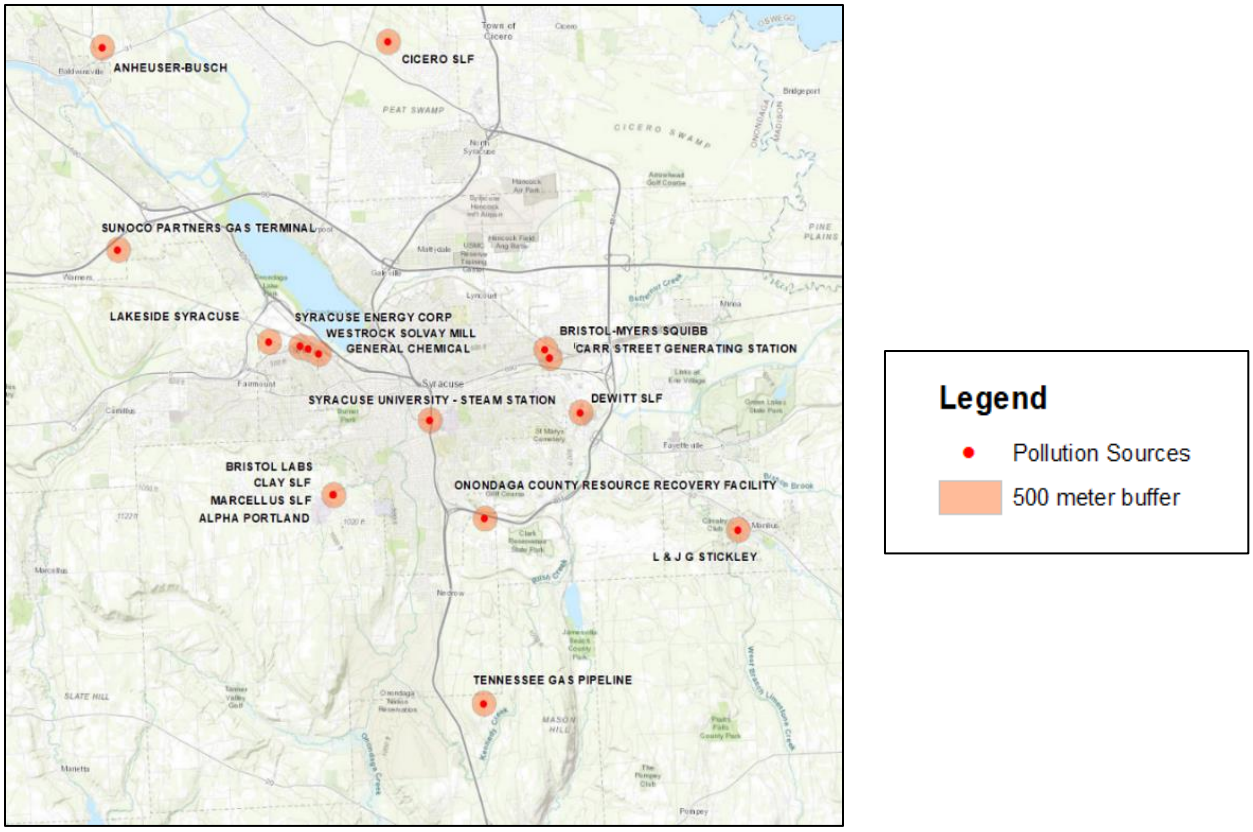

Figure 3-3: Map of "major" and "hazardous" impact air pollution permit holders and the 500m site selection buffer (EPA, 2015)

Site selection also required a site visit to identify micro-scale sources of particulate contamination. Refuse bins, dog parks, dirt piles, excessive litter, broken appliances and used tires were all identified as potential contaminants and avoided. Final sites had large open spaces with access to undisturbed snow. In total, 15 sites were selected for the directional and transect studies [Figure 3-4]. Appendix A details the location, GPS coordinates and description of each site.

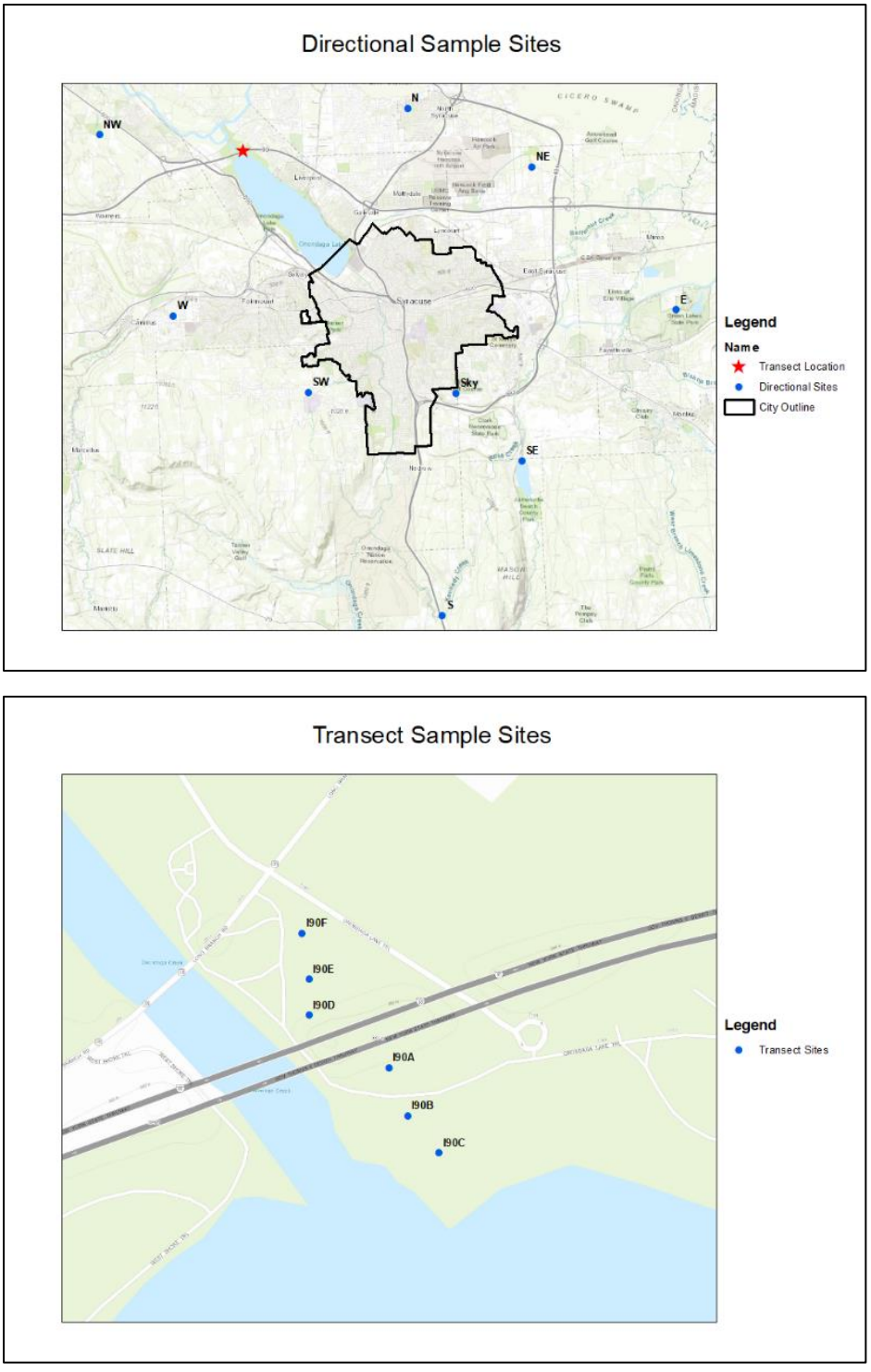

Figure 3-4: Map of the official directional (top) and transect (bottom) sites sampled in the second season; both maps exclude first season sites that were relocated in the second season

A number of sites were relocated in the second season. The E site was moved 1.5 km southwest as a result of parking lot construction within Green Lakes State Park. Two of the six transect sites (I90B and I90E) were unmeasurable during the first season. One site was located in a parking lot (that was unplowed during site selection) and second in an ephemeral streambed. Suitable alternatives could not be identified. In order to keep the transect intact, all six sites were relocated 170-210 m to the southwest [Figure 3-5]

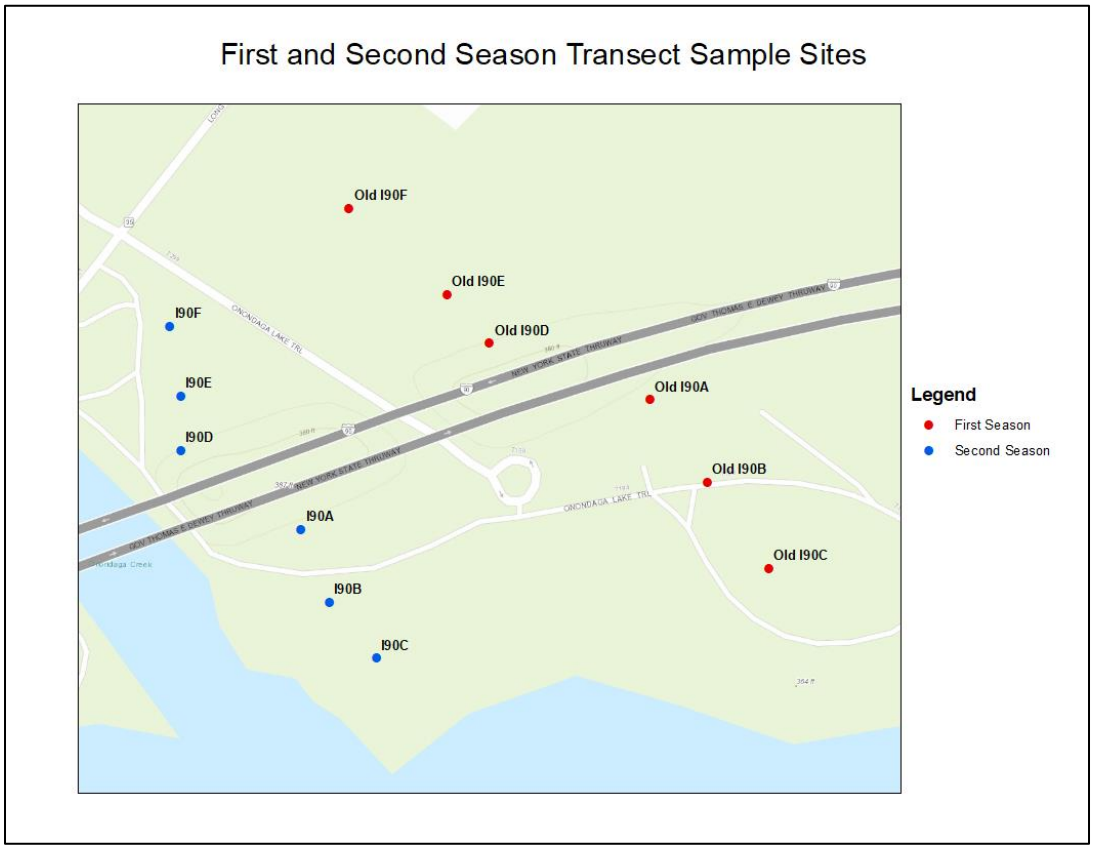

Figure 3-5: Map of transect sites in the first season (red) and second season (blue)

Sample Collection

Particulate pollution is incorporated into snow through wet and dry deposition (Bond et al., 2013; Persad et al., 2012). Wet deposition occurs during precipitation and deposits

particulates throughout the entire snowpack. In contrast, dry deposition causes particulates to settle on the surface of the snow (Zhang et al., 2015). Two rounds of samples were scheduled for each snow event. The first set was collected within 24 hours after the end of snow accumulation. This set was used to determine the amount of wet deposition associated with the storm. If possible, a second set of samples was collected three to seven days after the first sample. This was used to examine both wet and dry deposition. A minimum of 15 cm of new accumulation was required to provide enough snow for laboratory analysis

Field work followed a standard procedure. Directional sites were sampled clockwise beginning with the N site. Transect sites were sampled in alphabetical order beginning with the sites south of the interstate. It was difficult to standardize fieldwork collection times. According to Dirmhirn and Eaton (1975), the amount of reflected radiation measured by a pyranometer (a solar radiation meter used to measure incoming and reflected radiation) is significantly affected by sun angle. A smaller sun angle increases the amount of specular reflectance and causes the pyranometer to underestimate the amount of reflected radiation. This error is minimized near solar noon (Millar, 2017). Samples were collected with this restriction in mind, however, it was not possible to visit each site between 11:00 and 13:00 (12:00 and 14:00 EDT). In most cases, the first directional site was sampled between 09:30 and 10:00, the final near 15:30. The timing of transect sampling was less consistent and was dependent on the timing of the snow event. If accumulation ended in the morning, transect sites were sampled that afternoon (one day prior to the directional sites). If snow ended in the evening, transect sites were sampled one day after directional sites. If snow ended in the evening and more snow was predicted within two days, the transect sites were sampled immediately after the directional sites.

Precipitation (options = no precipitation, light snow, moderate snow, heavy snow, rain) and sky cover (options = clear, few clouds, partly cloudy, mostly cloudy, overcast) were recorded at each sample site. Air temperature and wind speed were measured using a handheld digital anemometer. The device was allowed 30-60 seconds to acclimate to the surrounding air before recording the temperature. To record wind speed, the device was faced into the wind approximately 150 cm above the snow surface. Wind speed was monitored for 10-15 seconds – the highest speed and most consistent direction was recorded. A handheld infrared thermometer was used to determine the temperature of the snow. To record this, the device was pointed at the snow surface from a height of approximately 50 cm. Snow depth was measured using a standard aluminum meter stick [Figure 3-6].

Figure 3-6: Field gear for the second season

Incoming and reflected solar radiation were measured using a PCE-SPM 1 solar radiation meter. The radiation meter has a resolution of 0.1 W/m^2 and accuracy of ±10 W/m^2 (Millar, 2017). Incoming radiation was recorded by holding the radiation meter perpendicular to the

snow with the sensor pointing directly overhead. The reading was observed for 10-15 seconds and the highest value recorded. To measure reflected radiation, the meter was rotated 180 degrees vertically until the sensor was pointed directly at the snow. Both incoming and reflected radiation were measured at a height of 25-35 cm above the snow surface. These data were later used to calculate the albedo of the snowpack.

Photos of the snow and the surrounding area were taken for the photo analysis whenever a sample was collected. Throughout the first season, a minimum of two photos were captured of the snow itself. One was taken directly above the snow surface from a height of approximately 30 cm. The sample container and ruler were included in the photo to identify the sample site and give the photo perspective. A second photo was taken with a wider angle in order to show the entire sample area. Occasionally, additional photos were taken to document unusual conditions in the surrounding area, local sources of particulates, snow cover changes or interesting landscape features [Figure 3-7].

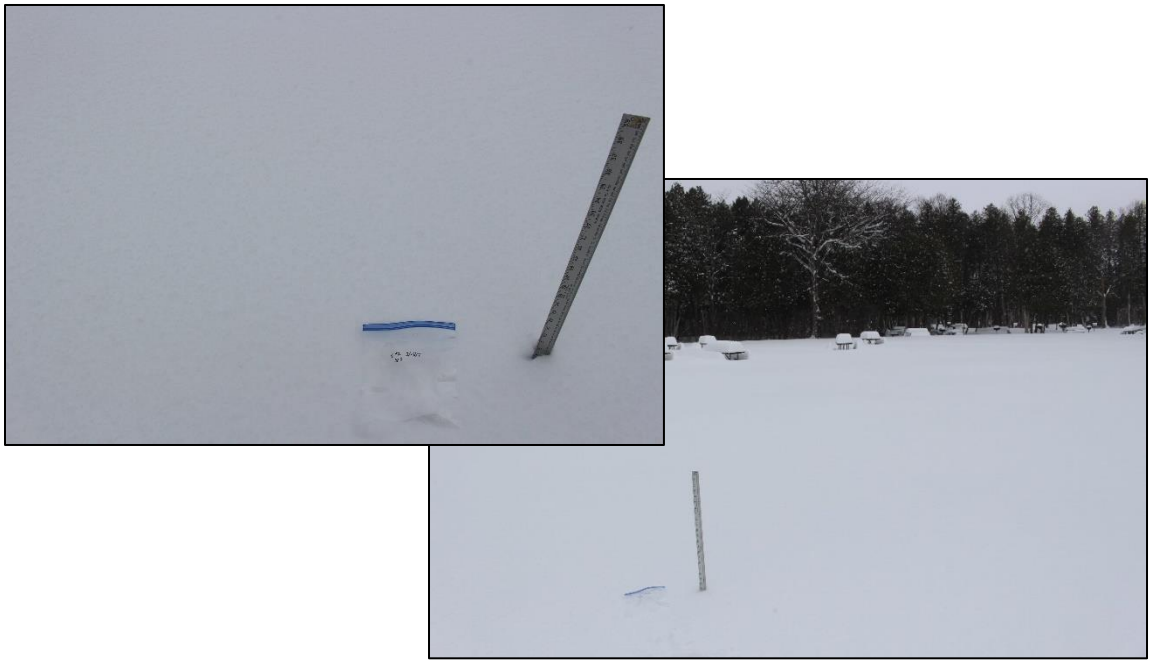

Figure 3-7: First season photos showing the snow surface (top left) and site overview (bottom right) at the E site (this site was moved to a new location in the second season)

In the second season, photo collection followed a standardized procedure. A minimum of ten photos were collected at each sample site, including two photos of the snow surface. Both images were taken directly above the surface at a 90 degree angle to the ground. The focal length of the lens was set at 18mm and a meter stick was placed flat on the snow surface. One image was collected from waist height (70-100 cm) above the surface and generally showed the meter stick from the 20 cm mark through the 75 cm mark. The second was taken from chest height (110-130 cm) and was framed to show the entire meter stick across the bottom of the photo [Figure 3-8].

Figure 3-8: Standardized snow surface photos taken at the relocated second season E site: chest height (left), waist height (right) and site overview (center)

The remaining eight images were used to document the snow and environmental conditions adjacent to the sample site. One photo was taken facing each of the cardinal directions in the following order: S, SW, W, NW, N, NE, E, SE. All photos were collected at eye level (150cm) with a focal length of 18mm. Additional photos were taken potential sources of contamination, unusual snow conditions or notable phenomena.

A snow core was collected from the same snow surface that was analyzed and photographed. This surface was utilized to allow for the comparison of analysis methods, however, on occasion the core was collected a short distance away (<2 m). In this case, the variability of snow conditions and particulate concentration was assumed to be negligible. In the first season, a small plastic tube (30 cm length by 3.2 cm diameter) was inserted vertically into the snow to collect the core. Snow was removed from the tube with a wooden dowel. The dowel, marked in 1 cm increments, was also used to measure the core length. A small section (<2 cm) of the core was removed to prevent dirt/debris contamination from the ground.

First season samples did not yield enough snowmelt volume for laboratory analysis. To correct this, a “4 inch” rain gauge was used in the second season instead of the small plastic tube [Figure 3-9]. In addition, a second core was collected at each site. This sample was a “composite” core where 2-3 individual cores were collected and combined together in the same storage bag. To collect the composite, the first core was taken, measured and added to the sample bag using the standard procedure. This process was repeated for 1-2 additional cores, until a total of 20-30 cm of combined core length was collected.

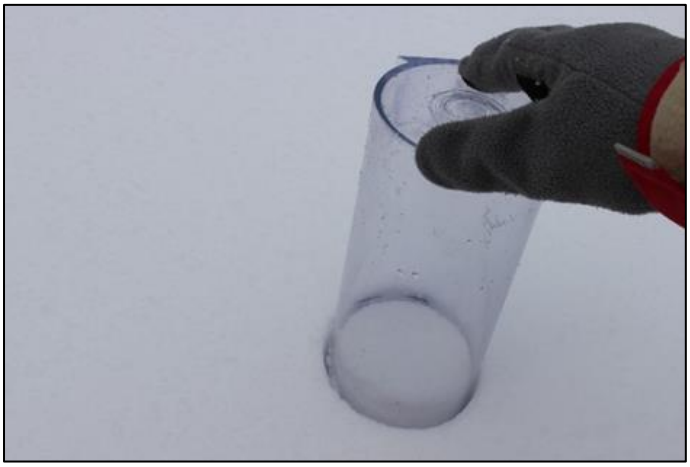

Figure 3-9: Core collection in the second season

Core samples were stored in food grade plastic bags (Doherty et al., 2014). A number of first season samples leaked before analysis. To prevent this in the second season, quart size glass canning jars were considered as a cost effective, high quality and leak proof alternative. However, practically in the field and limited freezer space in the lab reduced their functionality. Doherty et al. (2014) note that there is no measurable difference in particulates stored in plastic bags or glass jars. Therefore, samples were again stored in plastic bags. To combat leakage, bags were upgraded to gallon size, freezer grade plastic bags with a zipper closure

(instead of snap-close). This type of bag was tested for leaks before use. In the field, filled bags were stored upright and transferred to the laboratory freezer as soon as possible.

Laboratory Analysis

Four laboratory methods were selected to examine the concentration of particulate matter. These include: Particulate Mass by Weight, Light Absorption Heating Method, Spectroradiometer Filter Analysis and Light Meter Filter Analysis. While these methods are all described briefly in the literature, the Single Particle Soot Photometer (SP2) method is the generally accepted method to measure black carbon in snow and rain. The SP2 employs a nebulizer to aerosolize the snow, which is then sent to the SP2 for analysis. The quantity of black carbon is measured by quantifying the mass of each individual particle that passes through the SP2 (Wendl et al., 2014). The SP2 is an expensive piece of laboratory equipment and no access was found throughout Syracuse or the immediate surrounding area. In late winter 2018, one lab was identified that provided analysis, however, most samples were already processed using alternative methods.

To prepare for analysis, snow and rain samples were removed from the freezer and allowed to melt for one hour [Figure 3-10]. Sample baggies were partially immersed in tepid water to speed up melting. The bag opening remained outside the water bath to prevent sample loss. Once melted, samples were analyzed as soon as possible to prevent algal growth (Doherty et al., 2010).

Figure 3-10: Frozen snow samples before melting in the lab

Initially, samples were analyzed using the Particulate Mass by Weight method. This method utilizes a precision balance to determine the weight of particulates in a sample. While filtering almost always accompanies particulate analysis in the literature, weighing does not (Doherty et al., 2010; Doherty et al., 2014; Hewen Niu et al., 2017b). Only two studies, performed by Kuchiki et al. (2015) and Moran and Morgan (1973), detail this method. Particulate Mass by Weight measures total particulate concentration, instead of individual species (Bond et al. 2013). Since this study examines particulates in general, not specific types, this was an appropriate method to test.

To execute Particulate Mass by Weight, the filter was weighed using a precision balance. Immediately after the sample was filtered it was dried for 60 hours then weighed again. The initial filter weight was subtracted from the final filter weight to determine the total particulate concentration. Samples for all analyses were filtered using a 47 mm, 0.2 µm nylon filter. Doherty et al. (2010) suggest using a 0.4 µm filter, however, they note that this size yields a 12-15% particulate undercatch. The smaller filter pore size was used in this study to prevent

particulate loss. Filtration followed a standard procedure. Each sample was mixed thoroughly to reincorporate any particulates stuck to the side of the bag. Water was poured into a 250 ml graduated cylinder. If a sample measured less than 20 ml, a 25 ml graduated cylinder was substituted. A funnel and tea strainer were used to remove large debris and dead insects from the sample and the volume was recorded the nearest ml. The sample container, graduated cylinder, funnel and strainer were rinsed with DI water in order to remove any remaining particulates. The sample was poured into the filtration apparatus and the pump was engaged. Filtration times varied substantially, ranging from 30 seconds to 3 hours.

Once completed, the filter was removed using forceps and placed on weigh paper. The filter was covered with a glass beaker to prevent dust contamination and allowed to air dry for a minimum of 60 hours. A small subset of samples were dried in the oven at 105 °C for 24 hours. Results were compared to the air-dried samples and no difference was found. Dried filters were stored in the lab with the glass beaker cover for future analysis [Figure 3-11].

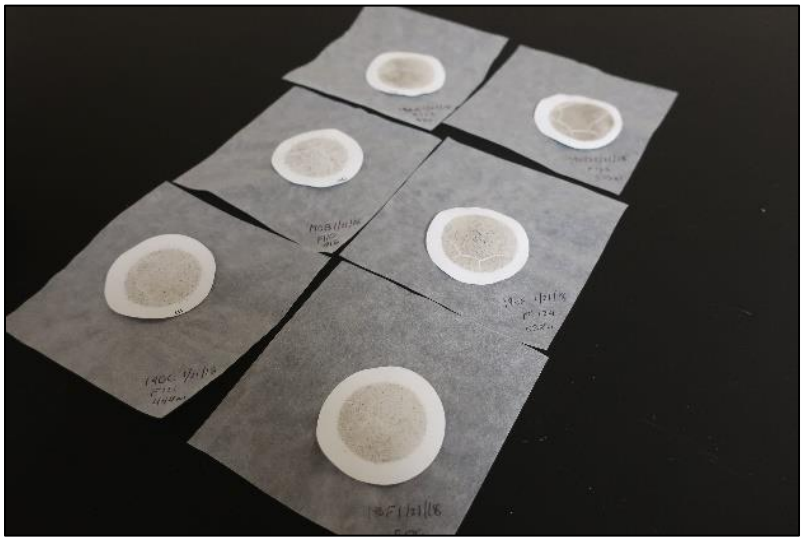

Figure 3-11: Dried filters showing particulate matter from the transect sites

While the Particulate Mass by Weight method seemed to be an easy solution to determine concentration, the method was not successful at quantifying particulates. The laboratory balance was unable to find a weight difference between the pre and post filtration measurements and was unable to self-calibrate to correct this. It is likely that the ongoing construction may have unsteadied the balance or that the amount of filtrate was too small to properly register.

The Light Absorption Heating Method (LAHM) was developed by Schmitt et al. (2014), as a cost effective technique to encourage further particulate research. The experiment takes advantage of the light absorbing properties of particulate matter. To execute this method, a filter is illuminated by a light source for a period of 30 seconds and the resultant temperature change measured. Kahn et al. (2017) tested the LAHM against the SP2 and found that there is ±40% uncertainty in the results. That said, much of this uncertainty can be attributed to particulate size limitations of the SP2 (<2 μm).

To test this technique in the lab, a large cardboard box was spray painted black in order to limit reflection. A filter was placed on small glass beaker approximately 10 cm from the bottom of the box. A full spectrum light was placed at a 45° angle to the filter and a small container of water was placed below the filter to absorb any extraneous radiation. An infrared thermometer was placed on the top of the box directly above the filter. The filter was illuminated for 120 seconds and the temperature of the filter was recorded manually at 10 second intervals [Figure 3-12]. Unfortunately, the LAHM technique did not show a substantial difference in heating times between experimental and blank filters.

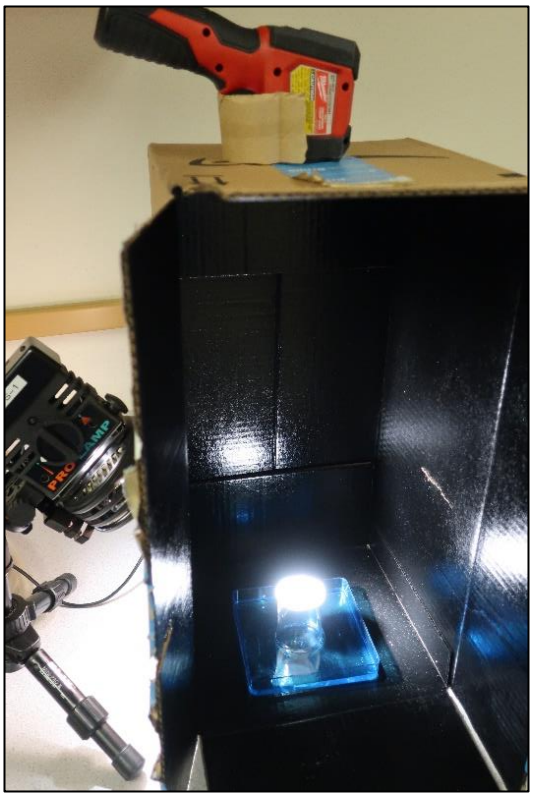

Figure 3-12: The LAHM laboratory analysis apparatus

Spectroradimetry of particulates looks to be a promising method for future identification. A few authors explore the use of a hand-held field spectrometer to identify spectral reflectance. Kahn et al. (2017), includes this method in the comparison of the SP2 and LAHM. They note a substantial decrease in reflectance across all wavelengths as the concentration of black carbon increases (as identified by the SP2). Before analysis, the spectrometer was calibrated using a white disk. The filter was placed on a cream-colored background to reduce interference from the table. A full spectrum bulb was used to illuminate the filter while the spectrometer sent continuous readings to an attached computer. The spectra for each filter were saved, however, little difference was observed between the spectra at the time of analysis [Figure 3-13].

Figure 3-13: Laboratory analysis using the Spectrometer

The final laboratory method tested was the Light Meter Filter Analysis. This method, while developed specifically for this study, was based on a similar method described by Du et al. (2011). Originally a digital camera, was set to take a photograph of a particulate-laden filter. A full spectrum light was used to illuminate the filter from behind. Du et al. (2011) use a complicated computer algorithm to determine the amount of light that passes through the filter and reaches the camera sensor as it snaps a photo. In order to avoid damage to the digital camera, this study substituted the PCE-SPM 1 solar radiation meter to determine the amount of light radiation that passes through the filter.

The experiment was set up in a similar way to the LAHM. The filter was placed on a small cardboard stand with a 25 mm opening under the filter to let light pass through. A full spectrum lamp was placed above the filter and the radiation meter was placed directly below. When the lamp was turned on, the radiation that passes through the filter to reach the radiation meter was recorded in W/m^2 [Figure 3-14].

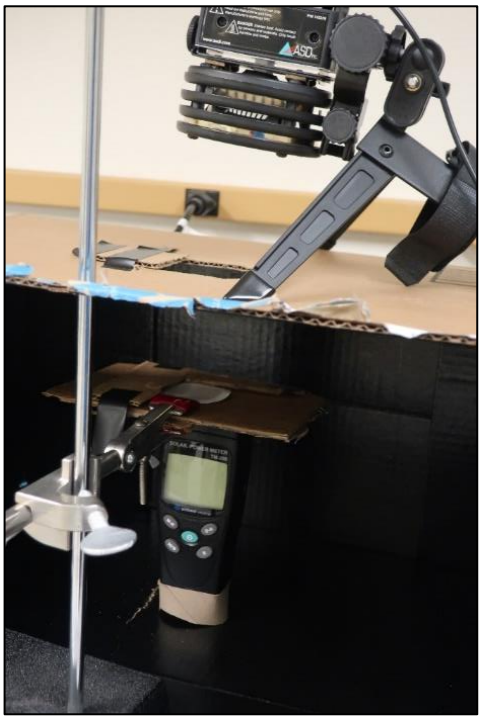

Figure 3-14: The Light Meter Filter Analysis

To test the consistency of the Light Meter Filter Analysis, one sample set (1/7) was tested multiple times at various brightness settings. A Pearson Correlation was calculated to identify the relationship between the 50% brightness and 100% brightness iterations. An r value of 0.996 and p value of <0.00001 (n=9) was calculated, suggesting an almost perfect correlation between brightness levels [Figure 3-15]. The Light Meter Filter Analysis was selected as the most consistent laboratory technique and was used for the bulk of the analyses reported in the next chapter.

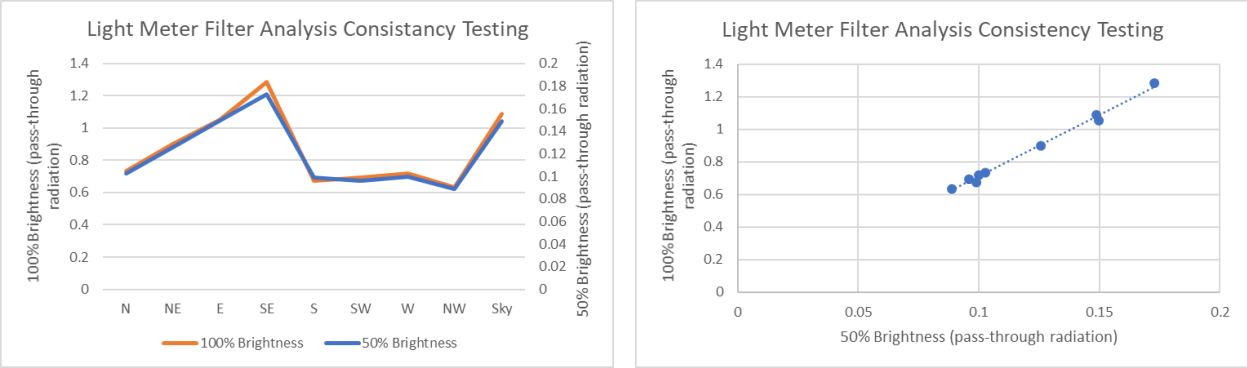

Figure 3-15: Left: Two iterations of consistency testing at 50% brightness (blue) and 100% brightness (orange); Right: Correlation observed between 50% testing and 100% brightness

Chapter 4 – Results and Discussion

Notable Storms

In order to understand the distribution of particulates, it is important to explore snow conditions over the course of this study. Snow accumulation totaled 342.6 cm in the first season and 390.1 cm in the second. Compared to historical data, the total accumulations for both seasons is within one standard deviation of the 1981 to 2010 average seasonal snowfall normal (321 cm) for Syracuse Hancock Airport. While they do not approach the station record low of 150.9 cm (2001-2002) nor the high of 487.9 cm (1992-1993), the two seasons show remarkable differences in the timing of snowfall and melting of the snowpack (MRCC, 2018).

The first season experienced the bulk of its accumulation in early and late season. Figure 4-1 shows the daily snow accumulations measured at Syracuse Hancock Airport. It is difficult to objectively classify high intensity snow events. Call (2004) suggests a severe storm must accumulate a minimum of 7.6 cm each day, amounting to a storm total accumulation of at least 35.6 cm. Using this definition, the first winter experienced only two severe storms. The first took place from November 19-21. Over 60 cm of snow fell on the city, distinguishing November 21st, 2016 as the second snowiest November day on record (O'Toole, 2016). The second storm, from March 14-15, again left Syracuse buried under 60 cm. Combined, these two storms accounted for almost 40% of the first season snowfall.

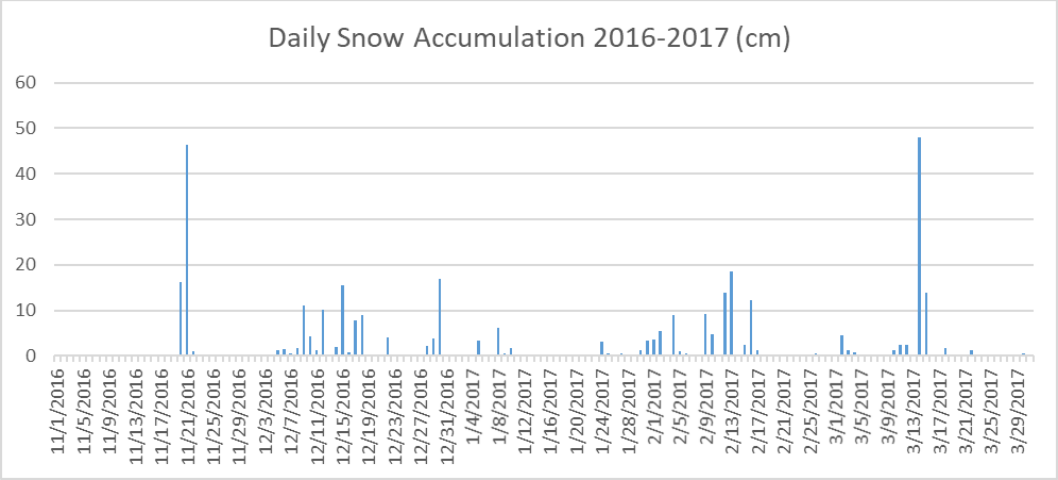

Figure 4-1: Depth of the snowpack at Syracuse Hancock Airport from 11/1/16 to 3/31/17 (MRCC, 2018)

Mid-season was marked by only two periods of sustained snow – mid to late December and early February. Mid-January and early March experienced unseasonably warm weather. Mean temperatures reached a high of 13.6 °C on March 1st, over 15 °C above normal [Figure 4-2]. The warm temperatures substantially reduced the chance for winter precipitation and delayed sample collection until mid-February. The first snow event was sampled from a smaller storm lasting from February 9-13. After an additional month of warm temperatures, a second event was sampled – the severe March 14-15 storm.

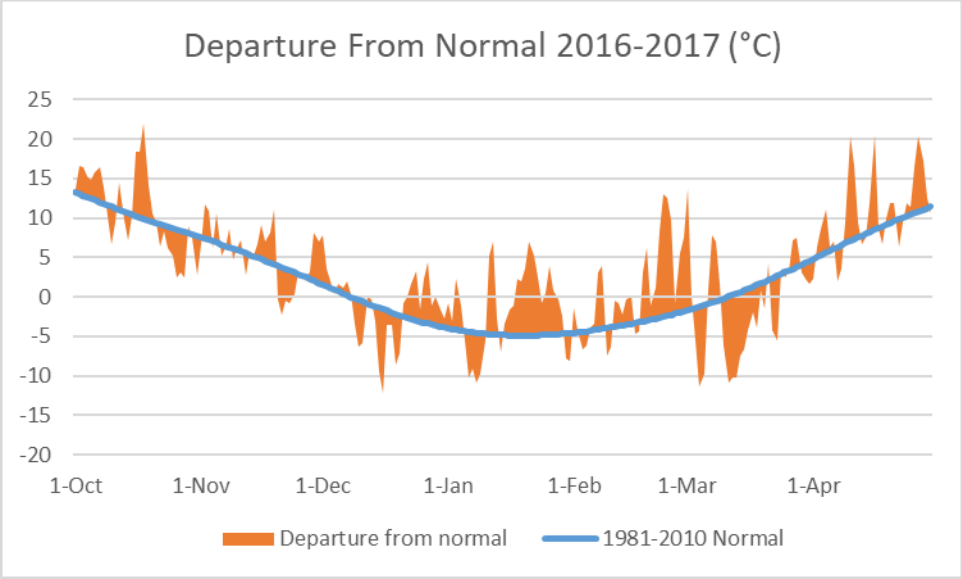

Figure 4-2: Departure from the mean daily normal temperature recorded at Syracuse Hancock Airport from 10/1/16 to 4/30/17 (MRCC, 2018)

The disappointing first season was offset by a long period of below average temperatures and abundant snow in the second season [Figure 4-3]. Four severe storms (≥35.6 cm) were observed as well as numerous smaller events. The first substantial accumulation was recorded about a month later than the first season. This storm lasted from December 12-13 and left only just enough snow (35.6 cm) to qualify as severe. A second major event was observed from January 4-6. In this event, 49 cm of snow accumulated. A number of smaller events continued through mid-January until a winter thaw melted the entire snowpack. A small number of snow-free days were observed at the end of the month. Beginning January 30th, 12 days of accumulating snow brought an additional 67 cm to Syracuse. The end of February and early March was unseasonably warm, but, this was offset by unseasonably cold temperatures through the end of April. Two additional severe storms brought 42 cm on March 2nd and 38 cm

on March 13-14. These storms were part of a series of four Nor'easters to impact the east coast in March (Coin, 2018).

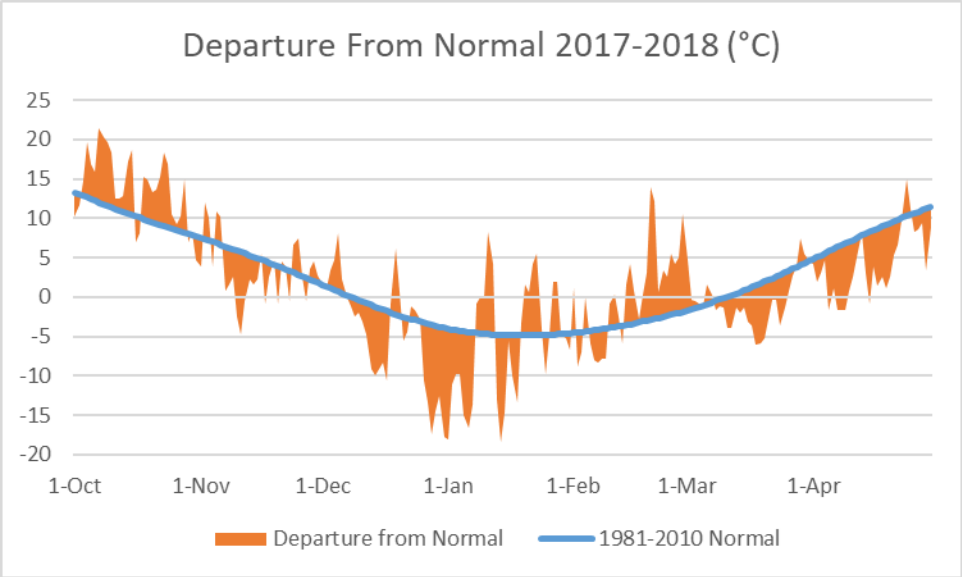

Figure 4-3: Departure from the mean daily normal temperature recorded at Syracuse Hancock Airport from 10/1/17 to 4/30/18 (MRCC, 2018)

Total accumulation in the second season was near 50 cm above the first season. Both seasons experienced substantial differences in snowpack stability. Only 75 days with at least 2.5 cm were observed from 11/1/16 to 3/31/17. Ninety-two days were observed from 1/1/17 to 3/31/18. More importantly, only 26 days were observed with 15 cm snowpack compared to 60 days respectively [Figure 4-4]. This impacted the number of available sampling days significantly.

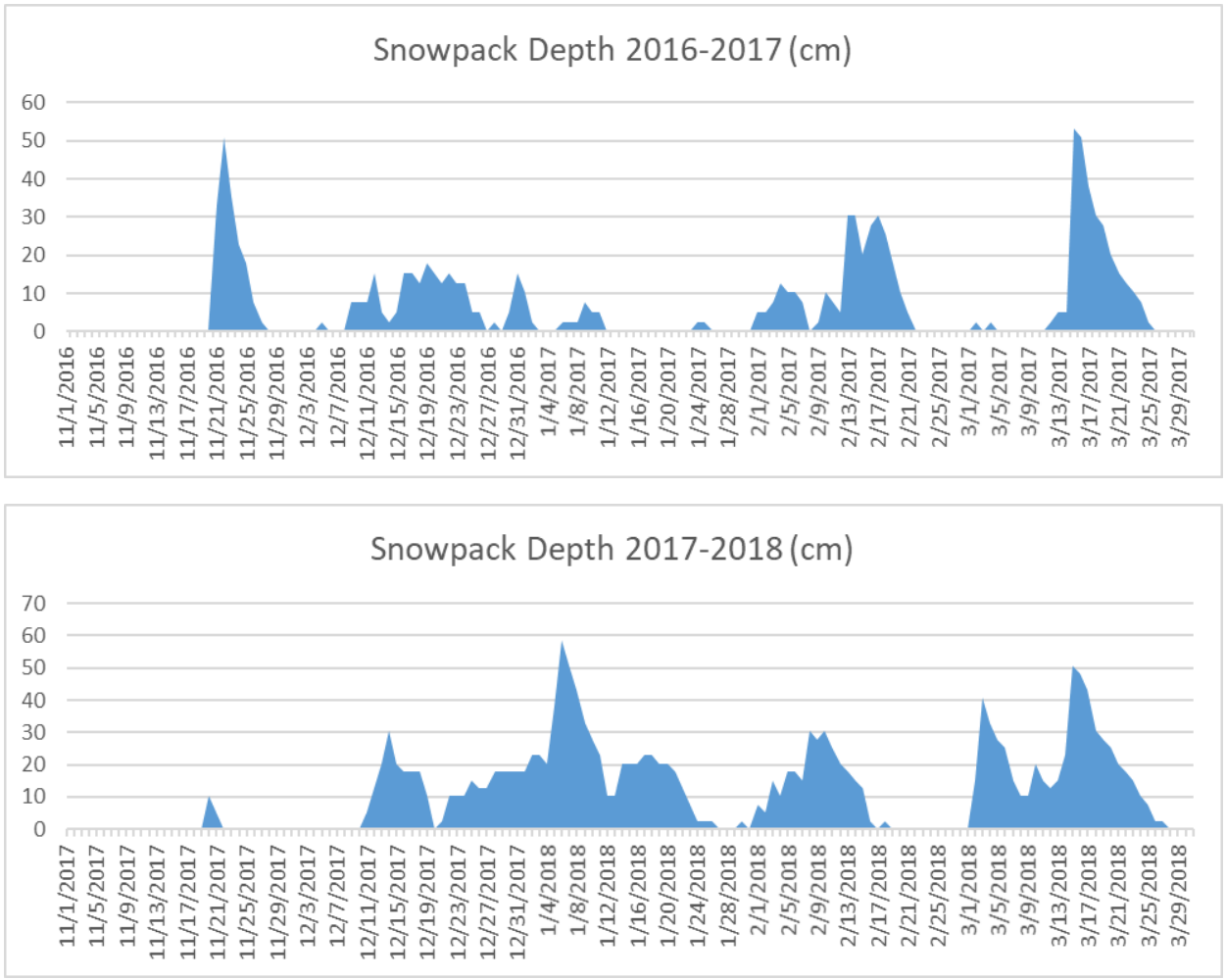

Figure 4-4: Total daily snowpack observed in the first season (top) and second season (bottom) (MRCC, 2018)

The Directional Study

The directional study explores the spatial distribution of particulate matter around Syracuse. This experiment was designed to determine the concentration both upwind and downwind of the urban core in order to see how the city changes particulate distribution. Most samples were collected within 24 hours of a snow event and used to determine the spatial distribution of particulates that fall as wet deposition. When possible, a second sample was collected four to seven days later to quantify particles that fell as dry deposition after the

storm. The second set of samples was used to assess the accumulation of particulates over time.

Seven snow events were sampled over two seasons, however, only two events were sampled twice [Table 4-1]. Clear weather is required to accurately assess the dry deposition of particulates. Any additional snow accumulation that falls after the first sample has been collected can alter the results of the second sample. Even a light accumulation of 10 cm can impact the surface albedo (Cereceda-Balic et al., 2018). Five storm events experienced additional accumulation within three days of the first sample. As a result, no second sample was collected for these events.

Sample date	**Snow event dates (dry deposition dates)**	**Snow depth (cm)**	**Type of distribution assessment**	**Samples collected**	**Notes**
2/18/17	2/12/17-2/17/17	25.4	Spatial	8*	Measurements were suspect as a result of abnormal albedo values
3/15/17	3/14/17-3/15/17	53.3	Spatial	8	
3/22/17	3/14/17-3/15/17 (3/15/17-3/22/17)	12.7	Temporal	8	
11/21/17	11/19/17-11/20/17	5.1	Spatial	5*	Warm temperatures melted all the snow by the 5th site
12/15/17	12/12/17-12/14/17	20.3	Spatial	9	
1/7/18	1/4/18-1/6/18	50.8	Spatial	9	
2/9/18	2/7/18	27.9	Spatial	9	
2/13/18	2/7/18 (2/8/18-2/13/18)	17.8	Temporal	8	
3/6/18	3/2/18-3/3/18* (3/3/18-3/6/18)	40.36	Temporal*	9	Sample was collected three days after the snow event

Table 4-1: List of all samples that were collected for the directional analysis. An asterisk (*) represents an abnormal sample: see notes column

Wind patterns

The direction of prevailing wind was identified in order to determine the direction of particulate movement across Syracuse [Figure 4-5]. Of the nine sample sets collected, seven experienced a WSW to NW wind. This is consistent with the general circulation pattern observed in Central NY (NCEI, n.d.). This range of wind direction is ideal to generate lake effect snow from Lake Ontario (NW wind) or Lake Erie (WSW wind) (Monmonier, 2012).

2/12/17-2/17/17

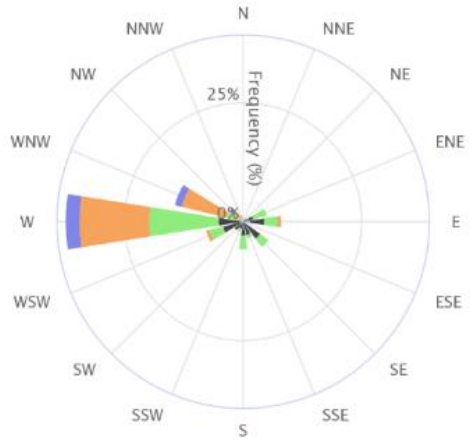

3/14/17-3/15/17

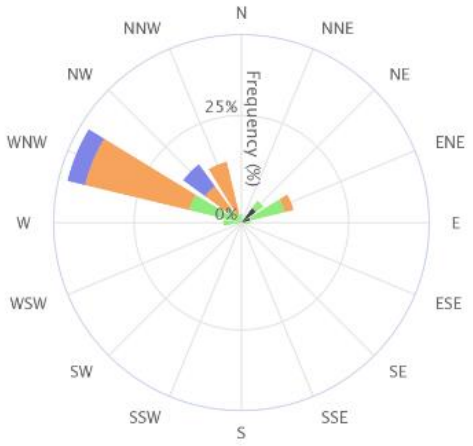

3/15/17-3/22/17*

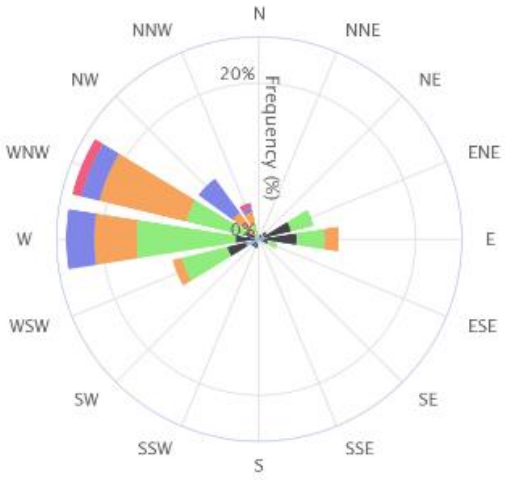

11/19/17-11/20/17

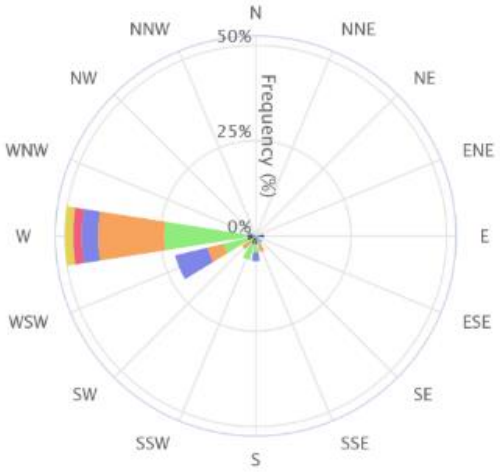

12/12/17-12/14/17

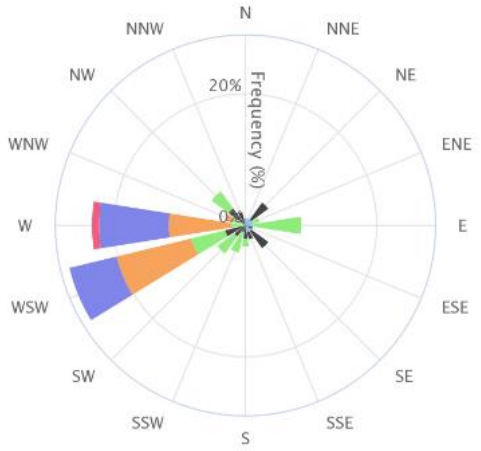

1/4/18-1/6/18

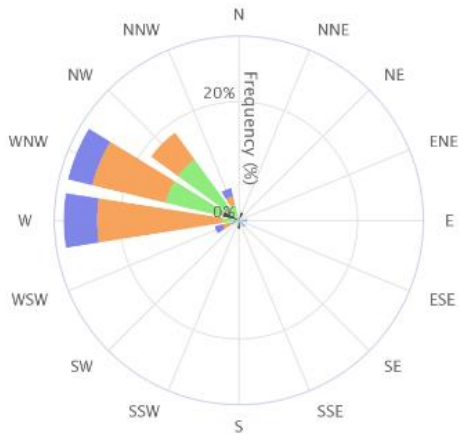

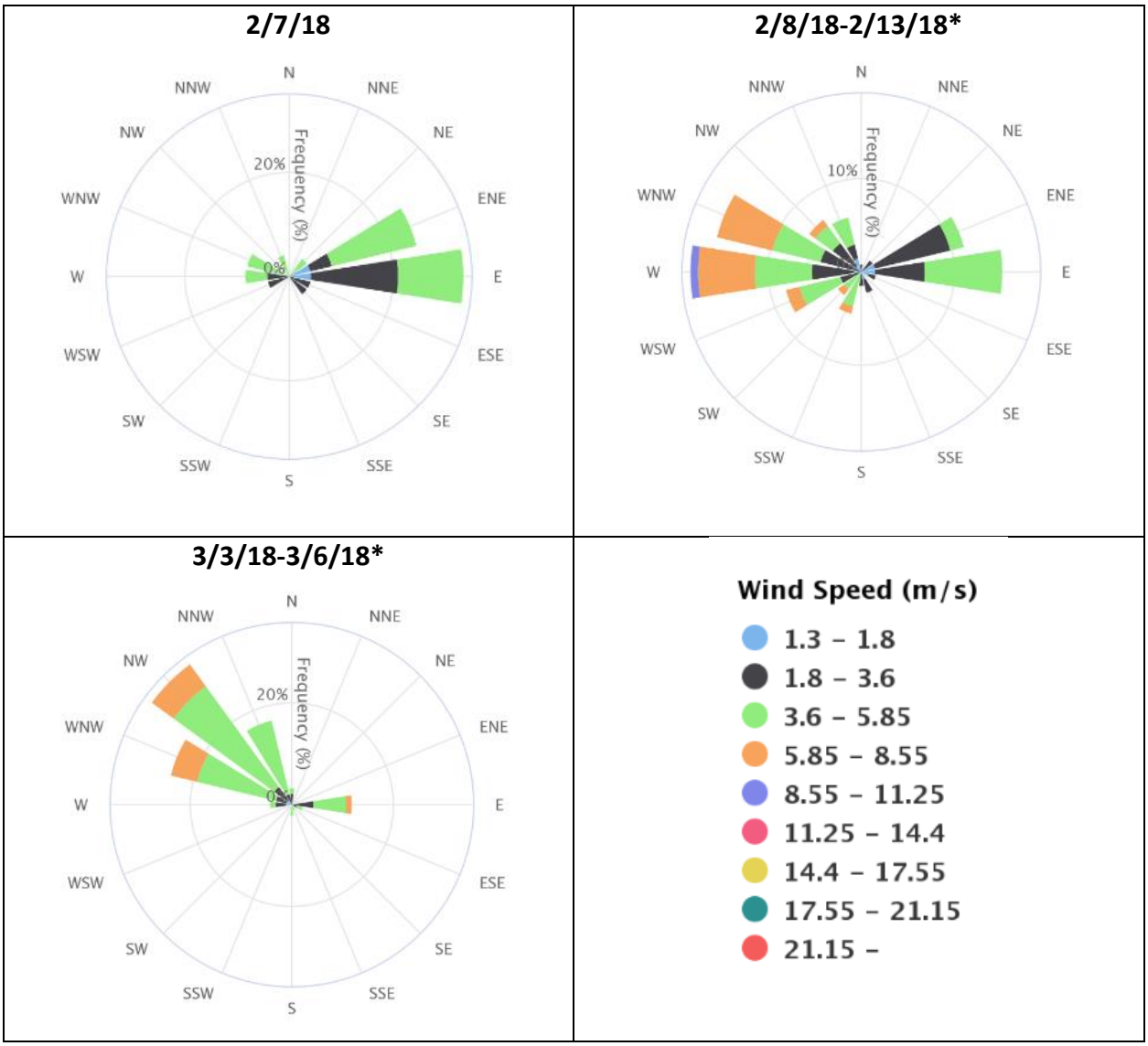

Figure 4-5: Frequency of wind direction (%) and speed (m/s) for each snow event; an asterisk (*) indicates a temporal sample (MRCC, 2018)

The two remaining samples, both associated with the February 7, 2018 snow event, do not match this pattern. This massive east-coast storm accumulated nearly 30 cm of heavy wet snow over the span of 12 hours (Greenlar, 2018). Instead of the typical westerly flow, winds associated with this snow event originated in the east. The National Weather Service (2018) surface analysis map for February 7, 2018 shows that as the coastal storm deepens the cyclonic

flow to the north of its central low pressure draws air from the SE towards Syracuse [Figure 4-6]. This system is responsible for the easterly wind associated with first sample (2/9). The second sample, collected on 2/13 is the only sample to include particulates associated with variable winds.

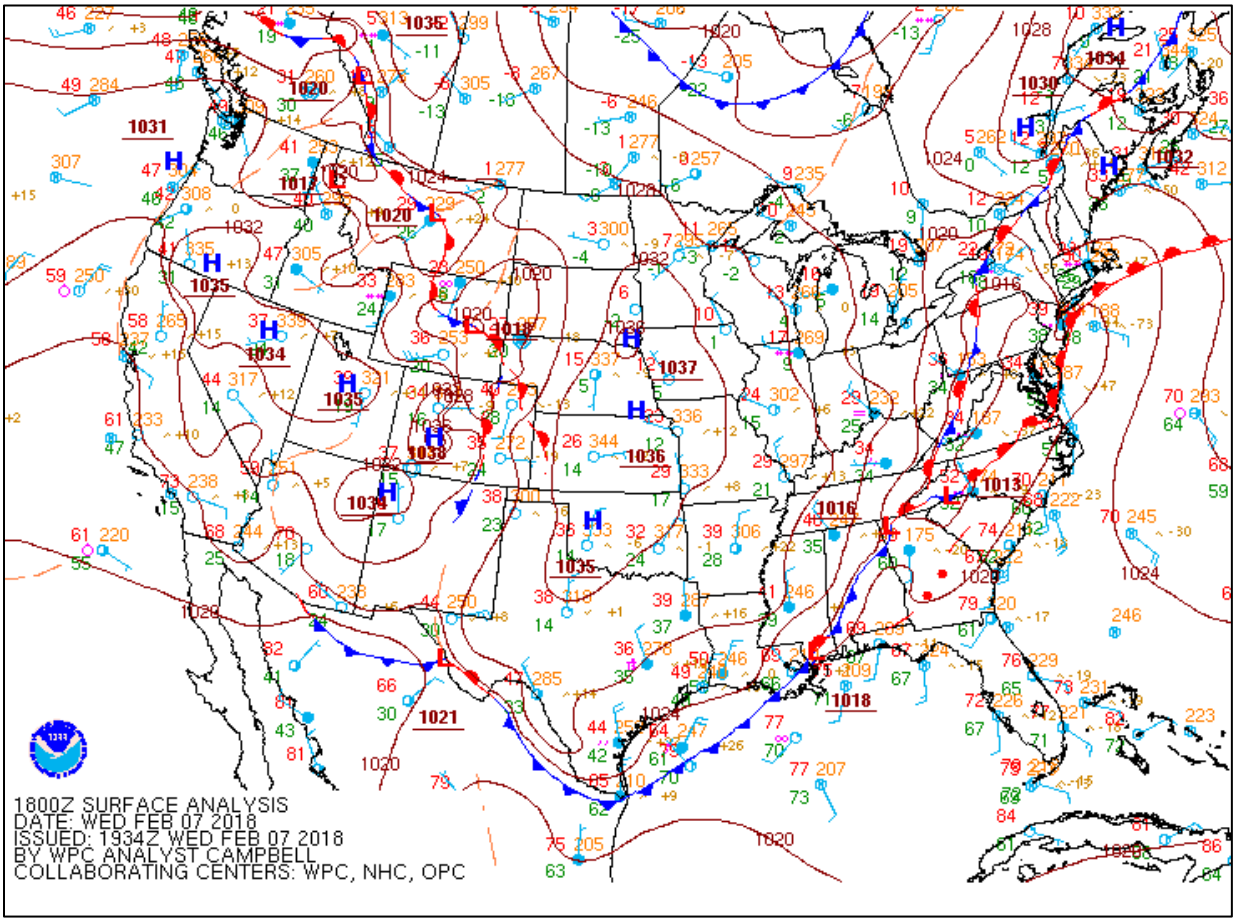

Figure 4-6: Surface analysis map from 14:00 EST, 2/7/18 showing the massive warm, cold and stationary fronts associated with the 2/7/18 snow event (National Weather Service, 2018)

Albedo

Particulate matter significantly influences the albedo of the snow. This is especially true of black carbon, however, all forms of particulates have some effect. Snow absorbs little to no radiation in the ultraviolet or visible spectrum. The addition of particulates to the snowpack

increases this absorption significantly (Dang et al., 2017). The shift supports the use of albedo measurements as a proxy for particulate concentration. In a controlled setting, a direct relationship can be measured – an increase in particulates yields a decrease in albedo. However, uncontrollable factors in the field, including snow grain size, snow temperature, snow depth, snow age and SWE make it difficult to determine the percentage of albedo reduction that is a direct result of particulate pollution (Gray & Male, 1981).

Albedo for each site was calculated by measuring incoming and reflected radiation. The equation:

$$A_s = Q_r/Q_{si}, \quad (1)$$

where A_s is the surface albedo, Q_r is the amount of reflected solar radiation and Q_{si} is the amount of incoming (incident) solar radiation, was used to calculate the ratio of reflected radiation to the total incoming radiation that reaches the snow surface (Gray and Male, 1981). Values varied substantially across the dataset – ranging from 0.58 (N site, 3/22, old snow) to 0.97 (E site, 1/7, fresh snow). Within each sample set, the albedo varied by up to 0.23. The largest range was observed at the E site (0.71 on 2/13 to 0.97 on 1/7); the smallest at the NE site, about 6.5km away (0.71 on 3/22 to 0.81 on 1/7). Figure 4-7 shows the albedo measurements on 1/7 and 3/6 as well as the average albedo recorded for all sites. Only four sample sets include an albedo measurement for Skytop, therefore, the average was not comparable to the other sites and it was removed from analysis. The graphs for 1/7 and 3/6 show that the highest albedo values were usually recorded at sites to the south and east of the

city (E, SE, S and SW sites) and the lowest values were recorded to the north and west (W, NW, N and NE sites). This distribution was observed in most sample sets. Albedo measurements for all samples can be found in Appendix B.

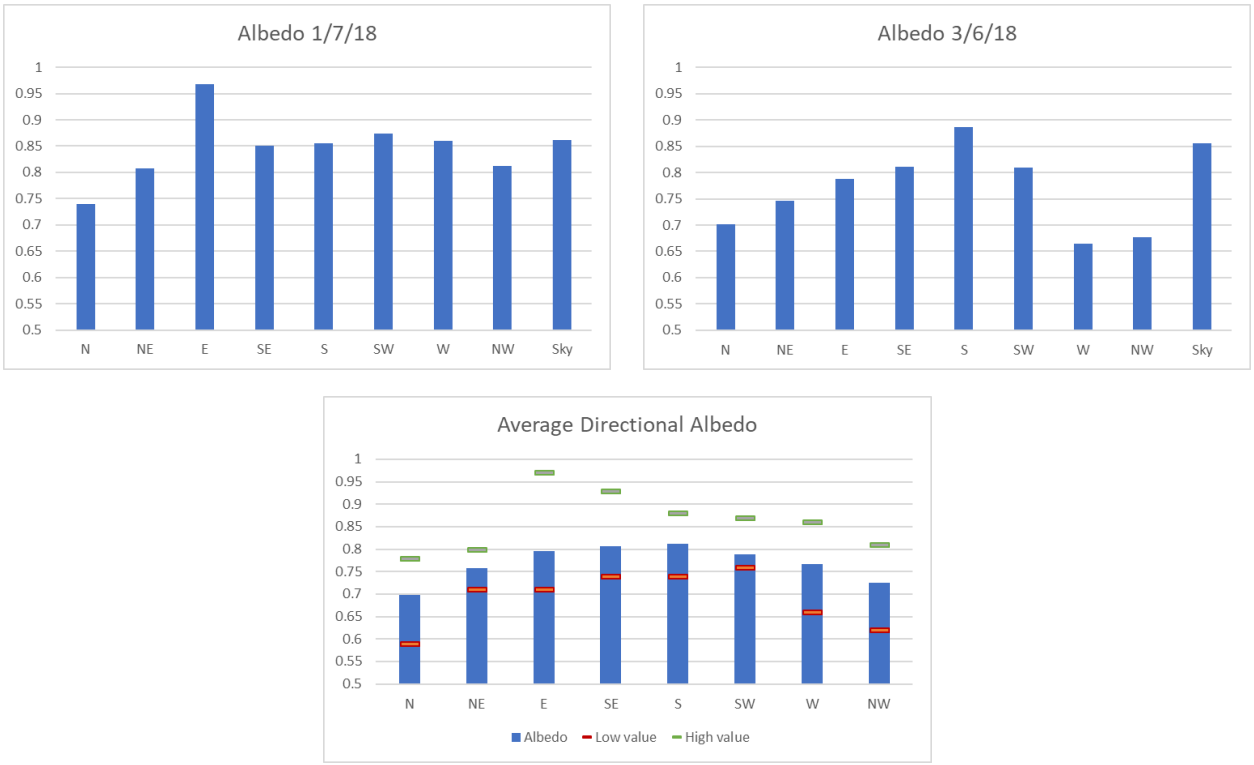

Figure 4-7: Top left: Albedo values measured on 1/7; Top right: Albedo values measured on 3/6; Bottom: Average (blue), highest (green) and lowest (red) albedo values recorded at each directional site

The 2/7/18 storm event is a notable exception to the typical distribution [Figure 4-8]. Here, samples collected immediately after the storm, show little to no variation in albedo. The temporal sample (2/13), however, shows a unique pattern. It is substantially different from both the 2/9 sample and the average albedo that was observed in both seasons. In this case, the highest albedo was recorded at the W site, the lowest at the E site. It is likely that dry deposition decreased the albedo of the N, SE and S sites. However, it is worth noting that the

albedo of the SW and W sites actually increases from 2/9 to 2/13. This effect is unlikely. As snow ages albedo decreases (Gray and Male, 1981). Even without any dry deposition of particulates, albedo should have decreased between the two samples. This discrepancy is likely a result of sampling error. In contrast to other sample sets, the 2/9 samples were collected under overcast skies and late in the afternoon. Typically, measurements collected late in the day demonstrate reduced light conditions and increased spectral reflection as a result of a low observed sun angle (Dirmhirn & Eaton, 1975). In this case, extensive cloud cover obscured the sun, eliminating the reflection effect. That said, reduced light conditions were observed at the sample sites. Two samples, N and NE, were excluded as a result. It is likely that low light simply did not provide enough incoming radiation to accurately assess albedo.

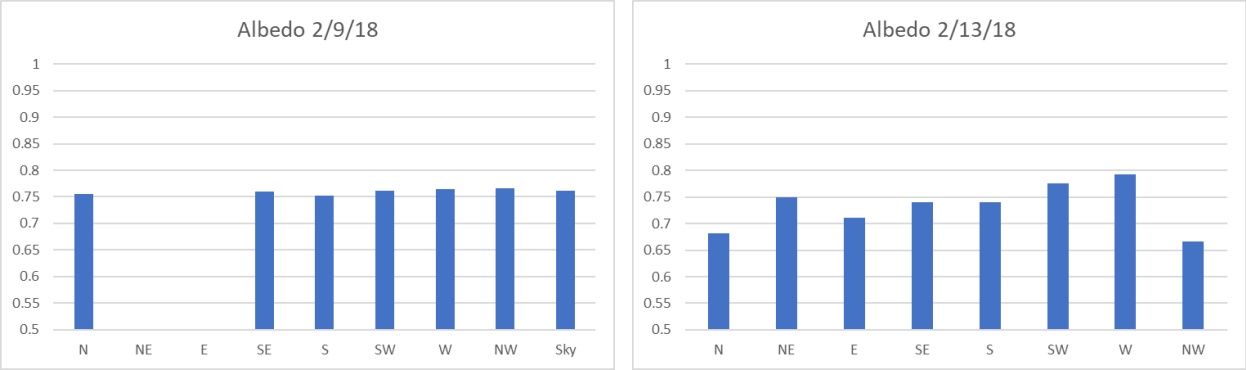

Figure 4-8: Albedo values measured after the 2/7/18 snow event: 2/9 (left) and 2/13; the 2/9 albedo for the NE and E sites excluded as a result of an extremely low sun angle

A number of other factors also affect albedo and may have influenced the observed results. These include, sun angle, snow type, snow age, snow grain size, SWE, snow depth and snow temperature (Adolph et al., 2016; Dirmhirn & Eaton, 1975; Gray and Male, 1981). Two variables were selected for measurement in the field – snow depth and snow temperature. The

remainder were not measured due to time constraints, however, they are likely responsible for a non-negligible amount of the variation between sample sites.

The effect of snow depth on albedo is studied extensively in the literature. According to Kung et al. (1964), a snow depth less than 12 cm will allow radiation to penetrate to the ground surface and reduce the albedo of the snowpack (as cited in Gray and Male, 1981). Bergen (1975) and Schlatter (1972), however, found that radiation can reach the ground surface at depths greater than 12 cm (as cited in Wiscombe & Warren, 1980). They cite 30 cm and 50 cm, respectively, as the required depth to mask this effect. Wiscombe and Warren (1980) note that snow density and grain size can alter the masking depth – a likely explanation for the wide range of minimum depths reported in the literature. Snow depth at the directional sites ranged from 3 cm to 59 cm. A Pearson Correlation was performed to determine the effect of snow depth on albedo [Figure 4-9]. An r value of 0.160 (n=48) and p value of 0.277 were calculated (the incomplete sample set collected on 2/9 was excluded from analysis). While the albedo increases slightly with snow depth, the p value indicates that this correlation is not statistically significant.

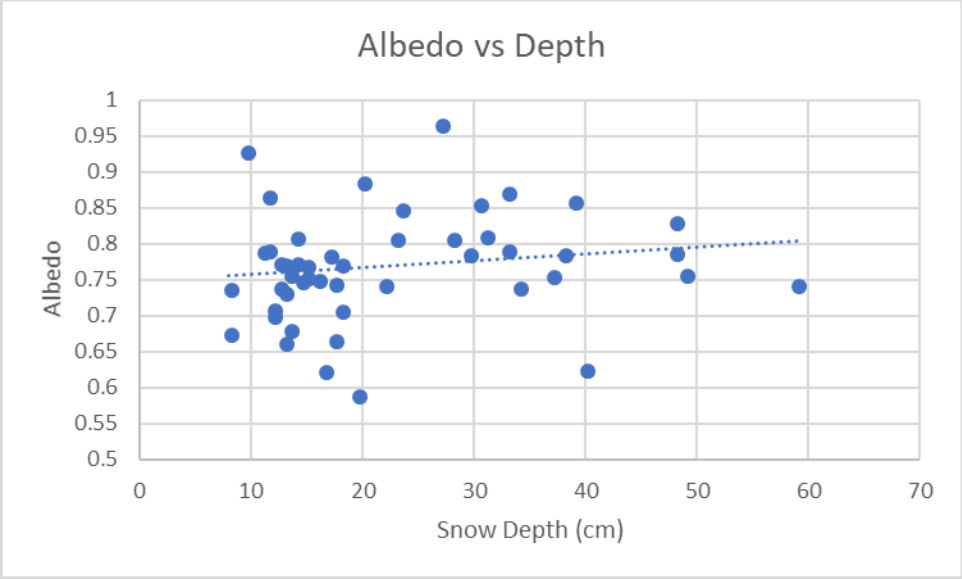

Figure 4-9: Correlation between albedo and snow depth at the directional sites

The 50 cm minimum depth noted by Schlatter (1972) suggests that albedo should not be affected by snow depth if the snowpack is deeper than 50 cm. A second Pearson Correlation was performed to determine if the directional samples that were collected from a deep snowpack reduced the r value of the first correlation. For this test, only samples collected from a snowpack <50 cm deep were selected for analysis – one sample was excluded (3/15, W site, 59 cm snow depth). The r value increased to 0.202 (n=47) and the p value decreased to 0.173, however, the correlation was not significant [Figure 4-10]. A third Pearson Correlation was performed to test the 30 cm limit suggested by Bergen (1975) (as cited in Wiscombe & Warren, 1980). In this case, the r value increased to 0.252 (n=35) and the p value decreased to 0.144. Once again the correlation was not significant [Figure 4-11].

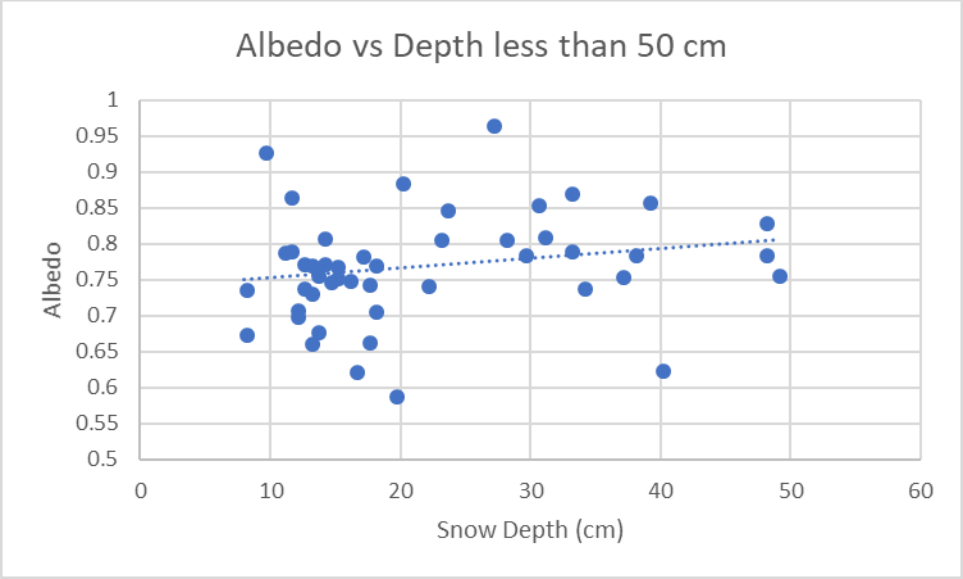

Figure 4-10: Correlation between albedo and snow depth for sample sites with a depth <50 cm

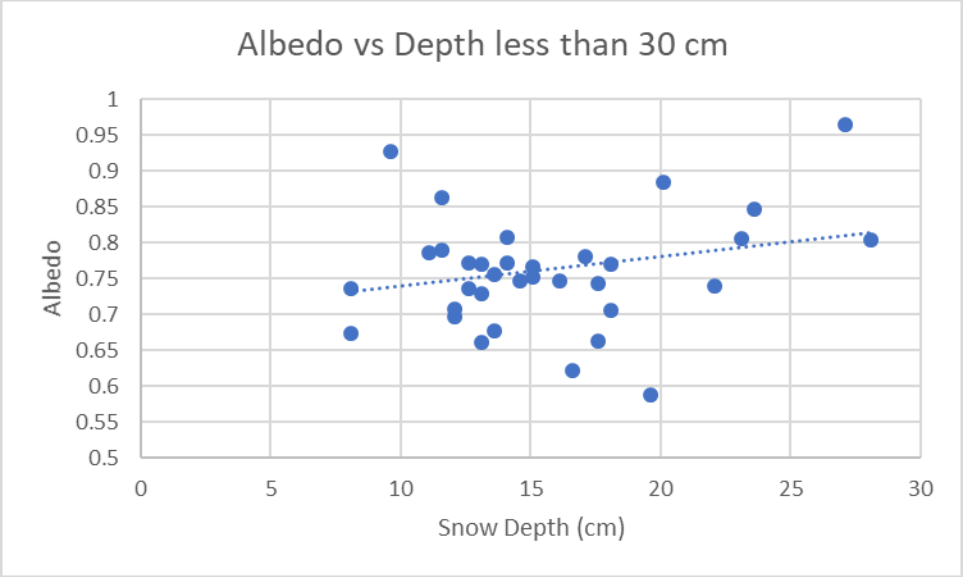

Figure 4-11: Correlation between albedo and snow depth for sample sites with a depth <30 cm

Snow temperature also affects albedo, albeit, indirectly. Individual snow grains increase in size as the snowpack ages (Jacobi et al., 2015). This process occurs naturally, but, can be accelerated by a high snow surface temperature. Large snow grains have a lower albedo, and

increase the amount of incoming radiation absorbed by the snow, therefore, as temperatures rise, albedo decreases (Bohren & Barkstrom, 1974 as cited in Gray & Male, 1981). A Pearson Correlation was run to identify the relationship between snow temperature and albedo at the directional sites [Figure 4-12]. An r value of -0.095 (n=32) and a p value of 0.605 were calculated. Similar to snow depth, this correlation was not statistically significant.

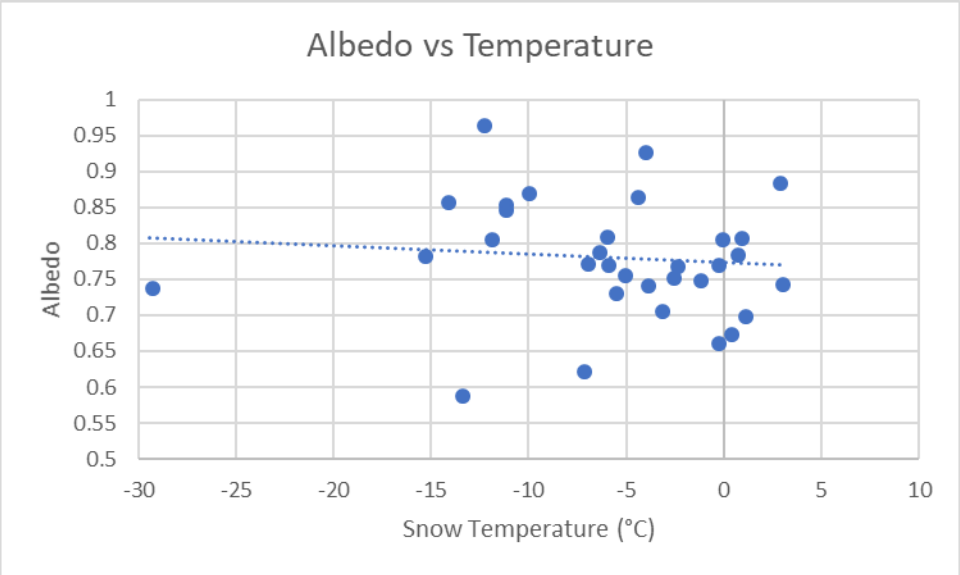

Figure 4-12: Correlation between albedo and snow temperature

The snow temperature recorded at the N site on 1/7, was exceedingly low (-29.4 ˚C). To determine how this data point influenced the correlation, the mean (-6.13 ˚C) and standard deviation (6.74 ˚C) were calculated for the snow temperature data. Thirty-one temperature measurements were found to be within 2 standard deviations of the mean. The 1/7 N measurement was the only data point outside of this range (3-4 standard deviations below the mean) [Figure 4-13]. The Pearson Correlation was re-run with this sample removed. For this test, the r value decreased to -0.198 (n=31) and the p value decreased to 0.306, once again, the correlation was not statistically significant [Figure 4-14].

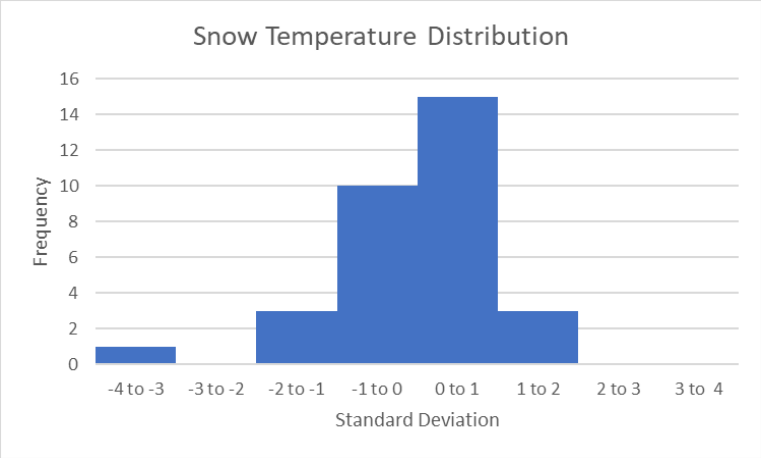

Figure 4-13: Frequency distribution of snow temperature measurements showing deviation from the mean

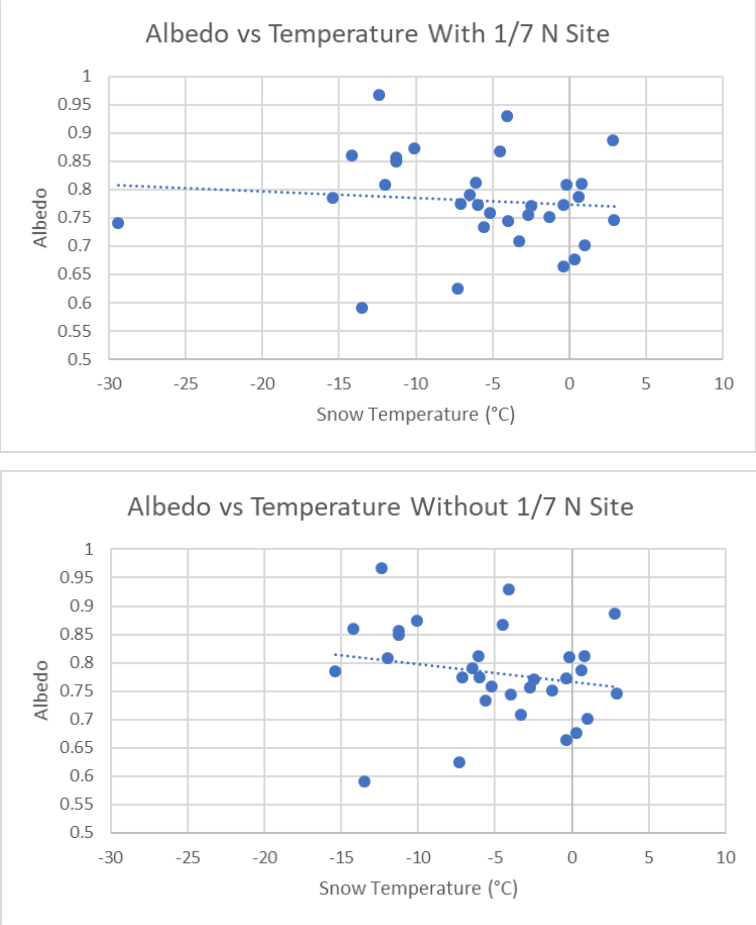

Figure 4-14: Correlation between albedo and snow temperature before (top) and after (bottom) the 1/7 N site was removed

It is surprising that all six correlations failed to show significance. The albedo/snow depth and albedo/snow temperature relationships are well tested throughout the literature (Grey & Male, 1981; Wiscombe & Warren, 1980). It is possible that non-standard sampling conditions affected the result. A stand-alone experiment examining snow depth, temperature and albedo at an isolated site may be able identify a significant relationship between albedo and snow depth or albedo and temperature.

Particulate concentration

Direct measurement of particulate concentration proved challenging. A number of first season samples were analyzed in summer 2017. Results revealed that sample volume was not large enough to accurately determine concentration. While this could be a result of exceptionally clean snow, it is unlikely. Schmitt et al. (2015) suggest a sample volume of 600 ml for accurate analysis. Most first season samples only measured 20-30 ml when fully melted. Larger samples were collected in the second season. This modification meant that first and second season samples were not comparable. Therefore, only the second season samples were analyzed for the final results.

Directional samples from four snow events (five sets of samples) were analyzed using the Light Meter Filter Analysis [Table 4-2]. Instead of direct particulate concentration, the equation:

$$P_{inv} = 10\text{-}P_{pass}, \quad (2)$$

where, P_{inv} is the inverse of the amount of light passing through the particulate filter and P_{pass} is the amount of light passing through the filter, was used to calculate the relative particulate concentration of each sample. Taking the inverse makes the Light Meter Filter Analysis output more intuitive. Low readings represent a higher quantity of light that passing through the filter to reach the radiation meter. This is indicative of low levels of particulate concentration. High readings represent the opposite – less light reaches the meter because it is absorbed by the high particulate concentration on the filter. Results were standardized to allow comparison between samples.

Sample date	**Deposition period**	**Type of deposition**	**Number of samples analyzed**
12/15/17	12/12/17-12/14/17	Wet	9
1/7/18	1/4/18-1/6/18	Wet	9
2/9/18	2/7/18	Wet	9
2/13/18	2/7/18-2/13/18	Wet and Dry	8
3/6/18	3/2/18-3/6/18	Wet and Dry	9

Table 4-2: List of sample sets analyzed to determine particulate concentration at the directional sites

Observed results varied substantially. A high concentration of 9.75 (W/m^2)/ml and a low of 8.49 (W/m^2)/ml was observed within the five sets of directional samples. Average particulate concentration showed a similar trend to albedo – low concentration was observed on the east side, high on the west [Figure 4-15]. An interesting exception, however, was observed at the S site. Here, both the highest albedo and the highest particulate concentration were recorded. As particulates cause a direct decrease in the albedo of a snowpack, this should not happen (Bond et al., 2013). Eight and a half kilometers away at the SE site, the lowest concentration of particulates was observed. This correlates with the high albedo also recorded at the site.

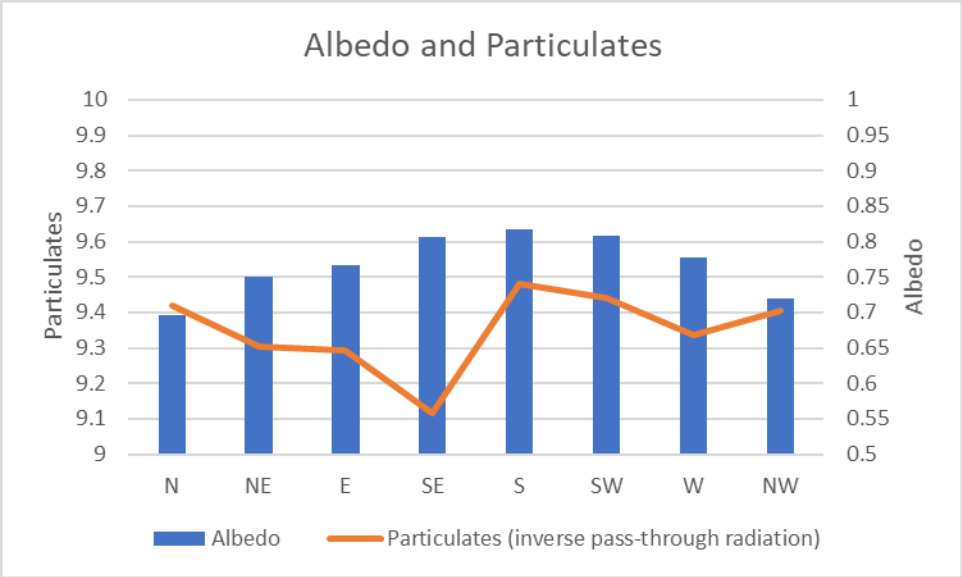

Figure 4-15: The average particulate concentration compared to albedo at each directional site

The location of the S site may partially explain this discrepancy. This site is situated in a small park adjacent to I-81 [Figure 4-16]. Samples were collected from a field approximately 100 m from the edge of the highway. Interstate 81 serves as a source of particulate pollution

(from vehicle exhaust) – the proximity to this highway explains the high particulate concentration but not the high albedo.

Figure 4-16: A 360° view of the S site, I-81 is located behind and right of the picnic pavilion

Further examination of the particulate methodology may help to explain this difference. Albedo and particulate measurements examine two slightly different parameters. The albedo of the snow surface includes particulates that were deposited from the most recent storm (wet deposition) as well as particulates that were deposited on the snow surface after the event ended (dry deposition). Particulates analysis, however, measures the particulate concentration in the entire snowpack, this includes particulates that accumulated from previous snow events. Essentially, particulate concentration includes total snowpack particulates. Albedo measurements only include particulates associated with the last snow event. Noting this difference, the high particulate level at the S site makes more sense. Overtime, the snowpack has accumulated significant particulates from vehicle emissions. When samples were collected, new, clean snow fell on top of the dirty snow, effectively masking any albedo reduction that should have accompanied the high particulate concentration.

Despite similar trends, more noise was observed in particulate results compared to albedo. Samples collected on 2/9, 2/13 and 3/6 show spikes in particulate concentration despite a gradual change in albedo [Figure 4-17]. These may be caused by local variability in

snow conditions, local particulate sources or wind re-distribution of airborne particulates (Bond et al., 2013). A table of all particulate concentrations can be found in Appendix B.

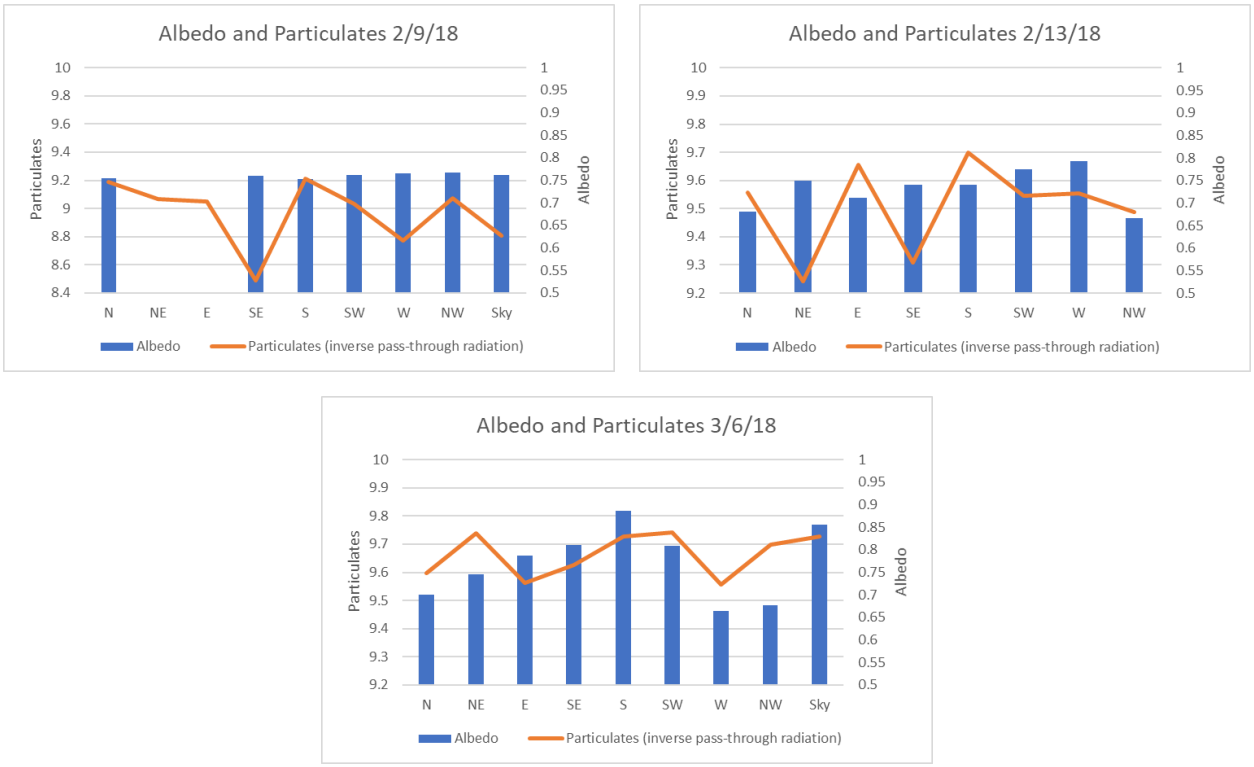

Figure 4-17: Particulate concentrations for 2/9 (top left), 2/13 (top right) and 3/6 (bottom)

Spatial distribution around Syracuse

Both albedo and particulate results were used to explore the spatial distribution of particulate matter around the city. The highest average albedo was found at the S site – this suggests that albedo increases from north to south across the city. The lowest particulate concentration was found at the SE site suggesting a decrease from northwest to southeast. A trend analysis was run in ArcGIS to verify this hypothesis [Figure 4-18]. Results show that albedo increases from NNW to SSE and particulates decrease from the W to E. This slight discrepancy is likely a result of the high particulate values discovered at the S site. Overall,

albedo and particulate analysis show that the snow on the west/northwest side of the city is relatively dirty and the snow on the east/southeast side is relatively clean.

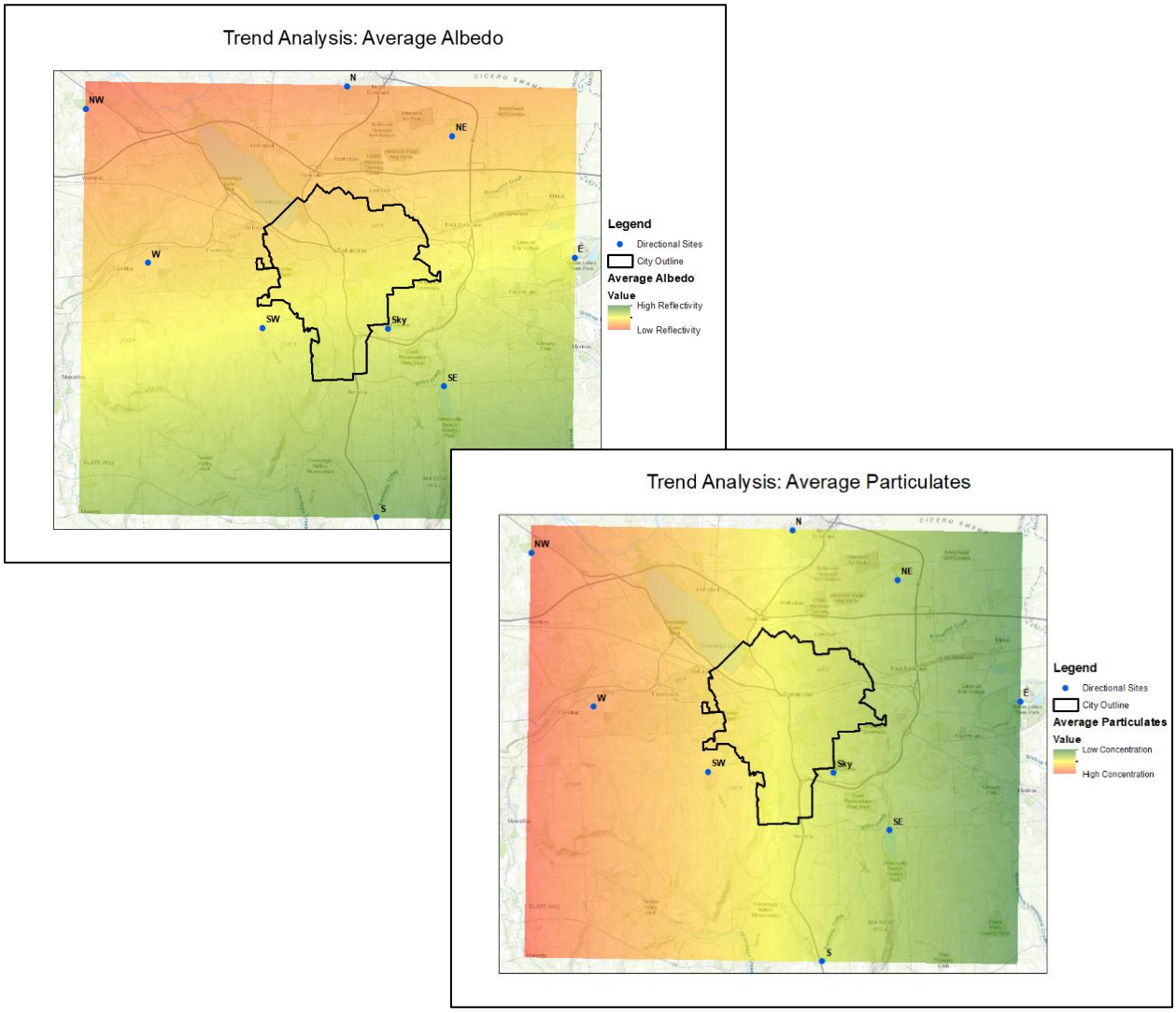

Figure 4-18: Trend analysis of albedo (top left) and particulates (bottom right); green = high albedo/low particulates, red = low albedo/high particulates

An additional trend analysis was run to compare these results to population distribution [Figure 4-19]. Outside of the urban core, the highest population is found in three suburbs Clay, DeWitt and Manlius – all are located to the north and east of the city center (USCB, 2010). According to Bond et al. (2013), the concentration of energy and transportation related

particulate correlates with high population density. Trend analysis shows that population decreases from NE to SW across the city. Some overlap is apparent when comparing population to albedo (specifically the N site in Clay), however, the site with the lowest average albedo does not match the overall population trend (the lowest albedo was at NW instead of NE). In sharper contrast, the particulate concentration trend bears little to no resemblance to the population trend. In fact the E site, generally one the cleanest, is located near the high population suburbs of Dewitt and Manlius. While it is possible that population density, especially at the local scale, played some role in the spatial distribution of albedo and particulates, it is unlikely the driving factor for this study.

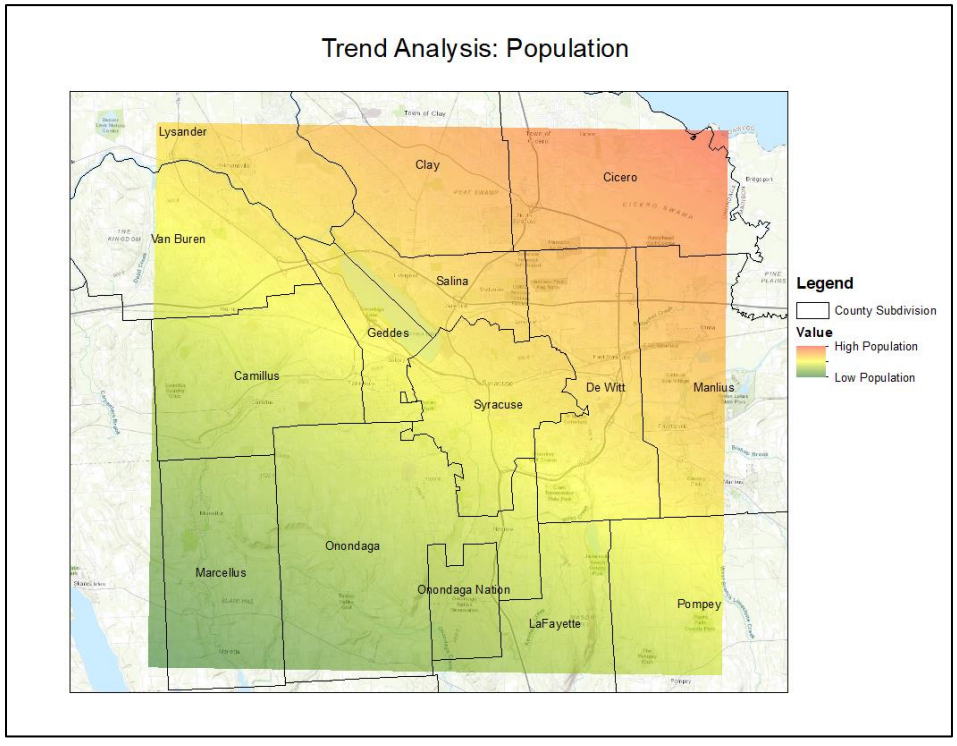

Figure 4-19: Trend analysis of population in the Onondaga County census subdivisions nearest to Syracuse (USCB, 2010)

Individual trend analyses were run for each sample set. These were compared to the direction of the prevailing wind during the particulate deposition period. Figure 4-20 shows albedo and particulate trends as well as the prevailing wind for the 1/7, 2/13 and 3/6 sample sets. Overall, the albedo is lowest upwind of Syracuse (as shown in 1/7 and 3/6). The connection between the measured particulate concentration and wind somewhat matches this trend.

Sample	Albedo	Particulates	Wind
1/7	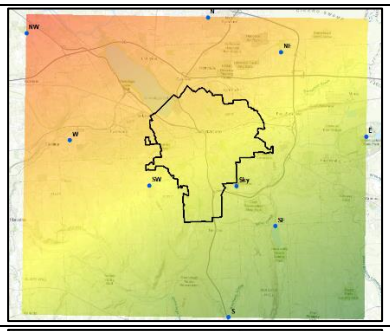	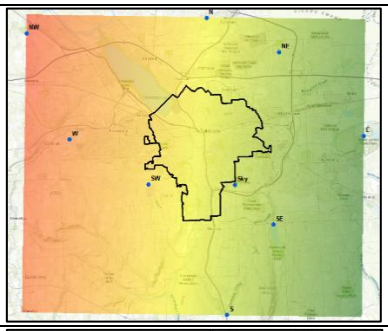	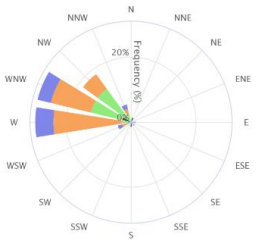
2/13	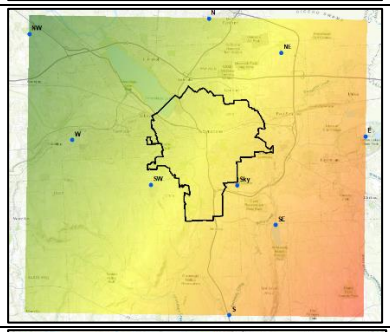	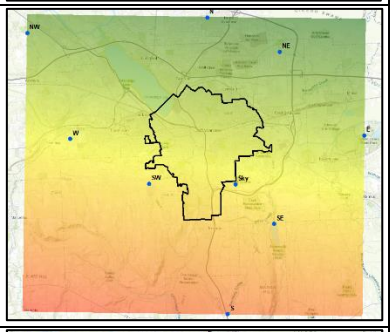	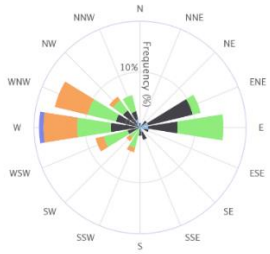
3/6	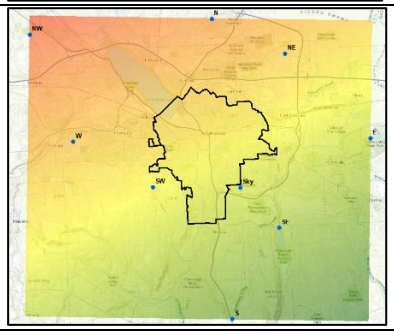	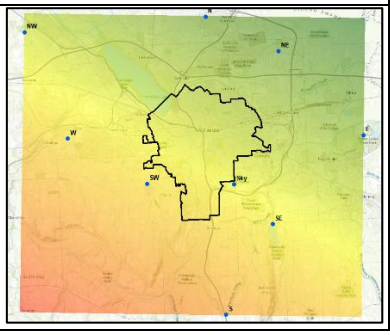	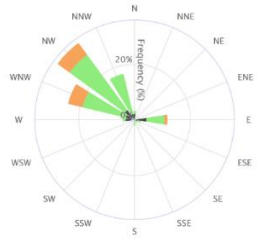

Figure 4-20: Selected albedo and particulate trend analyses; green = high albedo/low particulates, red = low albedo/high particulates

These results are surprising. Trend analysis was expected to show high albedo (low particulates) upwind of the city. Instead, results suggest that Syracuse actually cleans the air as a storm passes over the urban core. Few studies examine this effect at the city-scale, however, there is a robust literature that explores particulate transportation at a street-level scale.

Honghong Niu et al. (2017) identify the effect of buildings (both large and tall) on the transportation of particulates by wind. Their study uses a street level scale to map particulate distribution. When particulate-laden air moves through an urban canyon (ie: street with tall buildings), an eddy forms upwind of the leeward buildings. This circulation pattern traps particulates on the upwind side of the building and creates a rainshadow downwind (Honghong Niu et al. 2017). The magnitude of eddy depends on the porosity, the space between the buildings. This effect can be extrapolated to the city-scale. Cities with high urbanization and low porosity cause surface winds to blow back upwind of the urban core (Yuan, Ng & Norford, 2013). These winds recirculate air and over time accumulate additional particulates in the snowpack.

City-particulate rainshadow is likely one of many factors that influence the particulate concentration upwind of the city. In fact, long-range atmospheric transport may play a role in the high concentration observed west of Syracuse. Air masses travel to Central NY from Northern Canada, the Ohio Valley and the Atlantic (NCEI, n.d.). Of these, the Ohio Valley is a substantial source of particulate pollution. M. Kim (2002) found that up to 50% of the highly polluted air masses observed in eastern OH, move northeast to Central NY. As an air mass moves into the area, particulates can be deposited. The quantity and location depends on the track of the air mass.

An air mass track was developed for a high pressure system that affected the 3/6 sample set [Figure 4-21]. The high follows a NE trajectory before diverting N into Canada. This path skirts the west side of Syracuse on 3/3/18. It is possible that this airmass brought Ohio Valley particulates to the south and west side of the city and fewer particulates less to the north and east side. This distribution matches the particulate trend analysis for 3/6.

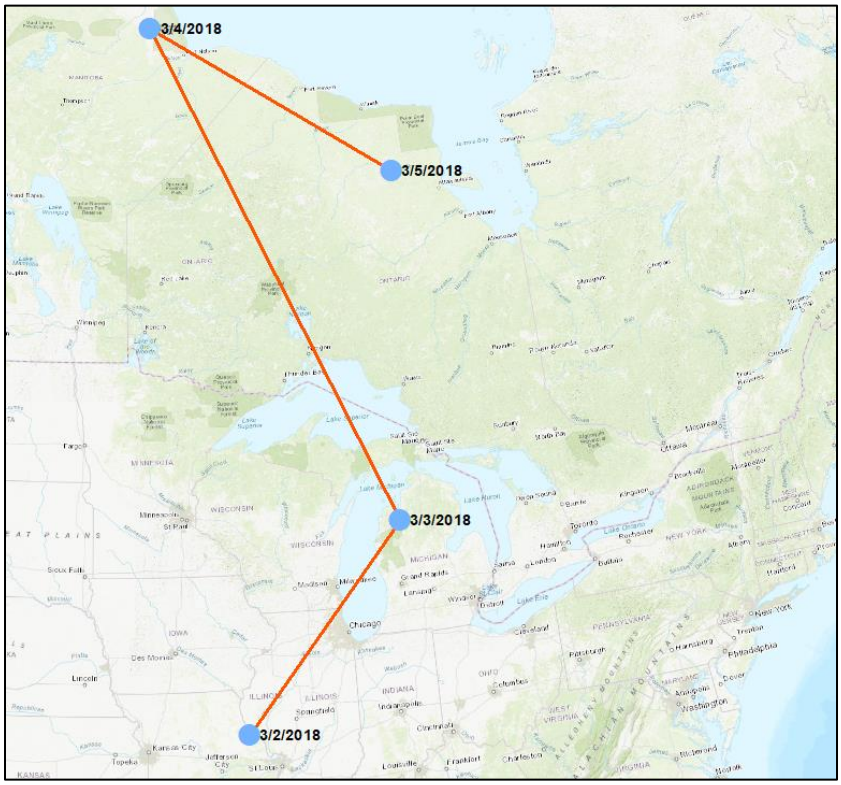

Figure 4-21: Backward projection of the air mass affecting Syracuse from 3/2/18 to 3/5/18; the blue dot marks the center of the airmass (National Weather Service, 2018)

Transect Analysis

A number of authors explore the impact of automobiles and traffic on pollution levels. Within this literature, highway dispersion of particulate matter is well documented, however, most research focuses on the human-health impact of particulates rather than the impact on the environment (Bowker, Baldauf, Isakov, Khlystov, & Petersen, 2007; Saha, Khlystov, &

Grieshop, 2018; Tong, Whitlow, MacRae, Landers, & Harada, 2015). Cereceda-Balic et al. (2018) conducted one of the few studies to explore the effect of highway pollution on the cryosphere (specifically the effect on albedo).

The transect study aims to explore the effect of vehicle emissions on particulate distribution in the near-road environment. In this experiment, I-90 acts as a point source of particulate pollution. A three-site transect was sampled on both sides of the interstate. These sites were oriented NW to SE in order to match the general wind pattern for each snow event. Sites D, E and F were located upwind of the highway while sites A, B, C were located downwind. All sites were sited approximately 10 km away from the urban center [Figure 4-22]. Most transect samples were collected from the same snow events as the directional samples. One event was not sampled (2/7), however, one additional sample set was collected (1/21, January 13-17 storm event). For this set, winds were variable, shifting between west and east [Figure 4-23].

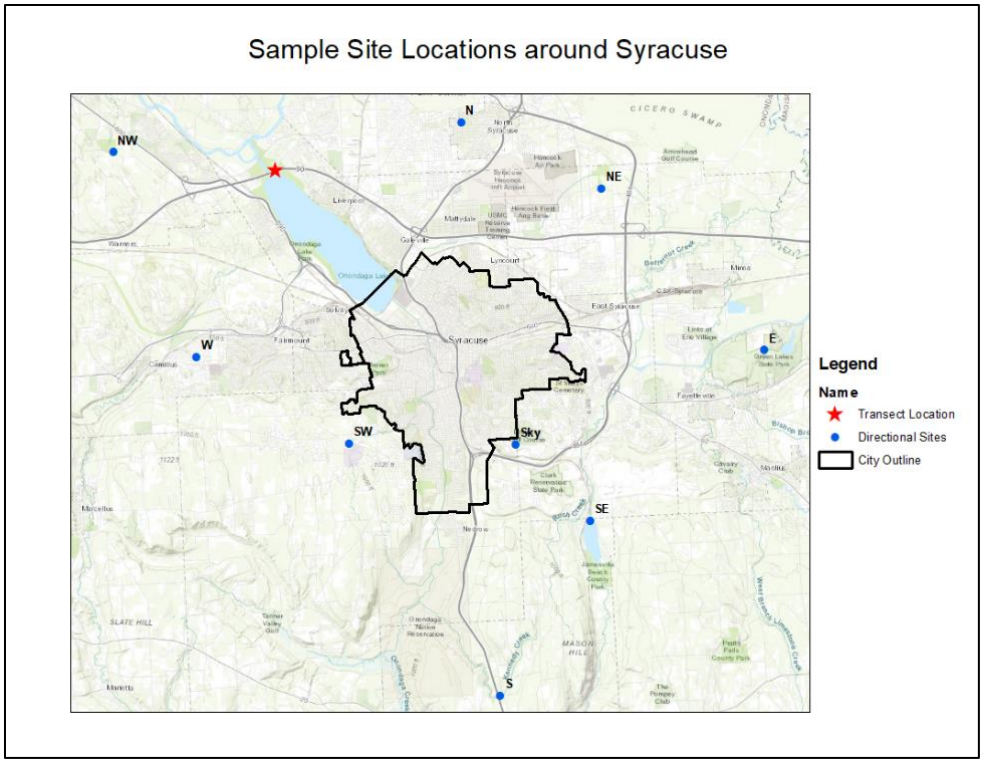

Figure 4-22: The location of the transect sample sites in relation to Syracuse

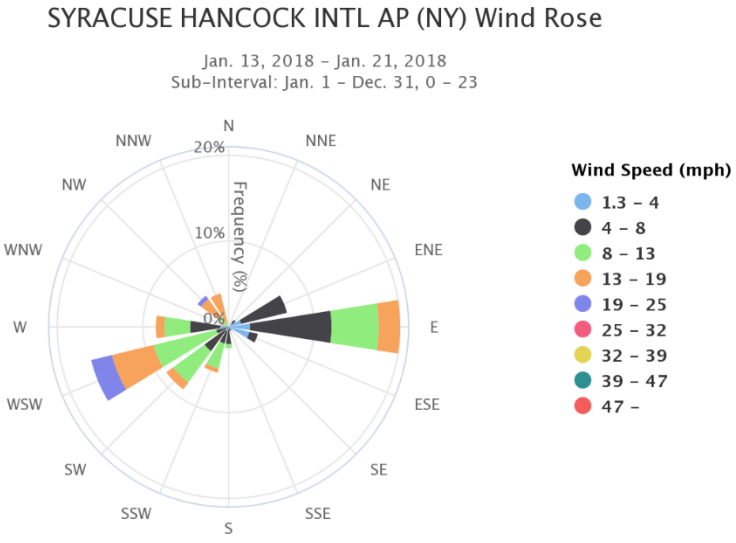

Figure 4-23: Wind rose for the 1/21 transect sample (MRCC, 2018)

A total of seven sample sets were collected over two field seasons [Table 4-3]. Two sets were collected from a transect located to the southeast of Onondaga Lake Parkway (east transect). On 3/22, two sites were not able to be sampled. Site I90B was located in a plowed parking lot (this site was unplowed on 3/15). Site I90E was flooded by an ephemeral stream. On 3/15, snow depth at these sites was 30.5 cm and 38 cm, respectively. The deep snow likely masked any albedo reduction that may have been observed from the underlying pavement and stream. Therefore, these results were not excluded from analysis. The I-90 transect was relocated for the second season (west transect). New sites were selected approximately 250 m to the WSW of their original locations. An additional five sample sets were collected from the west transect.

Sample date	Snow event dates	Transect location	Number of samples	Notes
3/15/17	3/14/17-3/15/17	East	7*	One duplicate sample was collected at site F
3/22/17	3/14/17-3/15/17	East	4*	Sample site B was located in a plowed parking lot; sample site E was located in a stream. No suitable alternative sites were found
11/20/17	11/19/17-11/20/17	West	6	
12/15/17	12/12/17-12/14/17	West	3*	Samples were collected late in the day, only three samples were successfully collected before dark
1/7/18	1/4/18-1/6/18	West	6	
1/21/18	1/13/18-1/17/18*	West	6	Sample was collected four days after the snow event, however, no comparison sample collected immediately following the storm
3/6/18	3/2/18-3/3/18*	West	6	Sample was collected three days after the snow event, however, no comparison sample collected immediately following the storm

Table 4-3: Summary of all transect samples collected; An asterisk (*) represents an abnormal sample: see notes column

Albedo and particulate concentration

Vehicle exhaust increases the amount of particulate matter available for deposition on snow. The type of vehicle, type of fuel and intensity of traffic all affect the quantity and quality of particulates produced (Bond et al., 2013; Lund et al., 2014). Of these effects, traffic intensity is most influential. Cereceda-Balic et al. (2018) found that intense traffic (at least 2000 vehicles per day) produces enough particulates in 24 hours to reduce snow albedo by 0.08. This effect is greater than the albedo reduction associated with a background level of particulate matter deposition (about 0.02), but not greater than the reduction associated with deposition on old

snow (about 0.11) (Gul et al., 2018). While few authors quantify the amount of particulate matter required for a 0.08 albedo reduction, Bond et al. (2013) note that the addition of about 0.4 μm of specifically black carbon will reduce albedo by 0.08.

Unfortunately, the change in albedo observed by Cereceda-Balic et al. (2018) is not directly comparable to this study. Daily traffic in Onondaga Lake County Park is substantially higher than levels observed in Chile. Over 32,000 vehicles pass the I-90 transect each day (New York Department of Transportation [NYDOT], 2018). Of these, 17.6% are considered heavy duty vehicles (trucks and maintenance vehicles) which contribute up to 90% of particulate emissions (Lund et al., 2014; New York Department of Transportation [NYDOT], 2004). It was not possible to determine daily variation in particulates or albedo, however, it was assumed that an increase in vehicles will lead to greater particulate emissions and a greater daily albedo reduction.

Both albedo and particulates were measured using the same method as the directional study. Sites I90A and I90D were located closest to the interstate, I90C and I90F were furthest away. Average albedo ranged from 0.58 (site I90A, 3/15/17, new snow) to 0.87 (site I90B, 1/21/18, old snow). Within each sample set, albedo varied by up to 0.27 [Figure 4-24]. The albedo range was similar across most sites. Interestingly, a range of 0.16 was measured at sites I90A and I90D, 0.17 at I90E and I90F and about 0.21 at I90C and I90B. These groupings, near road (I90A, I90D), upwind (I90E, I90F) and downwind (I90C, I90B) suggest that a location-based pattern of atmospheric transport exists along the transect.

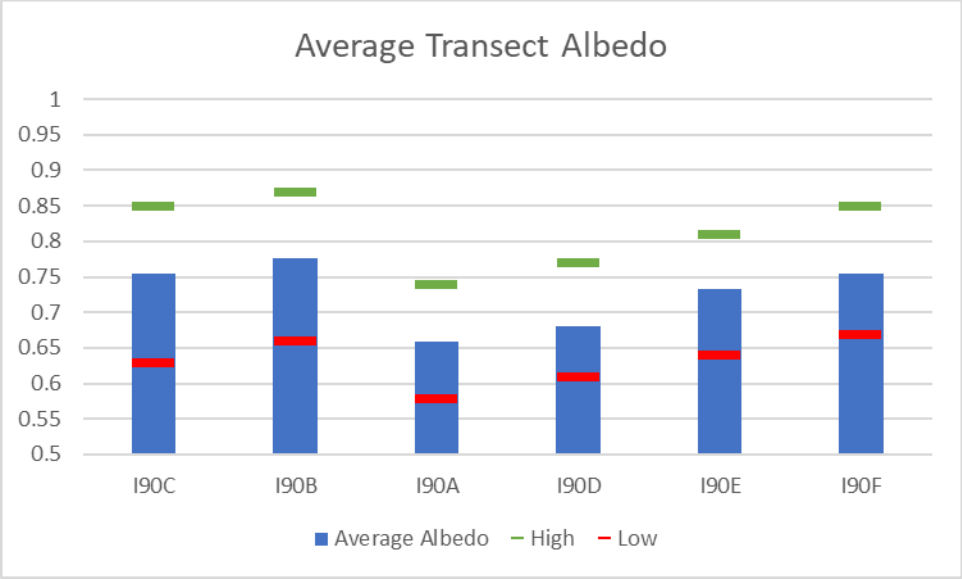

Figure 4-24: Average (blue), highest (green) and lowest (red) albedo values that were recorded at transect site; I-90 is located between sites I90A and I90D

Figure 4-25 shows the albedo of two individual transect samples. The graph for 1/7 represents a common observed distribution of albedo. In this case, the highest albedo was recorded at I90C, furthest away from the pollution source. The lowest albedo, recorded at I90A was likely the result of its proximity to the interstate (20 m) and its downwind location. The 1/21 sample is an interesting exception. Here, the lowest albedo was measured at I90C (0.63) instead of I90A (0.64). Between these two sites, an albedo of 0.86 was measured at I90B. This discrepancy suggests that the interstate was not influencing albedo on 1/21. In fact, prevailing wind direction for this period was parallel to the highway (variable out of the W or E). This zonal pattern likely blows particulates further down the road, limiting deposition on the snow.

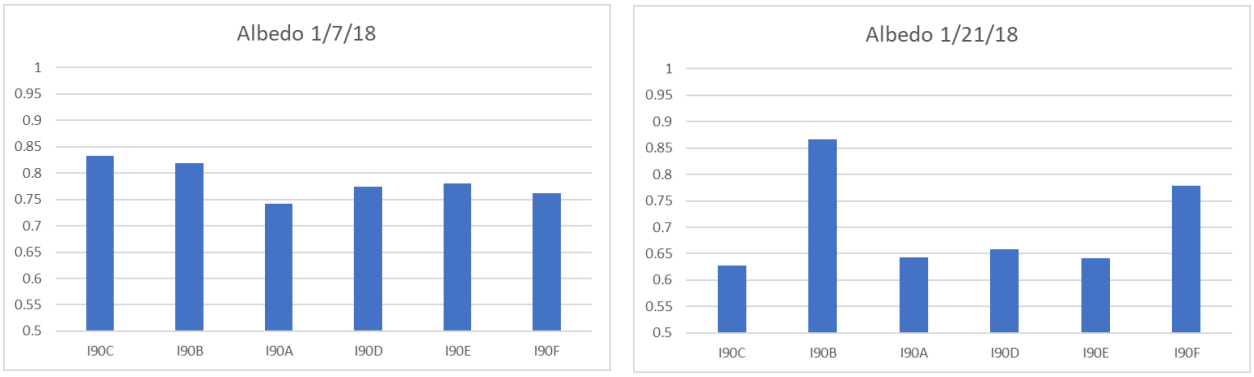

Figure 4-25: Left: transect albedo measurements recorded on 1/7; right: transect albedo measurements recorded on 1/21; I-90 is located between sites I90A and I90D

On average, particulate concentration followed a similar trend as albedo [Figure 4-26]. Results varied from 9.75 $(W/m^2)/ml$ to 9.29 $(W/m^2)/ml$. Highest concentrations were found at site I90D while lowest were found at I90C. In general, concentration decreased with distance from the edge of the interstate, the highest concentration was found upwind of the highway at I90D. This contrasts to the lowest albedo measurement, recorded at I90A (downwind of the highway).

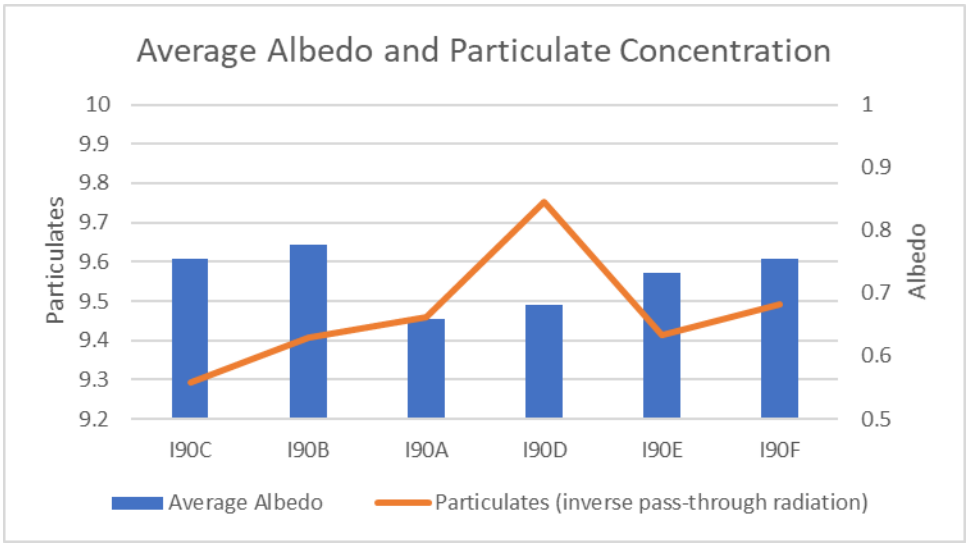

Figure 4-26: Average particulate concentration compared to albedo at each transect site; I-90 is located between sites I90A and I90D

This discrepancy is likely a result of excluded data. Particulate concentrations measured on 11/20 were exceedingly low (8.70 (W/m^2)/ml to 7.48 (W/m^2)/ml). Site I90D was found to have the lowest concentration of the entire transect study. This result is unlikely given its proximity to the interstate (Bowker et al., 2007). To test this, the mean (9.38 (W/m^2)/ml) and standard deviation (0.65 (W/m^2)/ml) were calculated for all transect samples. Five of the 11/20 samples were found to be 1-2 standard deviations away from the mean. These sites were retained for analysis. The I90D sample was found to be over 3 standard deviations away from the mean and was excluded [Figure 4-27]. Unfortunately, excluding this data point removed the effect of a generally low particulate concentration sample set from the I90D average, likely increasing the I90D concentration.

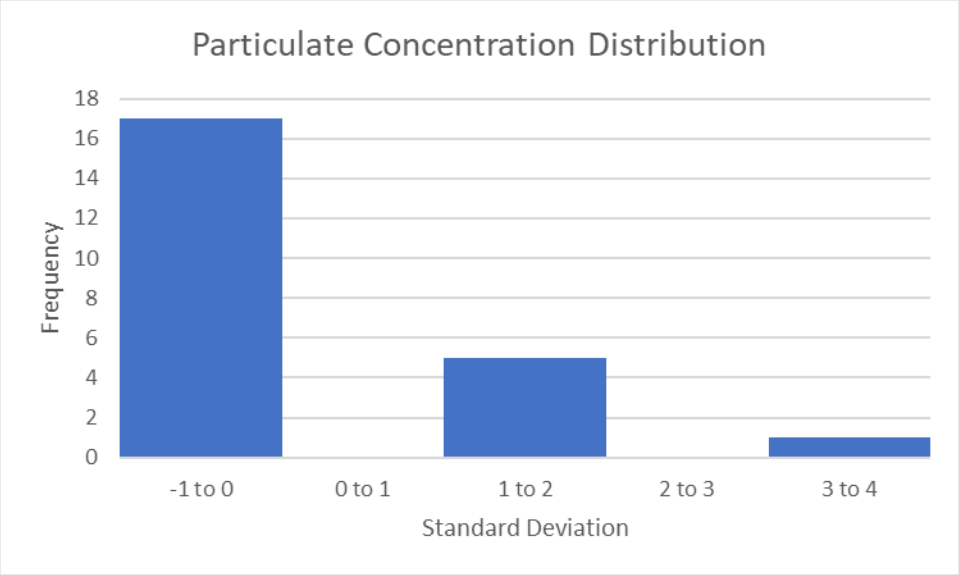

Figure 4-27: Frequency distribution of transect samples showing deviation from the mean

Limited data made individual sample set analysis difficult. Saha, Khlystov and Grieshop (2017) and Tong et al. (2015) suggest continuous monitoring to accurately access the quantity of near-road particulates. This was not feasible for the transect study, however, samples still

include a form of continuous data in the results. Similar to the particulate build-up at S site, each sample contains the total quantity of particulates within the snowpack. Therefore, a snow core should yield the concentration of all particulates that were deposited since snow first accumulated. Framing the particulate samples in this way may also help to explain the difference between albedo and particulate concentration at the transect sites.

Figure 4-28 shows the distribution of particulate matter measured on 1/21 and 3/6. The 1/21 sample shows that the concentration of particulates at sites I90B, I90E and I90F was greater than the concentration observed immediately downwind of the highway (site I90A). This contrasts with the distribution observed on 3/6 (particulates are lowest at I90B and I90E), which represents an average distribution. In addition, a relatively high albedo was measured at I90B and I90F on 1/21. A Pearson Correlation was performed to identify the relationship between particulates and albedo on 1/21, however, the test was not statistically significant ($r = 0.224$, $n = 6$, $p = 0.669$) [Figure 4-29]. Nevertheless, an increase in particulate matter should not result in an increase in albedo. Bond et al. (2013) note that particulate absorption properties can change when two or more types are mixed together (ie: an increase in dust concentration reduces the effectiveness of black carbon). This scenario, however, would still result in a net albedo decrease.

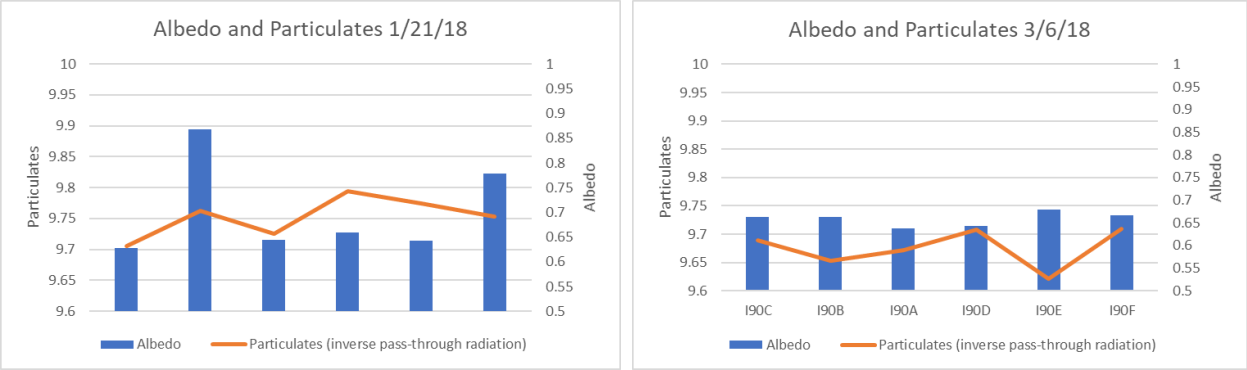

Figure 4-28: Albedo and particulate concentrations measured on 1/21 (left) and 3/6 (right)

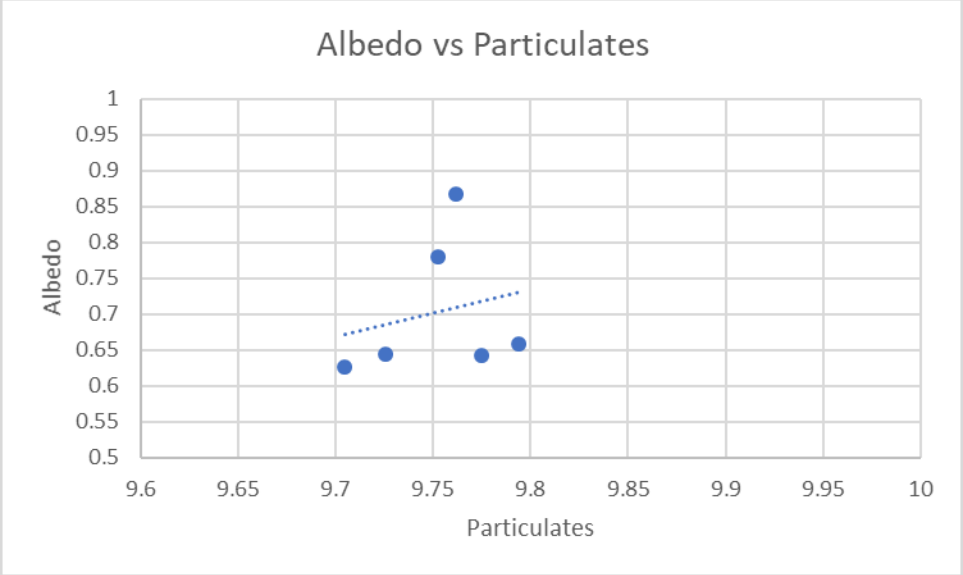

Figure 4-29: Correlation between albedo and particulate concentration for the 1/21 transect

The 1/21 and 3/6 measurements were compared to snowpack data recorded at the Syracuse Hancock Airport [Figure 4-30]. Samples collected on 1/21 were taken from a snowpack that began accumulating on 12/21/17. As a result, the snow core contained particulates that accumulated from 12/21/17 until 1/21/18. Samples collected on 3/6 were taken from a snowpack that began accumulating on 3/2/18. Doherty et al. (2016), note that as a snowpack ages it continues to accumulate particulates. Over time, these become concentrated in deeper

layers. The 1/21 snowpack aged for 31 days, therefore, particulate samples included deposition from this entire period. In contrast, albedo measurements only quantified surface particulates. The difference was manifested as the discrepancy between measured albedo and particulate concentration that was observed on 1/21.

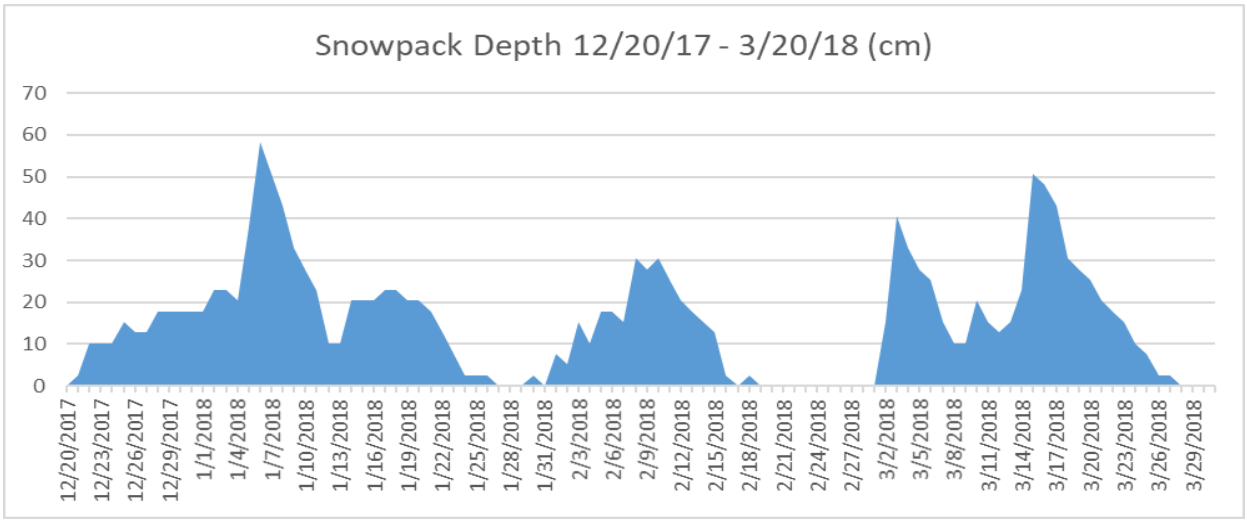

Figure 4-30: Snow depth recorded at Syracuse Hancock Airport from 12/20/17 to 3/31/18 (MRCC, 2018)

Distance analysis

Albedo and particulate concentration were both used to explore how particulate pollution is affected by source proximity. While the two measurements examine slightly different parameters, they both agree that pollution is greatest in near I-90. This result is not surprising. Vehicles act as a significant source of particulate pollution, therefore, close proximity should increase the concentration (Bond et al., 2013; Lund et al., 2014). It was assumed that this trend would continue as distance from the highway increased. This would result in the cleanest snow at sites I90C and I90F. This was not always the case. On average, I90C showed an

albedo decrease compared to I90B. Likewise, I90F showed an increase in particulate concentration compared to I90E [Figure 4-31].

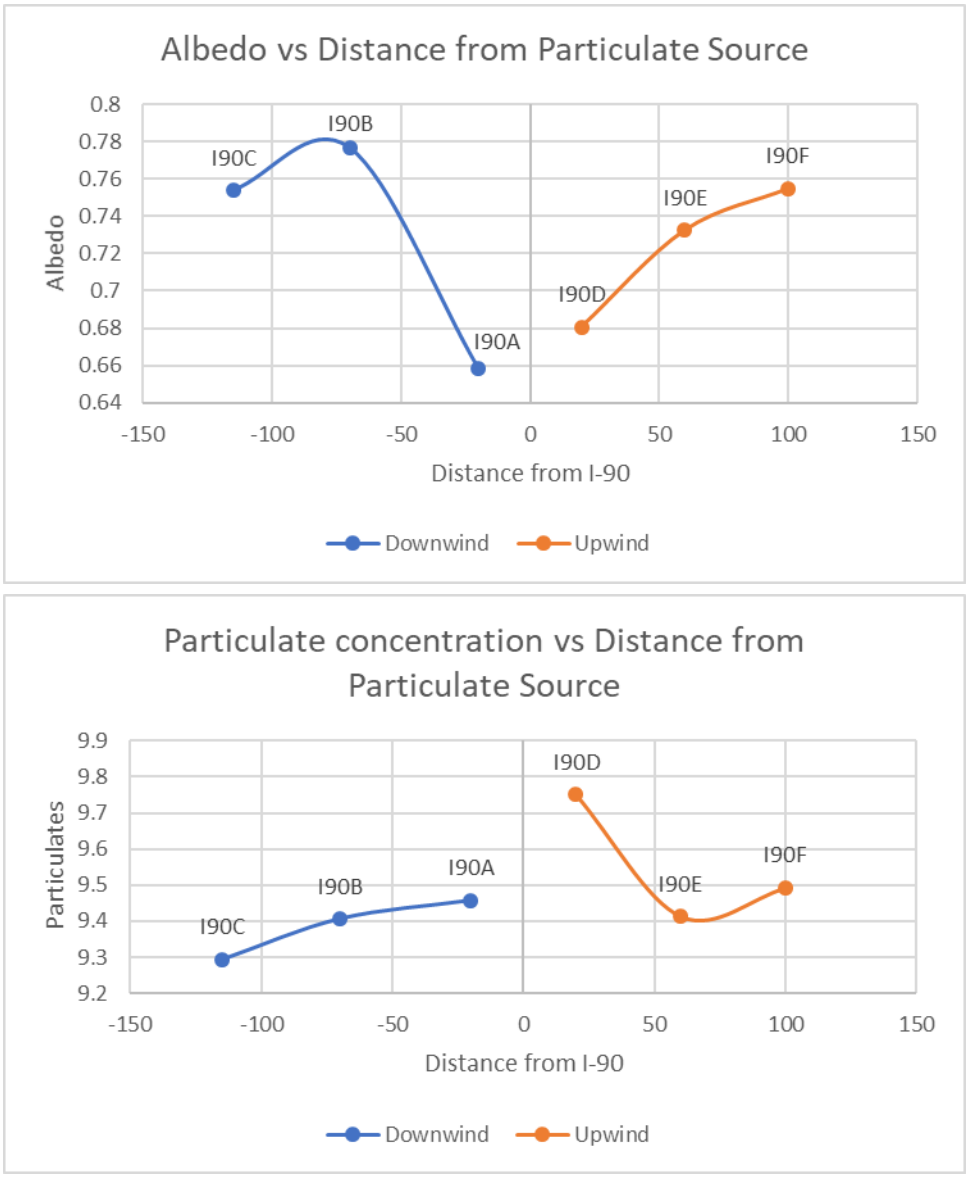

Figure 4-31: Top: albedo values and distance from particulate source; bottom: particulate concentration values and distance from source; I-90 is located at distance 0; Negative values represent distance to the south of I-90

According to Bowker et al. (2007) a number of other factors influence particulate distribution. Local obstructions often direct wind circulation patterns. Sound barriers, buildings, large trailers and trees/vegetation all alter the dispersal of particulates (Tong et al., 2015). Normal dispersal patterns show that vehicle emissions can travel up to 400 m away from the source. When an obstacle is placed in this dispersal field the effect is similar to the city-particulate rainshadow – particulates tend to accumulate in front of the obstacle leaving the space directly downwind relatively clean (Bowker et al., 2007). This circulation pattern is likely why I90A was found to have the lowest recorded albedo and I90B the highest. A large stand of trees is situated between I90A and I90B [Figure 4-32]. This likely act as a partial barrier, increasing the concentration at I90A and decreasing it at I90B.

Figure 4-32: Trees blocking particulate dispersal on the downwind transect

This effect may also explain the apparent decrease in albedo at I90C. Bowker et al. (2007) note that particulate-laden air is forced upwards when it comes in contact with a barrier.

This air returns to the ground some distance downwind of the obstruction. When the air returns to the ground a recirculation zone is created increasing the concentration of particulates on the snow (Tong et al., 2015). Bowker et al. (2007) suggest that a 12 m barrier will cause the plume to return to the ground 80 m downwind. The trees between I90A and I90B begin at 10 m from the edge of the interstate. Assuming the trees are taller than 12 m, the plume should return to the ground at least 90 m from the edge of the interstate – likely placing I90C (115 m) in the recirculation zone.

In addition to acting as a barrier, trees also act as a net to trap particulates as they are deposited from the road. Trapped particles can be re-aerosolized and deposited again at a later date (Tong et al., 2015). Site I90D is located directly under a large tree. The average albedo at the site was found to be 0.015 higher than I90A even though both sites are the same distance from the interstate. While it is possible this discrepancy is a result of the prevailing wind direction, it is equally likely that some particulates were caught in the tree. This would have reduced particulate deposition and increased albedo to some degree.

This effect may also account for the increase in particulate concentration observed at I90F. At this site, average particulate concentration increased even though albedo increased. Since the albedo measurement only accounts for particulates deposited in fresh snow, airborne particulates that get caught in the tree-net over site I90D may not be included. Over time, these particulates re-enter circulation and are deposited downwind, again likely close to I90F (100 m) (Bowker et al., 2007; Tong et al., 2015). As suggested by Doherty et al. (2016), these particulates could accumulate in the snowpack and be concentrated in deeper layers. If this

happens they would only be measured in the next snow core – effectively increasing the observed concentration while not affecting the albedo.

Photography Analysis

The use of digital photography in scientific research is a rapidly expanding tool for both qualitative and quantitative analysis of land surfaces. Traditionally, photographic analysis of snow has been limited to expensive aircraft acquisition or poor resolution, large scale satellite imagery. These data are useful for global or regional studies of snow, however, they do not provide the necessary resolution for micro-scale analysis (Pimentel, Herrero & Polo, 2012). Recently, improvements in consumer digital camera technology have opened access to a variety of new photographic based analysis methods. Many scientists now utilize Unmanned Aerial Vehicles (UAV) to assess local scale snowpack properties (Bernard et al., 2017; Lendzioch, Langhammer, & Jenicek 2016; Mizinski & Niedzielski, 2017). Others quantify micro-scale processes using terrestrial photography (Corripio, 2004; Pimentel, Herrero & Polo, 2012).

The photo study aims to identify a digital photographic analysis method to quantify particulate concentration in snow. This concept is not well developed in the literature. There are a few authors that use field photography to examine particulate matter in air, however, no authors examine the concentration in snow (Du et al., 2013). That said, quantification of albedo using digital photos is discussed briefly (Corripio, 2004; Gilchrist, 2011). As albedo is an integral part of the directional and transect studies, it was used as the basis for the photo analysis.

Digital photos were collected for 10 sample sets [Table 4-4]. Three of these were collected in the first season. Each first-season image is focused on the snow surface in order to maximize the sample area for analysis. The sampling ruler (to note snow depth) and collection

baggie (to identify the sample site) are included on the right side of the image [Figure 4-33].

One to three photos were taken whenever a snow sample was collected.

Sample date	Snow event dates	Type of sample	Number sites	Photo Method	Notes
2/18/17	2/12/17-2/17/17	Directional only*	8	Old	Could not compare to directional albedo values
3/15/17	3/14/17-3/15/17	Directional and transect	14	Old	
3/22/17	3/14/17-3/15/17	Directional and transect	14	Old	
11/21/17	11/19/17-11/20/17	Transect only	11	New*	Ruler was not included in photos
12/15/17	12/12/17-12/14/17	Directional only	9	New	
1/7/18	1/4/18-1/6/18	Directional and transect	15	New	
1/21/18	1/13/18-1/17/18	Transect only	6	New	
2/9/18	2/7/18	Directional only	9*	New	Two photos (NE & E) were taken in low light conditions
2/13/18	2/7/18	Directional only	8	New	
3/6/18	3/2/18-3/3/18	Directional and transect	15	New	

Table 4-4: List of all photo sets that were collected for analysis. An asterisk (*) represents an abnormal sample: see notes column

Figure 4-33: A first season photograph collected at the E site on 3/15/17

Most images were shot perpendicular to the snow surface, however, a substantial number were shot from a variety of other angles [Figure 4-34]. This substantially impaired comparability of the photos. As a result, the images were repurposed. Instead of using the photos for analysis they were examined in order to standardize photo collection methodology for the second season.

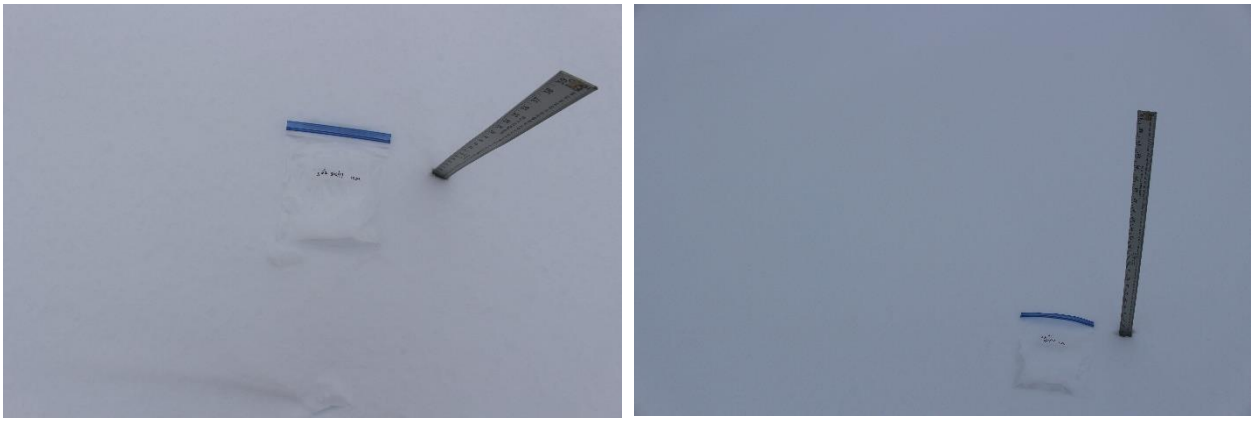

Figure 4-34: Two images collected in the first winter season; note the inconsistency between the left image (almost perpendicular to the snow) and the right (at an oblique angle)

Seven photo sets were collected in the second season. A standard method was employed at each site, resulting in highly standardized images. Two photos were taken perpendicular to the snow surface. The top two-thirds of each image focused on the snowpack, while, the bottom third contained the sampling ruler (and occasionally feet). The ruler was placed flat on the snow surface and used as a guide to frame the photo [Figure 4-35]. In the first image, a horizontal distance of about 55 cm of snow surface was captured. About 100 cm of horizontal distance was captured in the second image.

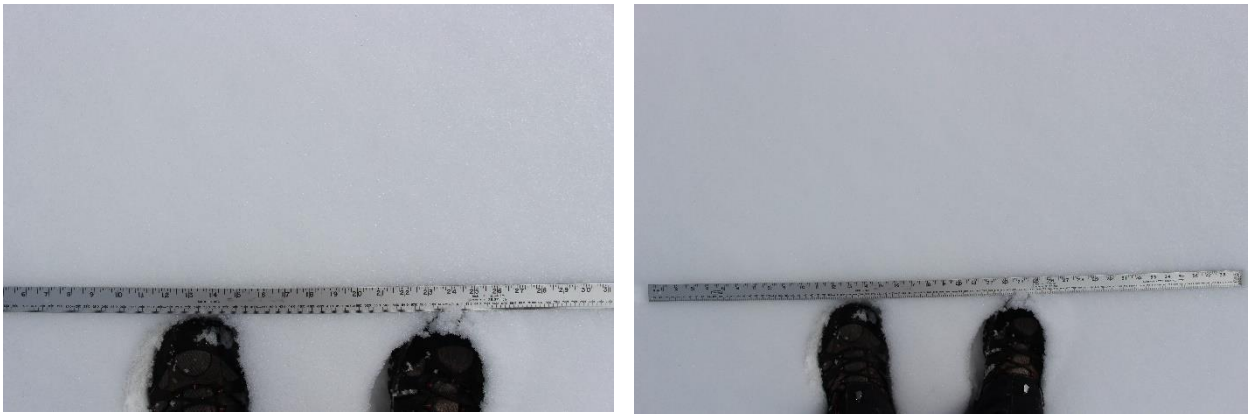

Figure 4-35: Two images collected in the second winter season using the new standardized methodology (3/6/18, N site)

Albedo

The albedo of each photo was calculated using ImageJ. This program is an open source software package, developed by the National Institute of Health. While the program is visually simple, it provides a robust toolset for image quantification and manipulation (Ferreira & Rasband, 2012). Applications include, cell counting (Grishagin, 2015), historical stain analysis (Jensen, 2013), particle size distribution (Igathinathane et al., 2008) and leaf shape measurement (Maloof et al., 2013), among others. In snow science, ImageJ is often used for

snow distribution analysis, snow depth analysis or individual snow grain measurement (Sturm et al., 2006; Yamaguchi et al., 2010).

Images from four second season, directional sample sets were analyzed using ImageJ: 12/15, 1/7, 2/13 and 3/6. The one remaining directional set, 2/9, was excluded as a result of the missing albedo measurements. A total of 35 images were processed using the platform. Before analysis, lens distortion and chromatic aberration were removed with Adobe Lightroom.

Each image was individually loaded into ImageJ. Albedo was calculated using a method developed by Corripio (2004) employed by *The Albedo Project* (Gilchrist 2011; Gorski, 2018). It is possible to measure the albedo of a surface by comparing the relative brightness of an object with unknown albedo to the relative brightness of a reference object. Gorski (2018) suggests a matte-white sheet of paper for the reference object (albedo = 0.65). The second season photo collection methodology did not incorporate a reference object. However, each image contained the metal meter stick to identify image scale. An average albedo of the meter stick was determined to be 0.45 and it was used as the reference object for analysis.

To analyze an image, the meter stick was selected in ImageJ. A histogram was created to determine the mean brightness of the reference. This process was repeated to determine the brightness of the snow [Figure 4-36]. The equation:

$$A_{rel} = B_u/B_r, \quad (3)$$

where A_{rel} is the relative albedo, B_u is the mean brightness of the snow and B_r is the brightness of the reference object, was used to calculate the relative albedo of the image (Gilchrist, 2011). This result was then compared to the reference albedo. The equation:

$$A_{ab} = A_{ref} \times A_{rel}, \quad (4)$$

where A_{ab} is the absolute albedo of the snow, A_{ref} is the absolute albedo of the reference object and A_{rel} is the relative albedo calculated in Equation 3, was used to determine the actual albedo of the snow (Gilchrist, 2011).

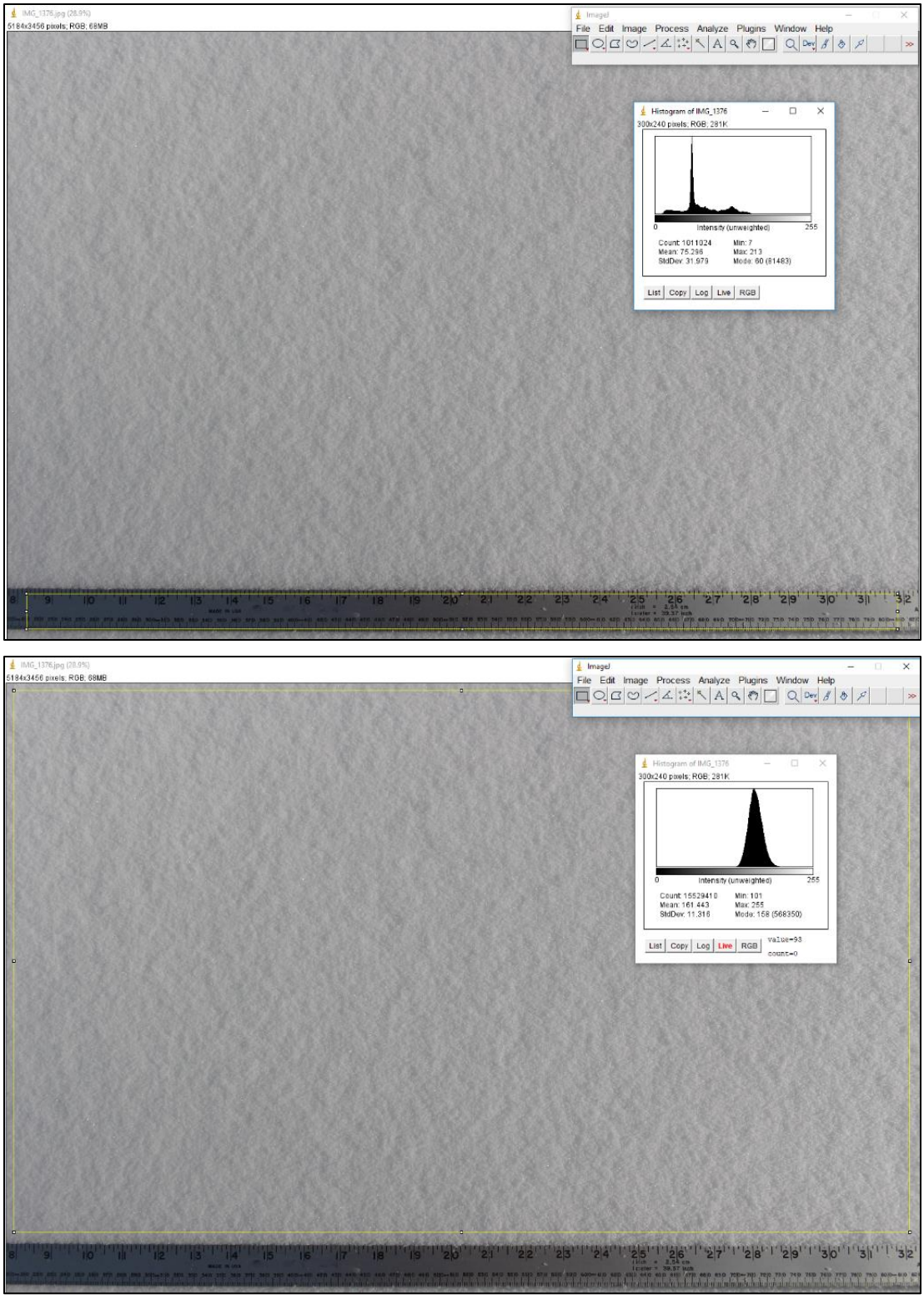

Figure 4-36: Reference (top) and unknown (bottom) object analysis in ImageJ

Results show that the average photo albedo ranged from a low of 0.70 at the W site to a high of 0.88 at the S site. The largest range was observed at Sky (low of 0.55, high of 1.00), the smallest at the E site (low of 0.62, high of 0.80). The highest albedo values were found to the south of the city. The lowest value, however, was inconsistent [Figure 4-37].

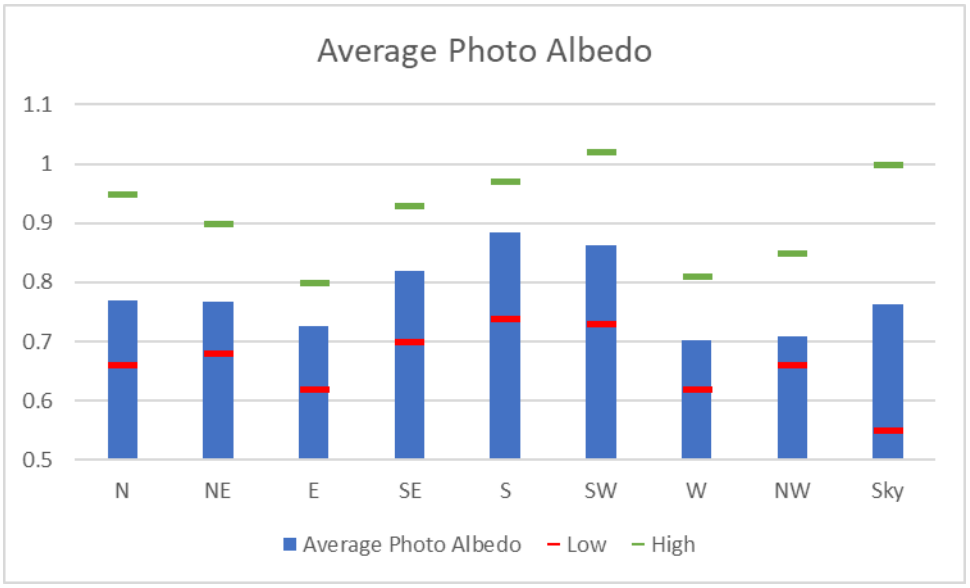

Figure 4-37: Average (blue), highest (green) and lowest (red) albedo values calculated from the photo analysis

Individual sites varied substantially. Figure 4-38 shows the photo albedo calculated at each site on 1/7. While the overall trend follows a similar pattern to the average, results range drastically. The lowest value was calculated at the NW site (0.66), the highest at the SW site (1.02). Interestingly, two albedo values were found to be greater than 1 (1.02 at the SW site, 1.004 at the Skytop site). This should not be possible. Albedo represents the percent of incoming solar radiation that is reflected off the surface (Gray and Male, 1981). An albedo value over 1 means that more radiation is reflected than reaches the snow in the first place. As snow

does not emit radiation in the visible spectrum, these values must be a result of experimental error.

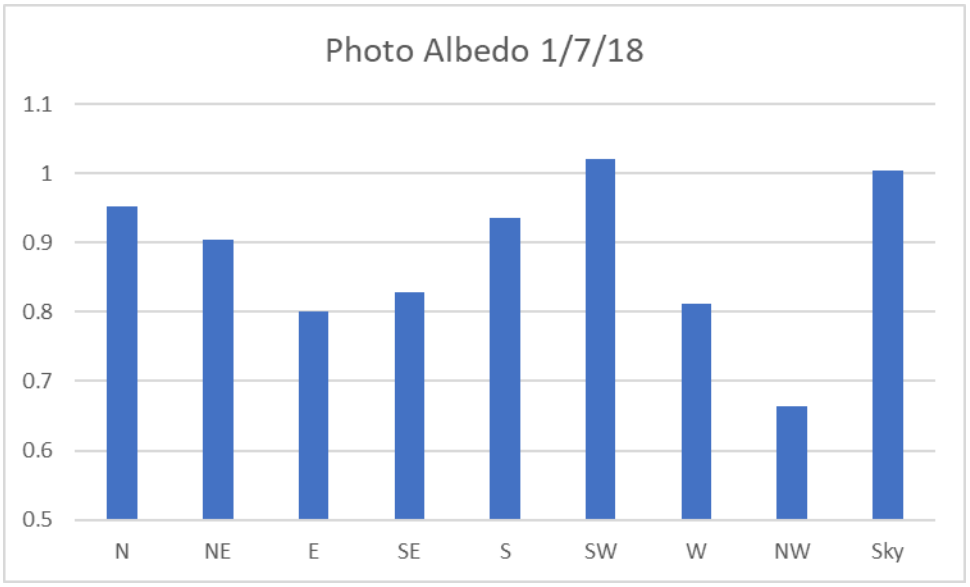

Figure 4-38: The photo albedo calculated at each site on 1/7

Images from these sites were reviewed to identify the error source [Figure 4-39]. Both show the reference object partially covered by shadow, while, this shadow is not observed on the snow. It is possible, that nearby objects reduced the amount of light reaching the ruler, thus reducing its brightness. According to equation 3 and 4, a decrease in B_r will result in an abnormally high absolute albedo (Gilchrist, 2011).

Figure 4-39: Photos taken at the Sky (top left) and SW (bottom right) sites on 1/7

Comparison analysis

The relationship between field albedo and photo albedo measurements was examined to explore the accuracy of the photo analysis. Corripio (2004) and Gilchrist (2011) claim that the ImageJ analysis method can calculate albedo to within 3% of field albedo measurements. To test this, a range of acceptable values was calculated using the average field albedo results [Figure 4-40]. The upper limit was determined by adding 3% to the average field albedo at each site, the lower limit by subtracting 3%.

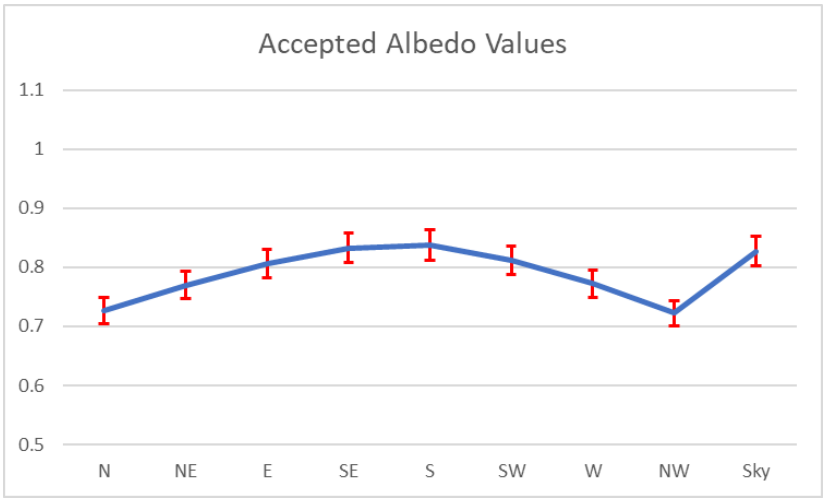

Figure 4-40: Average field albedo values; the red bars represent the range of accepted values for albedo accuracy

Figure 4-41 shows the average photo albedo at each site and the range of accepted albedo values. Only three sites fell within this range (NE, SE and NW). This suggests that these results are not comparable to field measurements. That said, the overall trend appears somewhat aligned to albedo results. To verify this, a trend analysis was run on the average photo albedo and compared to the field albedo trend [Figure 4-42].

Figure 4-41: Average photo albedo; the blue bars represent the accepted range of values for each site

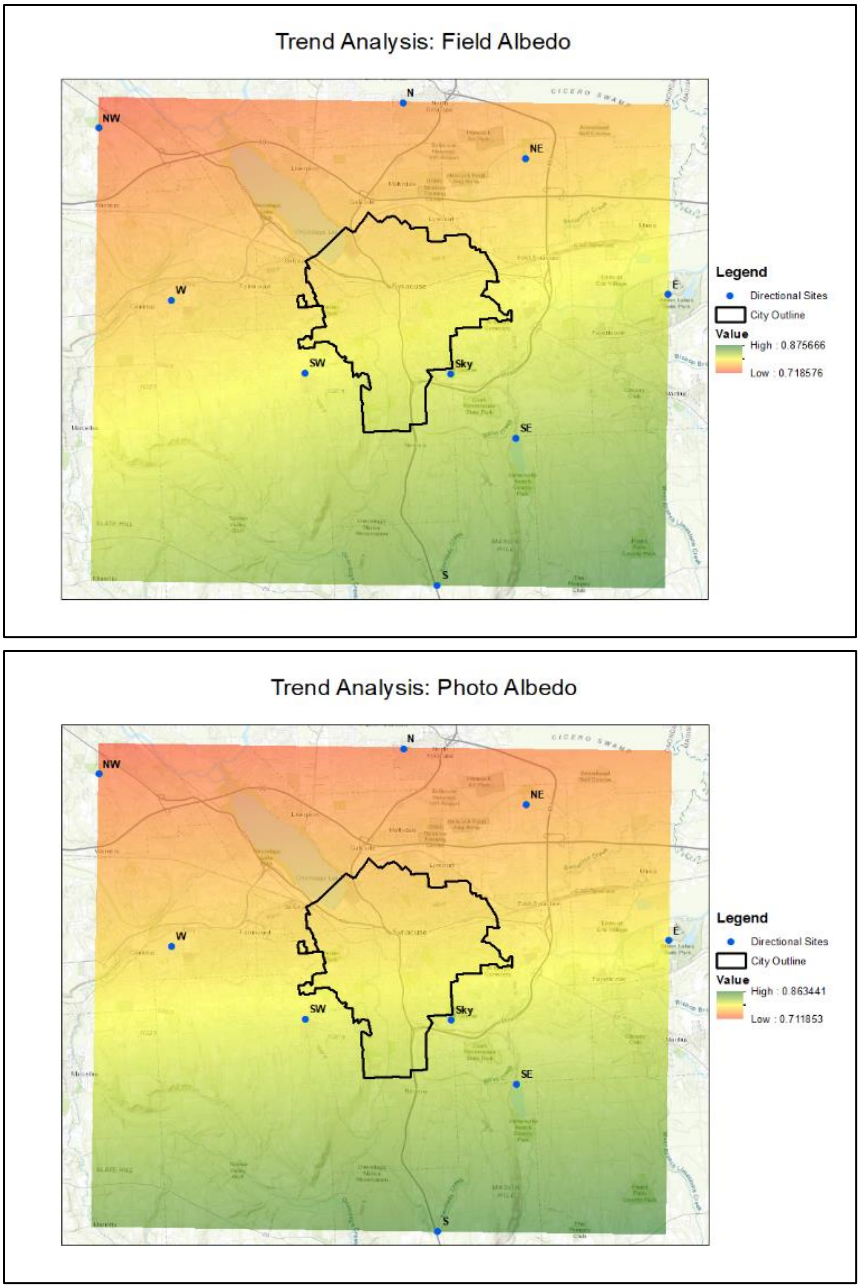

Figure 4-42: Trend analysis of field albedo (top) and photo albedo (bottom); green = high albedo, red = low albedo

Results show that albedo increases from NNW to SSE across Syracuse. While this does not exactly match field albedo results, the slight shift N is likely a result of the erroneously high value calculated at the S site (1/7). This suggests that while exact albedo values are not

comparable, the overall trend of photo albedo may show an accurate relative reflectivity. Despite this, individual sites, are less consistent [Figure 4-43]. The trend observed at each sample set is substantially different. The 2/13 inconsistency is likely a result of variable wind direction, however, the 12/15 variation remains unexplained. Overall, trend analyses show that the highest albedo could be found anywhere between the SW and SE.

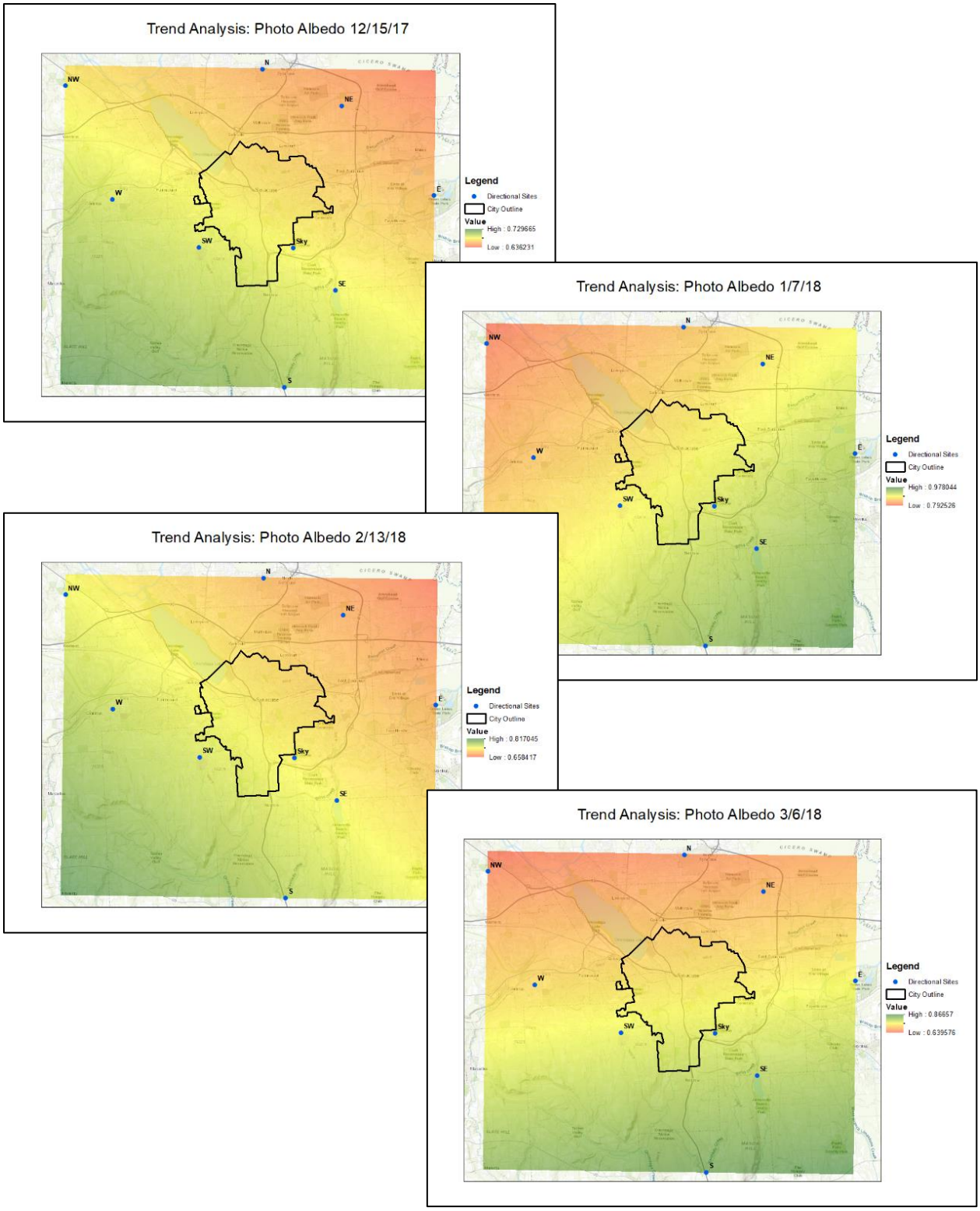

Figure 4-43: Trend analysis of photo albedo on 12/15 (top left), 1/7 (mid right), 2/13 (mid left) and 3/6 (bottom right); green = high albedo, red = low albedo

Corripio (2004) provides a possible explanation for the discrepancy between field and photo albedo measurements. According to the study, it is difficult for a camera to detect the many variables that affect albedo. In order to calculate an accurate measurement, a correction factor must be used to account for the influence of local topography on diffuse radiation. This correction involves calculating a shadow factor and skyview factor to determine number of pixels affected by diffuse radiation. Essentially, any object that increases scattering, will likely result in an inconsistent albedo calculation and a greater albedo range. This effect is observed at the Skytop site. The sample site is situated at the bottom of a small hill in a field of tall grass. Both the hill and the grass are likely to increase scattering at the snow surface. Without a correction value the calculated albedo should read abnormally high or low.

The directional, transect and photo explored analyses in this thesis examine the direct interaction between particulates, snow and the midlatitude city. The implications of increased particulate concentration, however, extend beyond alteration of the snowpack. These broader impacts can affect future climate conditions and impact people living in the midlatitudes. These effects are explored in the final chapter.

Chapter 5 – Conclusion

This thesis explores the distribution of particulate matter at the city-scale. Results show that at this scale, particulates are concentrated upwind of the city and near emission sources. The role of particulates in the local climate system, however, extends beyond snow distribution measurements. Using the research questions as a guiding framework, this chapter examines the broad impact of particulates on environmental processes and human health. Suggestions for future research are also presented.

The City-Particulate Rainshadow effect

The distribution of particulate matter is affected by city morphology. Overall, the highest particulate concentration is found upwind of the urban core, while, the lowest is located downwind. This effect, dubbed, the city-particulate rainshadow, is created by air circulation patterns that develop in a highly urbanized landscape. The flow of air around large and/or tall buildings encourage the recirculation and deposition of particulate-laden air upwind of the city.

There are a number of additional factors that likely influence this distribution, however, the rainshadow is poised to become increasingly relevant as cities expand. Both vertical and horizontal densification increases the surface roughness and the decreases porosity of an urban landscape. Following an urban canyon model, the upwind particulate concentration increases as the gap between buildings approaches zero (Honghong Niu et al., 2017). When extrapolated to the city-scale, an increase in density should intensify and expand particulate concentration upwind of the urban core. However, Honghong Niu et al. (2017) note that the concentration above ground level will increase if porosity ever reaches zero. In this case, particulates are

forced upwards to move around an obstacle. In high density cities this may lead to an increased quantity of particulate matter in the air above the urban core.

Urbanization is likely to increase overall particulate emissions. Logically, this should also increase the particulate concentration in snow and air. Yet, this effect is not always straightforward. Particulate emissions are not only linked to urbanization, but, also to economic growth. As economic prosperity increases over a certain level, particulate concentration actually declines (J. Wu et al., 2018). This is likely a result of increased access to green technology and the city-level implementation of federally mandated particulate reduction strategies.

An expansion of the rainshadow footprint or an increase in the intensity of its effect will have a substantial impact on the environment. Further, any increase in the concentration of particulates upwind of the city should result in reduced snow albedo and accelerated snow aging. These two factors degrade the snowpack and lead to an earlier melt-out date. A number of studies explore the effect of dust concentration on snowpack thinning and melt-out. On average, an accumulation of 1000 μg of dust on the snow surface will shift the melt-out date by 15 to 33 days (Skiles et al., 2012). Snow melt-out is also affected by the 2 °C to 4 °C increase in air temperature associated with elevated CO_2 levels. Together, dust concentration and CO_2, shift the melt-out date by 21 to 51 days. This effect is likely to be exacerbated in urban area as a result of extensive black carbon emissions (Bond et al., 2013; Lund et al., 2014).

Particulate induced early melt-out can alter local hydrology. Bayard et al. (2005) note that frozen soil tends to increase runoff. As particulate matter increases winter snowmelt, more water is released onto a frozen ground surface. While some infiltrates into the soil, the rate of

infiltration largely depends on the amount of pore and basal ice present (Bayard et al., 2005). High ice concentration can increase runoff by up to 30% and potentially cause localized flooding. If enough snow melts in the winter the snow-water equivalent (SWE) of the snowpack can become compromised. Low SWE decreases the soil moisture and the amount of water available in spring (Blankinship, 2014). Together these effects decrease transpiration, reduce crop yield and increase suburban water use. A significantly reduced SWE can result in localized drought.

An increase in particulate concentration can also impact human health. There is a robust literature that details the link between air pollution (especially fine particulates, <0.2 μm) and the prevalence of cardiovascular, pulmonary and skin diseases (Brook et al., 2018; K. Kim, Cho & Park, 2016; Zeng et al., 2017). In general, high particulate exposure increases the disease mortality rate. An increase in the city-particulate rainshadow effect would likely result in increased exposure and mortality. This effect should be pronounced in cities that observe a fairly consistent wind direction as mortality is linked to long-term exposure (Brook et al., 2018). Results suggest that residents who live on the upwind side of the urban core experience are exposed to an elevated level of particulate matter.

While the directional study provides insight into the spatial distribution of particulates, a larger sample size would decrease variability and increase confidence in the data. That said, the time commitment required of additional fieldwork may render this study unfeasible. A simple solution is to expand the number of field technicians. If two teams collected samples simultaneously, sample collection could be accomplished in three hours. Another option is to utilize a continuous monitoring device to measure deposition on snow. Either option would

streamline collection and would constrain fieldwork to a short window of time with ideal sun angles (11a-2p). To improve the quantification of particulates, future research should utilize a SP2 if available.

Further research is required to analyze the city-particulate rainshadow. A transect study through the city could be implemented in parallel to the direction of prevailing wind. Quantification of particulates along this transect would provide insight into distribution of particulate matter relative to the urban core. Other variables (soil moisture, prevalence of respiratory disease) could be examined along the same transect to determine any relationship with particulate matter concentration.

Near-Highway Particulate Concentration

Both source proximity and the placement of obstacles affect particulate distribution in the near-road interface. The highest concentration is found immediately adjacent to the highway. The lowest concentration, however, is not necessarily furthest away. Instead, obstacles, including barrier walls, buildings and vegetation cause particulate matter to recirculate within 600 m of the emission source. Particulate concentration decreases immediately downwind of an obstacle and increases further away.

This effect, known as a recirculation zone, impacts the spatial distribution of particulates near high intensity traffic. According to Bowker et al. (2007), a secondary high concentration is often observed upwards of 550 m away from the interstate. The location of peak concentration depends on the morphology of the obstacle field. Modification of the field can alter this distribution. In many locations, including I-90 in Syracuse, the addition of new obstacles could shift peak particulate concentration into a residential neighborhood. Unlike the city-particulate

rainshadow, the recirculation zone is not constrained to the urban core or surrounding area. Instead, this effect observed near any source or particulate emissions (in this case a highway). Urbanization will likely result in the expansion of the current transportation network both inside and outside of urbanized areas. Increased particulate concentration should follow this growth.

An increase in the near-road particulate concentration has a substantial impact on the environment and human health. Similar to the city-particulate rainshadow, the recirculation zone increases exposure to particulates in affected areas and likely contributes to high mortality. Furthermore, it is possible for, residents to be exposed to both effects (living upwind of the city, near a particulate source). These people will likely suffer the greatest incidence of particulate induced diseases and the highest mortality.

Road expansion and the associated recirculation zone increase present new environmental challenges. These include an expansion of the urban heat island effect. While the urban core experiences the brunt of this temperature increase, suburbs experience some increase as well (Kantzioura, Kosmopoulos & Zoras, 2011). Ye, Wang & Li (2017) note that the urban heat island expands outward from the urban core following the established road network. Near to the city center, this expansion is likely a result of increased urban densification. Outside of this area, however, the effect still exists. An elevated level of particulate matter in the recirculation zone may provide an explanation. On average, the presence of particulate matter in snow increases the surface (0-2 m) air temperature by up to 1 °C (Qian et al., 2009). This causes the snowpack to melt faster and eventually reveals bare ground. The presence of soil or vegetation instead of snow further decreases albedo and warms

the surface via absorption of excess solar radiation. This effect further increases the surface air temperature and intensifies the urban heat island effect.

Elevated levels of near-road particulate matter are not limited to cities. A high-traffic road through an undeveloped area will produce particulate deposition up to 600 m away. Therefore, construction of new roadways can introduce particulate pollution into a pristine environmental system. Once this occurs, any snowmelt in this area will likely carry a substantial amount of particulate matter into the nearby rivers or lakes. Odhiambo and Routh (2016) suggest that an increase in the concentration of black carbon in lake waters may accelerate eutrophication, however, few authors have explored this effect. Nevertheless, an increase in particulate concentration in any waterbody increases exposure of wildlife to particulates. Likewise, an increase in a drinking water supply is likely to increase human consumption of particulate matter and increase mortality.

The transect study provides a preliminary assessment of particulate concentration near an interstate highway or other high traffic road. Results show that spatial patterns of distribution are extremely nuanced. An increase in spatial and/or temporal resolution would provide an opportunity to examine the recirculation zone in more detail. To do this additional sample sites should be added to fill in data gaps along the transect. To address temporal variability, each site should be outfitted with a continuous monitoring device in order to examine deposition patterns over time.

Future research is required to test the relationship between particulate concentration and the spread of urban heat island. A simple experiment could be set up to examine concentration on three transects – in the city, suburbs and in a rural area. Temperature

measurements could be collected alongside particulate concentration and albedo to identify a relationship between the three parameters.

A more complex experiment would be required to test the impact of particulate matter on the local water supply. To do this meltwater should be tested for particulates near a highly trafficked highway and a seldom used backroad. These results would detail the difference in concentration at both locations and could be compared to particulate concentration in water quality samples collected throughout the watershed.

Digital Photography for Particulate Analysis

Digital photography is a cost-effective method to measure snow albedo and by proxy, particulate concentration. This method can accurately determine relative concentration using a digital image and a reference object of known albedo. It is possible to use the results to identify albedo trends within a set of photos, however, a correction factor is required to calculate absolute albedo (Corripio, 2004).

In either case, photo analysis improves the efficiency and accessibility of particulate analysis. Without the correction factor, fieldwork is simple – only one photo of the snow surface is required to assess albedo. This will significantly speed up sampling and limit necessary equipment to a digital camera and reference material (Gilchrist, 2011; Gorski, 2018). Most people have access to a camera (via smartphone technology) and could be easily trained for a photo analysis citizen science project (S. Kim et al., 2011). *The Albedo Project* strives to do this by asking volunteers to collect photos and analyze them in ImageJ. Photos of 91 sites were collected on June 21st, 2011, well beyond the capabilities of an individual sampler (Gorski, 2018). The addition of correction factor measurements makes fieldwork more complicated.

Even so, photo analysis can still streamline data collection. A number of topographic measurements are required to calculate the correction, however, only one set of measurements need to be collected at each sample site. Calculation of the correction factor for each sample set can be completed in the lab using the original topographic measurements (Corripio, 2004).

The photo analysis method removes a significant cost and time barrier to particulate-snow research. Without these constraints, scientists are more likely to conduct extensive studies or create snow-based citizen science projects. A citizen science approach could add substantially to the scarce research on particulate pollution in midlatitude snow. At the city-scale this would help scientists to better understand the city-particulate rainshadow effect. Findings could be disseminated to federal, state or city government and used to develop a particulate mitigation strategy. Currently, city-scale particulate mitigation only addresses airborne particulate matter. Suggested strategies include planting trees for air filtration, street wetting to reduce re-aerosolization and traffic restrictions to reduce overall emissions (Pugh et al., 2012; Slisane & Blumberga, 2013). Additional research could justify new federal regulation to reduce fossil fuel combustion in order to further decrease particulate emissions.

The photo study identifies an efficient method to analyze particulate concentration. While this study is able to identify albedo trends, the quantification of absolute albedo was not successful. To address this, measurements of local topography should be collected and used to create a diffuse radiation correction factor. Additionally, a large, non-reflective and more uniform reference material will help to make measurements more precise and eliminate

brightness variation. Collection of samples at the same time of day and the standardization of camera settings will also make photos more comparable.

Future research is needed to explore the capability of photo analysis for long term particulate study. Citizen scientists could be employed to collect snow surface photos over multiple winter seasons. These data could be used to determine changes in particulate concentration over the long term. In addition, a large number of samplers could be recruited in and around another mid-size, midlatitude city in order to duplicate this study and further examine the city-particulate rainshadow. This method could be paired with UAV collection of snow surface photos. A UAV could be flown near a source of particulate emissions. Collected imagery would be analyzed in ImageJ to determine how albedo patterns change near the source. Results could be compared to in situ monitoring of snow, reflectivity and wind in order to determine the microscale aerodynamic forces that affect particulate dispersal.

Final Thoughts

The distribution of particulate matter in midlatitude seasonal snow is not well understood. This thesis addresses this deficiency by exploring particulate distribution at the city-scale. Results show that particulates are concentrated upwind of the urban core, whereas, the area immediately downwind remains relatively clean. This effect, dubbed the city-particulate rainshadow, is the opposite of the original assumed hypothesis. Further study is needed to examine the extent and intensity of the particulate rainshadow in greater detail. The use of citizen scientists may prove to be an effective means to accomplish this. Continued exploration of particulate matter concentration in midlatitude seasonal snow is essential to better understand how particulate-snow interactions affect the broader environmental system.

Appendix A

Location, GPS coordinates and brief description of sites selected for this study

Site Code	Type of site	Site Location	GPS Coordinates	Local Description
N	Directional	Heritage Park	43.13731, -76.141905	Samples were collected from a grass field. There is a gravel walking path 8 m NW, a baseball field 125 m NW, residential housing 36 m E and a paved parking lot 24 m SW.
NE	Directional	Maxwell Park	43.112119, -76.066616	Samples were collected from a large grass field. There is a gravel parking lot 30 m W, a baseball field 70 m NW, residential houses 60 m S. Low flying planes occasionally pass over the site.
E	Directional	Green Lakes State Park	43.049759, -75.978727	Samples were collected from a grass field. There is a dirt road encircling the field 10 m away as well as a number of campsites 20 m from the site. A playground sits 6 m to the NW.
SE	Directional	Jamesville Reservoir DEC fishing access	42.982072, -76.070449	Samples were collected from a grass field. A number of trees surround the site at a distance of 15 m, a paved parking lot is 31 m NW, Jamesville Reservoir is 45 m SE and the Onondaga County DOT is 100 m W.
S	Directional	Fred Stafford Memorial Park	42.913396, -76.116961	Samples were collected from a grass field. There is a paved walking path 12 m NE, a gravel parking lot 25 m NE, a picnic pavilion 25 m W, a dirt playground 20 m NW and a paved walking path 8 m N. Interstate 81 is about 100 m SW.

SW	Directional	Onondaga Community College	43.01105, -76.199476	Samples were collected from a grass field. There is a county road 35 m NE, a local road 18 m SW, a paved parking lot 75 m SW, a paved maintenance path 30 m SE and a turf baseball field 41 m SE.
W	Directional	Camillus Park	43.044042, -76.281193	Samples were collected from a grass field. There is a small paved parking area 10 m S, a water splash pad 10 m N, a paved sidewalk 12 m E and a large paved parking lot 37 m SE.
NW	Directional	Van Buren Central Park	43.123591, -76.327391	Samples were collected from a grass field. There is a paved access road 28 m W, a small lake 40 m N, a small creek 38 m E and a county road 75 m S. A well-used sledding hill is located 90 m W
Sky	Directional	Syracuse University South Campus	43.011631, -76.110553	Samples are collected from a meadow. There is a dirt road 30m south and a gravel parking lot 100m south. The lot is occasionally used for event parking.
I90A	Transect	Onondaga Lake County Park	43.116392, -76.242041	Samples were collected from a grass field 20 m from the edge of the interstate. There is a paved walking path 28 m SE, an unplowed parking lot 25 m E, Onondaga Lake 75 m SW and a large number of trees 15 m S and W.
I90B	Transect	Onondaga Lake County Park	43.115973, -76.241807	Samples were collected from a grass field 70 m from the edge of the interstate. There is a paved walking path 14 m N, an unplowed parking lot 33 m NE, Onondaga Lake 45 m SW and a large number of trees 8 m E and W.

I90C	Transect	Onondaga Lake County Park	43.115651, -76.241426	Samples were collected from a grass field 115 m from the edge of the interstate. There is a kayak rental shop 60 m SE, Onondaga Lake 17 m W and a large number of trees 10 m E, W and S.
I90D	Transect	Onondaga Lake County Park	43.11684, -76.243005	Samples were collected from a grass field 20 m from the edge of the interstate. There is a paved walking path 25 m NW, NE, Onondaga Lake 55 m W and a large number of trees within 5 m of the site.
I90E	Transect	Onondaga Lake County Park	43.117157, -76.243011	Samples were collected from a grass field 60 m from the edge of the interstate. There is a paved walking path 23 m NW, Onondaga Lake 91 m SW and a large number of trees within 5 m of the site.
I90F	Transect	Onondaga Lake County Park	43.11756, -76.243103	Samples were collected from a grass field 100 m from the edge of the interstate. There is a paved walking path 14 m W, Onondaga Lake 70 m SW, a local road 30 m NE and a large number of trees 11 m N.

Appendix B

Selected data collected throughout the study

Date	Study type	Sample Site	Snow Depth (cm)	Snow Temperature (°C)	Field Albedo	Particulates ((W/m2)/ml)	Photo Albedo
2/18/2017	directional	N	14	0.6	0.26173913	nm	nm
2/18/2017	directional	NE	12.5	-0.9	0.258899676	nm	nm
2/18/2017	directional	E	12.5	0.2	0.279310345	nm	nm
2/18/2017	directional	SE	10	-0.2	0.269819193	nm	nm
2/18/2017	directional	S	14.5	-1	0.861111111	nm	nm
2/18/2017	directional	SW	11	-0.9	0.942622951	nm	nm
2/18/2017	directional	W	9	-1.1	0.909426987	nm	nm
2/19/2017	directional	NW	7	0.1	0.663507109	nm	nm
3/15/2017	directional	N	40	-5.5	0.62704918	nm	nm
3/15/2017	directional	NE	49	-4.1	0.757925072	nm	nm
3/15/2017	directional	E	48	-3.9	0.787974684	nm	nm
3/15/2017	directional	SE	38	-6.1	0.787072243	nm	nm
3/15/2017	directional	S	48	-8.7	0.83125	nm	nm
3/15/2017	directional	SW	37	nm	0.757009346	nm	nm
3/15/2017	directional	W	59	nm	0.743589744	nm	nm
3/15/2017	directional	NW	33	nm	0.79245283	nm	nm
3/15/2017	transect	I90C	27	-7	0.853846154	nm	nm
3/15/2017	transect	I90B	30.5	-3.6	0.774774775	nm	nm
3/15/2017	transect	I90A	34	-4.4	0.582758621	nm	nm
3/15/2017	transect	I90D	41	-3	0.613207547	nm	nm
3/15/2017	transect	I90E	38	-2.2	0.810720268	nm	nm
3/15/2017	transect	I90F	30	-1.3	0.847145488	nm	nm
3/22/2017	directional	N	19.5	-13.5	0.590994371	nm	nm
3/22/2017	directional	NE	18	-3.3	0.709026128	nm	nm
3/22/2017	directional	E	15	-2.7	0.75549806	nm	nm
3/22/2017	directional	SE	15	-2.5	0.770676692	nm	nm
3/22/2017	directional	S	22	-4	0.743651753	nm	nm
3/22/2017	directional	SW	16	-1.3	0.751219512	nm	nm
3/22/2017	directional	W	18	-0.4	0.773314204	nm	nm
3/22/2017	directional	NW	16.5	-7.3	0.624793388	nm	nm
3/22/2017	transect	I90C	8	-4.5	0.696907216	nm	nm
3/22/2017	transect	I90B	nm	nm	nm	nm	nm
3/22/2017	transect	I90A	12	-3.2	0.777996071	nm	nm
3/22/2017	transect	I90D	17	-6	0.823529412	nm	nm
3/22/2017	transect	I90E	nm	nm	nm	nm	nm

Date	Study type	Sample Site	Snow Depth (cm)	Snow Temperature (°C)	Field Albedo	Particulates ((W/m2)/ml)	Photo Albedo
3/22/2017	transect	I90F	13	-6.6	0.687041565	nm	nm
11/21/2017	directional	N	5	-0.4	0.68556701	nm	nm
11/21/2017	directional	NE	4	1	0.711442786	nm	nm
11/21/2017	directional	E	3	1.6	0.59602649	nm	nm
11/21/2017	directional	W	5	-2.5	0.716535433	nm	nm
11/21/2017	directional	NW	5.5	-1.1	0.738636364	nm	nm
11/20/2017	transect	I90C	8.5	-3	0.791666667	8.488636364	nm
11/20/2017	transect	I90B	8	-2.9	0.759259259	8.432098765	nm
11/20/2017	transect	I90A	12	-2.8	0.684931507	8.568181818	nm
11/20/2017	transect	I90D	6.5	-0.3	0.714285714	7.479166667	nm
11/20/2017	transect	I90E	9	-0.4	0.75	8.529411765	nm
11/20/2017	transect	I90F	11	-1	0.719298246	8.697247706	nm
12/15/2017	directional	N	17	-15.4	0.784615385	9.492857143	0.721626
12/15/2017	directional	NE	14	-7.1	0.774834437	9.369747899	0.676496
12/15/2017	directional	E	13.5	-5.2	0.75879397	9.25	0.616566
12/15/2017	directional	SE	9.5	-4.1	0.930232558	9.43220339	0.704279
12/15/2017	directional	S	11.5	-4.5	0.866995074	9.437246964	0.785637
12/15/2017	directional	SW	11	-6.5	0.79047619	9.581168831	0.729546
12/15/2017	directional	W	13	-6	0.773584906	9.518272425	0.622598
12/15/2017	directional	NW	13	-5.6	0.733333333	9.404958678	0.687129
12/15/2017	directional	Sky	15	-4.8	0.764705882	9.406779661	0.554219
12/14/2017	transect	I90C	16	nm	0.789473684	nm	nm
12/14/2017	transect	I90B	18	nm	0.790322581	nm	nm
12/14/2017	transect	I90A	17.5	-12.5	0.776041667	nm	nm
1/7/2018	directional	N	34	-29.4	0.74025974	9.268882175	0.953066
1/7/2018	directional	NE	28	-12	0.80781759	9.099337748	0.903943
1/7/2018	directional	E	27	-12.4	0.967741935	8.947368421	0.80081
1/7/2018	directional	SE	23.5	-11.3	0.85	8.714953271	0.82912
1/7/2018	directional	S	30.5	-11.3	0.856041131	9.325581395	0.935605
1/7/2018	directional	SW	33	-10.1	0.873303167	9.305084746	1.020485
1/7/2018	directional	W	39	-14.2	0.859649123	9.279411765	0.812571
1/7/2018	directional	NW	31	-6.1	0.8125	9.365591398	0.66434
1/7/2018	directional	Sky	23	-9	0.860759494	8.91322314	1.004683
1/7/2018	transect	I90C	29	-12.2	0.833333333	lost sample	nm
1/7/2018	transect	I90B	23	-12.2	0.818181818	9.780621572	nm
1/7/2018	transect	I90A	27.5	-13.3	0.741935484	9.865558912	nm
1/7/2018	transect	I90D	24	-11.9	0.774509804	9.751313485	nm
1/7/2018	transect	I90E	24	-14.5	0.780821918	9.728515625	nm
1/7/2018	transect	I90F	35	-14.4	0.761904762	9.8125	nm

Date	Study type	Sample Site	Snow Depth (cm)	Snow Temperature (°C)	Field Albedo	Particulates ((W/m2)/ml)	Photo Albedo
1/21/2018	transect	I90C	11.5	3.2	0.627118644	9.704954955	nm
1/21/2018	transect	I90B	12	2.1	0.866972477	9.761904762	nm
1/21/2018	transect	I90A	17	-0.4	0.643678161	9.725581395	nm
1/21/2018	transect	I90D	12.5	0.1	0.658536585	9.794059406	nm
1/21/2018	transect	I90E	12	2.1	0.642045455	9.774621212	nm
1/21/2018	transect	I90F	16.5	1.2	0.779141104	9.752598753	nm
2/9/2018	directional	N	23.5	-3.5	0.754716981	9.190972222	nm
2/9/2018	directional	NE	26	-4.6	too dark	9.069444444	nm
2/9/2018	directional	E	27.5	-5.5	too dark	9.046931408	nm
2/9/2018	directional	SE	18	-3.1	0.759689922	8.488764045	nm
2/9/2018	directional	S	28	-4.1	0.752688172	9.213017751	nm
2/9/2018	directional	SW	23.5	-3.1	0.761904762	9.02962963	nm
2/9/2018	directional	W	23	-3.2	0.764705882	8.771689498	nm
2/9/2018	directional	NW	24	-3.2	0.766666667	9.072413793	nm
2/9/2018	directional	Sky	22.5	-4.9	0.761904762	8.809090909	nm
2/13/2018	directional	N	13.5	-0.9	0.680981595	9.556561086	0.745868
2/13/2018	directional	NE	14.5	nm	0.75	9.242647059	0.783786
2/13/2018	directional	E	12	-4.1	0.711009174	9.656529517	0.754855
2/13/2018	directional	SE	8	-2.6	0.739726027	9.309701493	0.931738
2/13/2018	directional	S	12.5	-5.3	0.740384615	9.697520661	0.973617
2/13/2018	directional	SW	12.5	-6.9	0.775	9.544811321	0.825172
2/13/2018	directional	W	11.5	-10	0.793103448	9.554565702	0.734142
2/13/2018	directional	NW	17.5	-10	0.666666667	9.488607595	0.815111
3/6/2018	directional	N	12	1	0.701176471	9.596153846	0.65686
3/6/2018	directional	NE	17.5	2.9	0.745985401	9.738878143	0.706237
3/6/2018	directional	E	29.5	0.6	0.787550744	9.5625	0.730376
3/6/2018	directional	SE	14	0.8	0.81097561	9.62565445	0.808424
3/6/2018	directional	S	20	2.8	0.886877828	9.728464419	0.844575
3/6/2018	directional	SW	23	-0.2	0.809090909	9.740601504	0.872363
3/6/2018	directional	W	13	-0.4	0.663934426	9.555882353	0.638567
3/6/2018	directional	NW	8	0.3	0.676923077	9.697309417	0.665946
3/6/2018	directional	Sky	21.5	5.4	0.855384615	9.72761194	0.730016
3/6/2018	transect	I90C	6	-2.2	0.662921348	9.688679245	nm
3/6/2018	transect	I90B	8.5	-1.3	0.663716814	9.652892562	nm
3/6/2018	transect	I90A	12	0.9	0.637037037	9.671270718	nm
3/6/2018	transect	I90D	8	-2.7	0.642857143	9.708433735	nm
3/6/2018	transect	I90E	16	-2.3	0.679245283	9.620967742	nm
3/6/2018	transect	I90F	8	-2.1	0.666666667	9.709976798	nm

References

Adolph, A. C., Albert, M. R., Lazarcik, J., Dibb, J. E., Amante, J. M., & Price, A. (2017). Dominance of grain size impacts on seasonal snow albedo at open sites in New Hampshire. *Journal of Geophysical Research: Atmospheres, 122*(1), 121-139. doi:10.1002/2016JD025362

Allen, J. M. (1842). The Onondaga Salines: Locality of brine springs. sources of the brine. manufacture. use of salt. *Northern Light; Devoted to Free Discussion, and to the Diffusion of Useful Knowledge, Miscellaneous Literature, and General Intelligence (1841-1844), 1*(10), 153.

Anoplate. (2018). *Company Profile.* Retrieved from: https://www.anoplate.com/about/

Becker, M. (2018, February 9). An upstate town just hit the 300-inch mark for snow. *The Buffalo News.* Retrieved from: http://buffalonews.com/2018/02/09/an-upstate-town-just-hit-the-300-inch-mark-for-snow/

Bergeron, E. (2017). *From sovereignty to superfund: The Onondaga nation's legal battle for land rights, environmental justice, and the remediation of Onondaga Lake* (Doctoral dissertation, Cornell University).

Bernard, É., Friedt, J. M., Tolle, F., Griselin, M., Martin, G., Laffly, D., & Marlin, C. (2013). Monitoring seasonal snow dynamics using ground based high resolution photography (Austre Lovénbreen, Svalbard, 79°N). *ISPRS Journal of Photogrammetry and Remote Sensing, 75*, 92-100. doi:10.1016/j.isprsjprs.2012.11.001

Bernard, É., Friedt, J. M., Tolle, F., Griselin, M., Marlin, C., & Prokop, A. (2017). Investigating snowpack volumes and icing dynamics in the moraine of an arctic catchment using UAV photogrammetry. *The Photogrammetric Record, 32*(160), 497-512. doi:10.1111/phor.12217

Blankinship, J. C., Meadows, M. W., Lucas, R. G., & Hart, S. C. (2014). Snowmelt timing alters shallow but not deep soil moisture in the Sierra Nevada. *Water Resources Research, 50*(2), 1448-1456. doi:10.1002/2013WR014541

Boike, J., & Yoshikawa, K. (2003). Mapping of periglacial geomorphology using kite/balloon aerial photography. *Permafrost and Periglacial Processes, 14*(1), 81-85. doi:10.1002/ppp.437

Bond, T. C., Doherty, S. J., Fahey, D. W., Forster, P. M., Berntsen, T., DeAngelo, B. J., ... & Kinne, S. (2013). Bounding the role of black carbon in the climate system: A scientific assessment. *Journal of Geophysical Research: Atmospheres, 118*(11), 5380-5552.

Bowker, G. E., Baldauf, R., Isakov, V., Khlystov, A., & Petersen, W. (2007). The effects of roadside structures on the transport and dispersion of ultrafine particles from highways. *Atmospheric Environment, 41*(37), 8128-8139. doi:10.1016/j.atmosenv.2007.06.064

Briggs, N. L., & Long, C. M. (2016). Critical review of black carbon and elemental carbon source apportionment in Europe and the United States. *Atmospheric Environment, 144*, 409-427. doi:10.1016/j.atmosenv.2016.09.002

Bristol-Meyers Squibb. (2018). *Syracuse, New York: Facts and Figures.* Retrieved from: https://www.bms.com/about-us/our-company/worldwide-facilities/syracuse-new-york.html

Brook, R. D., Rajagopalan, S., Pope, C. A., Brook, J. R., Bhatnagar, A., Diez-Roux, A. V., . . . on behalf of the American Heart Association Council on Epidemiology and Prevention, Council on the Kidney in Cardiovascular Disease, and Council on Nutrition, Physical Activity and Metabolism. (2010). Particulate matter air pollution and cardiovascular disease: An update to the scientific statement from the American Heart Association. *Circulation, 121*(21), 2331-2378. doi:10.1161/CIR.0b013e3181dbece1

Buckley, S. M., & Mitchell, M. J. (2011). Improvements in urban air quality: Case studies from New York State, USA. *Water, Air, & Soil Pollution, 214*(1), 93-106. doi:10.1007/s11270-010-0407-z

Call, D. A. (2004). *Urban Snow Events in Upstate New York: An Integrated Human and Physical Geographical Analysis* (Thesis). Syracuse University, Syracuse, NY.

Call, D. A. (2005). Rethinking snowstorms as snow events: A regional case study from upstate New York. *Bulletin of the American Meteorological Society, 86*(12), 1783-1793. doi:10.1175/BAMS-86-12-1783

Cereceda-Balic, F., Vidal, V., Moosmuller, H., & Lapuerta, M. (2018). Reduction of snow albedo from vehicle emissions at Portillo, Chile. *Cold Regions Science and Technology, 146*, 43-52. doi:10.1016/j.coldregions.2017.11.008

Changnon, D., Merinsky, C., & Lawson, M. (2008). Climatology of surface cyclone tracks associated with large central and eastern U.S. snowstorms, 1950–2000. *Monthly Weather Review, 136*(8), 3193-3202. doi:10.1175/2008MWR2324.1

Coin, G. (2018, March 20). Fourth winter storm in three weeks should just graze Upstate NY. *Syracuse.com.* Retrieved from: http://www.syracuse.com/weather/index.ssf/2018/03/fourth_winter_storm_in_three_weeks_should_just_graze_upstate_ny.html

Corripio, J. G. (2004). Snow surface albedo estimation using terrestrial photography. *International Journal of Remote Sensing, 25*(24), 5705-5729. doi:10.1080/01431160410001709002

Crucible Industries. (2018). *Our History.* Retrieved from: http://www.crucible.com/history.aspx

Cui, X., Wang, X., Yang, L., Chen, B., Chen, J., Andersson, A., & Gustafsson, Ö. (2016). Radiative absorption enhancement from coatings on black carbon aerosols. *Science of the Total Environment*, 551, 51-56. doi:10.1016/j.scitotenv.2016.02.026

Dang, C., Warren, S. G., Fu, Q., Doherty, S. J., Sturm, M., & Su, J. (2017). Measurements of light-absorbing particles in snow across the arctic, North America, and China: Effects on surface albedo. *Journal of Geophysical Research: Atmospheres, 122*(19), 10,149-10,168. doi:10.1002/2017JD027070

Dickinson, J. L., Shirk, J., Bonter, D., Bonney, R., Crain, R. L., Martin, J., . . . Purcell, K. (2012). The current state of citizen science as a tool for ecological research and public engagement. *Frontiers in Ecology and the Environment, 10*(6), 291-297. doi:10.1890/110236

Di Mauro, B., Fava, F., Ferrero, L., Garzonio, R., Baccolo, G., Delmonte, B., & Colombo, R. (2015). Mineral dust impact on snow radiative properties in the European Alps combining ground, UAV, and satellite observations. *Journal of Geophysical Research: Atmospheres, 120*(12), 6080-6097. doi:10.1002/2015JD023287

Dirmhirn, I., & Eaton, F. (1975). Some characteristics of albedo of snow. *Journal of Applied Meteorology, 14*(3), 375-379.

Doherty, S. J., Warren, S. G., Grenfell, T. C., Clarke, A. D., & Brandt, R. E. (2010). Light-absorbing impurities in arctic snow. *Atmospheric Chemistry and Physics, 10*(23), 11647-11680. doi:10.5194/acp-10-11647-2010

Doherty, S. J., Dang, C., Hegg, D. A., Zhang, R., & Warren, S. G. (2014). Black carbon and other light-absorbing particles in snow of central North America: Black carbon in North American snow. *Journal of Geophysical Research: Atmospheres, 119*(22), 12-12,831. doi:10.1002/2014JD022350

Doherty, S. J., Hegg, D. A., Johnson, J. E., Quinn, P. K., Schwarz, J. P., Dang, C., & Warren, S. G. (2016). Causes of variability in light absorption by particles in snow at sites in Idaho and Utah. *Journal of Geophysical Research: Atmospheres, 121*(9), 4751-4768. doi:10.1002/2015JD024375

Dong, C., & Menzel, L. (2017). Snow process monitoring in montane forests with time-lapse photography. *Hydrological Processes, 31*(16), 2872-2886. doi:10.1002/hyp.11229

Du, K., Wang, Y., Chen, B., Wang, K., Chen, J., & Zhang, F. (2011). Digital photographic method to quantify black carbon in ambient aerosols. *Atmospheric Environment, 45*(39), 7113-7120. doi:10.1016/j.atmosenv.2011.09.035

Du, K., Shi, P., Rood, M. J., Wang, K., Wang, Y., & Varma, R. M. (2013). Digital optical method to quantify the visual opacity of fugitive plumes. Atmospheric Environment, 77, 983-989. doi:10.1016/j.atmosenv.2013.06.017

Effler, S. W. (Ed.). (1996). Limnological and engineering analysis of a polluted urban lake. New York, NY: Springer-Verlag.

Effler, S. W., & Hennigan, R. D. (1996). Onondaga Lake, New York: legacy of pollution. *Lake and Reservoir Management*, *12*(1), 1-12.

Ferreira, T. & Rasband, W. (2012). *ImageJ User Guide: IJ 1.46r.* Retrieved from: https://imagej.nih.gov/ij/docs/guide/user-guide.pdf

Gertler, A. W., Gillies, J. A., & Pierson, W. R. (2000). An assessment of the mobile source contribution to PM10 and PM2.5 in the United States. *Water, Air, and Soil Pollution, 123*(1), 203-214. doi:10.1023/A:1005263220659

Gertler, C. G., Puppala, S. P., Panday, A., Stumm, D., & Shea, J. (2016). Black carbon and the Himalayan cryosphere: A review. *Atmospheric Environment, 125*, 404-417.

Gilchrist, G. (2011). *A simple method to determine surface albedo using digital photography.* Retrieved from: https://www.semanticscholar.org/paper/A-simple-method-to-determine-surface-albedo-using-Gilchrist/e8bcd52452898dd1239679e24fbb5c19bb504657

Gorski, K. M. (2018). *The Albedo Project.* Retrieved from: https://sites.google.com/site/albedoproject/

Gray, D. M., & Male, D. H. (Eds.). (1981). *Handbook of snow: principles, processes, management & use.* Pergamon Press.

Greenlar, M. (2018, February 7). Live updates: Powerful snowstorm hits Upstate NY. *Syracuse.com.* Retrieved from: http://www.syracuse.com/weather/index.ssf/2018/02/live_updates_powerful_snowstorm_hits_upstate_ny.html#incart_river_index

Grenfell, T. C., Doherty, S. J., Clarke, A. D., & Warren, S. G. (2011). Light absorption from particulate impurities in snow and ice determined by spectrophotometric analysis of filters. *Applied Optics, 50*(14), 2037.

Grimmond, C. S. B., King, T. S., Cropley, F. D., Nowak, D. J., & Souch, C. (2002). Local-scale fluxes of carbon dioxide in urban environments: Methodological challenges and results from Chicago. *Environmental Pollution, 116*(1), S243-S254. doi:10.1016/S0269-7491(01)00256-1

Grishagin, I. V. (2015). Automatic cell counting with ImageJ. *Analytical Biochemistry, 473*, 63-65. doi:10.1016/j.ab.2014.12.007

Gul, C., Puppala, S. P., Kang, S., Adhikary, B., Zhang, Y., Ali, S., . . . Li, X. (2018). Concentrations and source regions of light-absorbing particles in snow/ice in Northern Pakistan and their impact on snow albedo. *Atmospheric Chemistry and Physics, 18*(7), 4981-5000. doi:10.5194/acp-18-4981-201

Heal, M. R., & Hammonds, M. D. (2014). Insights into the composition and sources of rural, urban and roadside carbonaceous PM_{10}. *Environmental Science & Technology, 48*(16), 8995.

Igathinathane, C., Pordesimo, L. O., Columbus, E. P., Batchelor, W. D., & Methuku, S. R. (2008). Shape identification and particles size distribution from basic shape parameters using ImageJ. *Computers and Electronics in Agriculture, 63*(2), 168-182. doi:10.1016/j.compag.2008.02.007

Jacobi, H-W., Lim, S., Ménégoz, M., Ginot, P., Laj, P., Bonasoni, P., . . . Arnaud, Y. (2015). Black carbon in snow in the upper Himalayan Khumbu valley, Nepal: Observations and modeling of the impact on snow albedo, melting, and radiative forcing. *The Cryosphere, 9*(4), 1685-1699. doi:10.5194/tc-9-1685-2015

Jensen, E. C. (2013). Quantitative analysis of histological staining and fluorescence using ImageJ. *The Anatomical Record, 296*(3), 378-381. doi:10.1002/ar.22641

Kappel, W. M., Teece, M. A., Geological Survey (U.S.), Onondaga Lake Partnership, & Onondaga Environmental Institute. (2007). *Paleoenvironmental assessment and deglacial chronology of the Onondaga trough, Onondaga county, New York*. Reston, Va: U.S. Geological Survey.

Kantzioura, A., Kosmopoulos, P., & Zoras, S. (2012). Urban surface temperature and microclimate measurements in Thessaloniki. *Energy & Buildings, 44*(1), 63-72. doi:10.1016/j.enbuild.2011.10.019

Keegan, K. M., Albert, M. R., McConnell, J. R., & Baker, I. (2014). Climate change and forest fires synergistically drive widespread melt events of the Greenland ice sheet. *Proceedings of the National Academy of Sciences of the United States of America, 111*(22), 7964-7967. doi:10.1073/pnas.1405397111

Khan, A. L., Dierssen, H., Schwarz, J. P., Schmitt, C., Chlus, A., Hermanson, M., . . . McKnight, D. M. (2017). Impacts of coal dust from an active mine on the spectral reflectance of arctic surface snow in Svalbard, Norway. *Journal of Geophysical Research: Atmospheres, 122*(3), 1767-1778. doi:10.1002/2016JD025757

Kim, K. E., Cho, D., & Park, H. J. (2016). Air pollution and skin diseases: Adverse effects of airborne particulate matter on various skin diseases. *Life Sciences, 152*, 126-134. doi:10.1016/j.lfs.2016.03.039

Kim, M. (2002). *Regional characteristics of fine particulate matter pollution in the upper Ohio River Valley.* (Thesis) Texas A&M University, Kingsville, TX.

Kim, S., Robson, C., Zimmerman, T., Pierce, J., & Haber, E. M. (2011, May). Creek watch: pairing usefulness and usability for successful citizen science. Proceedings from *SIGCHI Conference on Human Factors in Computing Systems* (pp. 2125-2134). ACM. doi:10.1145/1978942.1979251

Kinar, N. J., & Pomeroy, J. W. (2015). Measurement of the physical properties of the snowpack. *Reviews of Geophysics, 53*(2), 481-544. doi:10.1002/2015RG000481

Kirst, S. (2013, April 4). For the snowfall national championship: It looks like Syracuse, in a come-from-behind win. *Syracuse.com.* Retrieved from: http://www.syracuse.com/kirst/index.ssf/2013/04/post_465.html

Kirst, S. (2010, July 6). Steve Effler: The truth-teller of Onondaga Lake. *Syracuse.com*. Retrieved from: https://www.syracuse.com/kirst/index.ssf/2010/07/effler_onondaga_lake_truth-tel.html

Kuchiki, K., Aoki, T., Niwano, M., Matoba, S., Kodama, Y., & Adachi, K. (2015). Elemental carbon, organic carbon, and dust concentrations in snow measured with thermal optical and gravimetric methods: Variations during the 2007–2013 winters at Sapporo, Japan. *Journal of Geophysical Research: Atmospheres, 120*(2), 868-882. doi:10.1002/2014JD022144

Kuliński, K., Kędra, M., Legeżyńska, J., Gluchowska, M., & Zaborska, A. (2014). Particulate organic matter sinks and sources in high arctic fjord. *Journal of Marine Systems, 139*, 27-37. doi:10.1016/j.jmarsys.2014.04.018

Langone, A. (2018, March 25). Orange snow hit parts of Europe this weekend. *Time.* Retrieved from: http://time.com/5214941/orange-snow-europe/

Lendzioch, T., Langhammer, J., & Jenicek, M. (2016). tracking forest and open area effects on snow accumulation by unmanned aerial vehicle photogrammetry. *The International*

Archives of Photogrammetry, Remote Sensing and Spatial Information Sciences, XLI-B1, 917-923. doi:10.5194/isprs-archives-XLI-B1-917-2016

Lestari, P., Oskouie, A. K., & Noll, K. E. (2003). Size distribution and dry deposition of particulate mass, sulfate and nitrate in an urban area. *Atmospheric Environment, 37*(18), 2507-2516. doi:10.1016/S1352-2310(03)00151-1

Li, W., Wang, C., Wang, H., Chen, J., Yuan, C., Li, T., … & Tao, S. (2014). Distribution of atmospheric particulate matter (PM) in rural field, rural village and urban areas of northern china. *Environmental Pollution, 185*, 134-140. doi:10.1016/j.envpol.2013.10.042

Liu, J., Fan, S., Horowitz, L. W., & Levy, H. (2011). Evaluation of factors controlling long-range transport of black carbon to the arctic. *Journal of Geophysical Research Atmospheres, 116*(4), 1R. doi:10.1029/2010JD015145

Loveless, D. M., Godek, M.L. & Blechman, J. (2014). Developing a climatology of snowfall events in Oneonta, New York. *Northern Geoscience, 32*, 44-55.

Lund, M. T., Berntsen, T. K., Heyes, C., Klimont, Z., & Samset, B. H. (2014). Global and regional climate impacts of black carbon and co-emitted species from the on-road diesel sector. *Atmospheric Environment, 98*, 50-58. doi:10.1016/j.atmosenv.2014.08.033

Maloof, J. N., Nozue, K., Mumbach, M. R., & Palmer, C. M. (2013). LeafJ: An ImageJ plugin for semi-automated leaf shape measurement. *Journal of Visualized Experiment*s, (71) doi:10.3791/50028

Medrzycka, D., Benn, D. I., Box, J. E., Copland, L., & Balog, J. (2016). Calving behavior at rink Isbræ, West Greenland, from time-lapse photos. *Arctic, Antarctic, and Alpine Research, 48*(2), 263-277. doi:10.1657/AAAR0015-059

Midwestern Regional Climate Center. (2018). [A collection of mapping tools visualize long term climate data recorded at weather stations across the US]. *cli-MATE: MRCC Application Tools Environment.* Retrieved from: http://mrcc.isws.illinois.edu/CLIMATE/welcome.jsp

Millar, S. W. S. (2017). Plowing paradise: Snow clearing and urban solar radiation absorption. *Physical Geography, 38*(2), 197-209. doi:10.1080/02723646.2016.1242351

Miner, T. J., & Fritsch, J. M. (1997). Lake-effect rain events. *Monthly weather review, 125*(12), 3231-3248.

Miziński, B., & Niedzielski, T. (2017). Fully-automated estimation of snow depth in near real time with the use of unmanned aerial vehicles without utilizing ground control points.

Cold Regions Science and Technology, 138, 63-72. doi:10.1016/j.coldregions.2017.03.006

Monmonier, M. S. (2012). *Lake effect: tales of large lakes, arctic winds, and recurrent snows*. Syracuse, New York: Syracuse University Press.

Moran, J. M., & Morgan, M. D. (1973). Snow sampling: A student project for determination of urban air-borne particulate distribution. *The Science Teacher, 40*(8), 38-39.

National Centers for Environmental Information [formerly the National Climatic Data Center]. (n.d.). *Climate of New York.* Climate Services Branch: Asheville, NC. Retrieved from: https://www.ncdc.noaa.gov/climatenormals/clim60/states/Clim_NY_01.pdf

National Centers for Environmental Information [formerly National Climatic Data Center]. (2018). *Local Climatological Data Station Details: Syracuse Hancock International Airport, NY, US.* Retrieved from: https://www.ncdc.noaa.gov/cdo-web/datasets/LCD/stations/WBAN:14771/detail

National Weather Service. (2018). [A collection of maps, charts and discussions of past weather phenomena]. *Weather Prediction Center: WPC Product Archive.* Retrieved from: http://www.wpc.ncep.noaa.gov/archives/web_pages/wpc_arch/get_wpc_archives.php

Neff, W. D. (1997). The Denver Brown Cloud studies from the perspective of model assessment needs and the role of meteorology. *Journal of the Air & Waste Management Association, 47*(3), 269-285.

Neumann, N. N., Derksen, C., Smith, C., & Goodison, B. (2006). Characterizing local scale snow cover using point measurements during the winter season. *Atmosphere-Ocean, 44*(3), 257-269. doi:10.3137/ao.440304

New York State Department of Transportation. (2004). *2004 Traffic Data Report for New York State.* New York State Highway Data Services Bureau: Albany, NY. Retrieved from: https://www.dot.ny.gov/divisions/engineering/technical-services/hds-respository/Traffic%20Data%20Report%202004.pdf

New York State Department of Transportation. (2018). [Interactive map of daily traffic averages on New York State roads in 2015]. *NYS Traffic Data Viewer.* Retrieved from: https://www.dot.ny.gov/tdv

Ni, M., Huang, J., Lu, S., Li, X., Yan, J., & Cen, K. (2014). A review on black carbon emissions, worldwide and in China. *Chemosphere, 107*, 83-93. doi:10.1016/j.chemosphere.2014.02.052

Niu, H. [Hewen], Kang, S., Shi, X., Paudyal, R., He, Y., Li, G., ... & Shi, X. (2017a). In-situ measurements of light-absorbing impurities in snow of glacier on Mt. Yulong and implications for radiative forcing estimates. *Science of The Total Environment, 581*, 848-856.

Niu, H. [Hewen], Kang, S., Zhang, Y., Shi, X., Shi, X., Wang, S. … & He, Y. (2017b). Distribution of light-absorbing impurities in snow of glacier on Mt. Yulong, southeastern Tibetan Plateau. *Atmospheric Research, 197*, 474-484. doi:10.1016/j.atmosres.2017.07.004

Niu, H. [Honghong], Wang, B., Liu, B., Liu, Y., Liu, J., & Wang, Z. (2017). Numerical simulations of the effect of building configurations and wind direction on fine particulate matters dispersion in a street canyon. *Environmental Fluid Mechanics,* 1-19. doi:10.1007/s10652-017-9563-7

Niziol, T. A., Snyder, W. R., & Waldstreicher, J. S. (1995). Winter weather forecasting throughout the eastern United States. part IV: Lake effect snow. *Weather and Forecasting, 10*(1), 61-77. doi:10.1175/1520-0434(1995)010<0061:WWFTTE>2.0.CO;2

Odhiambo, M., & Routh, J. (2016). Does black carbon contribute to eutrophication in large lakes? *Current Pollution Reports, 2*(4), 236-238. doi:10.1007/s40726-016-0042-4

O'Toole, C. (2016, November 22). Syracuse sees 2nd snowiest day in November – ever. *Syracuse.com.* Retrieved from: http://www.syracuse.com/weather/index.ssf/2016/11/syracuse_sees_2nd_snowiest_day_in_november_--_ever.html

Pedersen, C. A., Gallet, J. C., Ström, J., Gerland, S., Hudson, S. R., Forsström, S., ... & Berntsen, T. K. (2015). In situ observations of black carbon in snow and the corresponding spectral surface albedo reduction. *Journal of Geophysical Research: Atmospheres, 120*(4), 1476-1489. doi:10.1002/2014JD022407

Persad, G. G., Ming, Y., & Ramaswamy, V. (2012). Tropical tropospheric-only responses to absorbing aerosols. *Journal of Climate, 25*(7), 2471-2480. doi:10.1175/JCLI-D-11-00122.1

Pimentel, R., Herrero, J., & Polo, M. J. (2012, October). Terrestrial photography as an alternative to satellite images to study snow cover evolution at hillslope scale. *Remote Sensing for Agriculture, Ecosystems, and Hydrology XIV, 8531*, 85310Y. doi: 10.1117/12.974419

Pugh, T. A. M., MacKenzie, A. R., Whyatt, J. D., & Hewitt, C. N. (2012). Effectiveness of green infrastructure for improvement of air quality in urban street canyons. *Environmental Science and Technology, 46*(14), 7692-7699. doi:10.1021/es300826w

Qian, Y., William I. Gustafson Jr, Leung, L. R., & Ghan, S. J. (2009). Effects of soot-induced snow albedo change on snowpack and hydrological cycle in western United States based on

weather research and forecasting chemistry and regional climate simulations. *Journal of Geophysical Research - Atmospheres, 114*(D3), D03108. doi:10.1029/2008JD011039

Rochette, S., Market, P., Gravelle, C., & Niziol, T. (2017). A case study of anomalous snowfall with an Alberta Clipper. *Advances in Meteorology, 2017* doi:10.1155/2017/8406379

Saha, P. K., Khlystov, A., & Grieshop, A. P. (2018). Downwind evolution of the volatility and mixing state of near-road aerosols near a US interstate highway. *Atmospheric Chemistry and Physics, 18*(3), 2139. doi:10.5194/acp-18-2139-2018

Schlatter, T. W. (1972). The local surface energy balance and subsurface temperature regime in Antarctica. *Journal of Applied Meteorology (1962-1982), 11*(7), 1048-1062. doi:10.1175/1520-0450(1972)011<1048:TLSEBA>2.0.CO;2

Schmitt, C. G., All, J. D., Schwarz, J. P., Arnott, W. P., Cole, R. J., Lapham, E., & Celestian, A. (2015). Measurements of light-absorbing particles on the glaciers in the Cordillera Blanca, Peru. *Cryosphere, 9*(1), 331-340. doi:10.5194/tc-9-331-2015

Skiles, S. M., Painter, T. H., Deems, J. S., Bryant, A. C., & Landry, C. C. (2012). Dust radiative forcing in snow of the upper Colorado River Basin: 2. interannual variability in radiative forcing and snowmelt rates. *Water Resources Research, 48*(7). doi:10.1029/2012WR011986

Slisane, D., & Blumberga, D. (2013). Assessment of roadside particulate emission mitigation possibilities. *Environmental and Climate Technologies, 12*(1), 4-9. doi:10.2478/rtuect-2013-0009

Solvents & Petroleum Service. (2018). *Company: Experts in Chemicals. Partners in Business.* Retrieved from: https://www.solventsandpetroleum.com/company.html

Steltzer, H., Landry, C., Painter, T. H., Anderson, J., Ayres, E., & Vincent, W. (2009). Biological consequences of earlier snowmelt from desert dust deposition in alpine landscapes. *Proceedings of the National Academy of Sciences of the United States of America, 106*(28), 11629-11634. doi:10.1073/pnas.0900758106

Sturm, M., Maslanik, J. A., Perovich, D. K., Stroeve, J. C., Richter-Menge, J., Markus, T., . . . Tape, K. (2006). Snow depth and ice thickness measurements from the Beaufort and Chukchi seas collected during the AMSR-Ice03 campaign. *IEEE Transactions on Geoscience and Remote Sensing, 44*(11), 3009-3020. doi:10.1109/TGRS.2006.878236

Suriano, Z. J., & Leathers, D. J. (2017). Synoptic climatology of lake-effect snowfall conditions in the eastern Great Lakes region. *International Journal of Climatology, 37*(12), 4377-4389. doi:10.1002/joc.5093

Thomas, B. C., & Martin, J. E. (2007). A synoptic climatology and composite analysis of the Alberta Clipper. *Weather and Forecasting, 22*(2), 315-333. doi:10.1175/WAF982.1

Tong, Z., Whitlow, T. H., MacRae, P. F., Landers, A. J., & Harada, Y. (2015). Quantifying the effect of vegetation on near-road air quality using brief campaigns*. Environmental Pollution, 201*, 141-149. doi:10.1016/j.envpol.2015.02.026

United States Census Bureau. (2010). *U.S. Census Bureau, 2010 Census* [Data file]. Retrieved from: https://factfinder.census.gov/faces/tableservices/jsf/pages/productview.xhtml?pid=DEC_10_SF1_P2&prodType=table

United States Environmental Protection Agency. (2010). *Our Nation's Air: Status and Trends Through 2008* (USEPA Publication No. 454-R-09-002). Research Triangle Park, NC. Retrieved from: https://www.epa.gov/air-trends/historical-air-quality-trends-reports

United States Environmental Protection Agency. (2015). EPA Region 2 ICIS-NPDES PERMITS [Data file]. Retrieved from: https://edg.epa.gov/metadata/catalog/search/resource/details.page?uuid=%7BCFBF6A76-94CD-4D8F-AC67-8BED32B318A1%7D

United States Environmental Protection Agency. (2018a). [A data visualization interface to explore the Toxic Release Inventory yearly fact sheet database]. *TRI Explorer.* Retrieved from: https://iaspub.epa.gov/triexplorer/tri_factsheet_search.searchfactsheet

United States Environmental Protection Agency. (2018b). [A selection of tools to map, visualize and download data collected from air quality monitoring stations across the US]. *Air Data: Air Quality Data Collected at Outdoor Monitors Across the US.* Retrieved from: https://www.epa.gov/outdoor-air-quality-data

Villani, J. P., Jurewicz Sr, M. L., Reinhold, K. (2017). Forecasting the inland extent of lake effect snow bands downwind of Lake Ontario. *Journal of Operational Meteorology, 5*(5), 53-70. doi:10.15191/nwajom.2017.0505

Wagstrom, K. M., & Pandis, S. N. (2011). Contribution of long range transport to local fine particulate matter concerns. *Atmospheric Environment, 45*(16), 2730-2735. doi:10.1016/j.atmosenv.2011.02.040

Wang, X., Doherty, S. J., & Huang, J. (2013). Black carbon and other light-absorbing impurities in snow across Northern China. *Journal of Geophysical Research: Atmospheres, 118*(3), 1471. doi:10.1029/2012JD018291

Wendl, I. A., Menking, J. A., Färber, R., Gysel, M., Kaspari, S. D., Laborde, M. J. G., & Schwikowski, M. (2014). Optimized method for black carbon analysis in ice and snow

using the single particle soot photometer. *Atmospheric Measurement Techniques, 7*(8), 2667-2681. doi:10.5194/amt-7-2667-2014

Wiscombe, W. J., & Warren, S. G. (1980). A model for the spectral albedo of snow. I: Pure snow. *Journal of the Atmospheric Sciences, 37*(12), 2712-2733. doi:10.1175/1520-0469(1980)037<2712:AMFTSA>2.0.CO;

Wu, G. M., Cong, Z. Y., Kang, S. C., Kawamura, K., Fu, P. Q., Zhang, Y. L., ... & Liu, B. (2016). Brown carbon in the cryosphere: Current knowledge and perspective. *Advances in Climate Change Research, 7*(1-2), 82-89.

Wu, J., Zheng, H., Zhe, F., Xie, W., & Song, J. (2018). Study on the relationship between urbanization and fine particulate matter (PM2.5) concentration and its implication in China. *Journal of Cleaner Production, 182*, 872-882. doi:10.1016/j.jclepro.2018.02.060

Yager, R. M., Kappel, W. M., & Plummer, L. N. (2007). Origin of halite brine in the Onondaga Trough near Syracuse, New York State, USA: modeling geochemistry and variable-density flow. *Hydrogeology Journal*, *15*(7), 1321-1339.

Yamaguchi, S., Katsushima, T., Sato, A., & Kumakura, T. (2010). Water retention curve of snow with different grain sizes. *Cold Regions Science and Technology, 64*(2), 87-93. doi:10.1016/j.coldregions.2010.05.008

Yasunari, T. J., Koster, R. D., Lau, W. K. M., & Kim, K. (2015). Impact of snow darkening via dust, black carbon, and organic carbon on boreal spring climate in the earth system. *Journal of Geophysical Research: Atmospheres, 120*(11), 5485-5503. doi:10.1002/2014JD022977

Ye, C., Wang, M., & Li, J. (2017). Derivation of the characteristics of the surface urban heat island in the greater Toronto area using thermal infrared remote sensing. *Remote Sensing Letters, 8*(7), 637-646. doi:10.1080/2150704X.2017.1312025

Yuan, C., Ng, E., & Norford, L. K. (2014). Improving air quality in high-density cities by understanding the relationship between air pollutant dispersion and urban morphologies. *Building and Environment, 71*, 245-258. doi:10.1016/j.buildenv.2013.10.008

Zeng, Q., Wu, X., Wu, Z., Jiang, G., Li, P., Li, G., . . . Pan, X. (2017). The association between ambient inhalable particulate matter and the disease burden of respiratory disease: An ecological study based on ten-year time series data in Tianjin, China. *Environmental Research, 157*, 71-77. doi:10.1016/j.envres.2017.05.004

Zhang, J., Liu, J., Tao, S., & Ban-Weiss, G. A. (2015). Long-range transport of black carbon to the Pacific Ocean and its dependence on aging timescale. *Atmospheric Chemistry and Physics, 15*(20), 11521-11535. doi:10.5194/acp-15-11521-2015

Vita

David J. Kelley

460 North Franklin Street #421 • Syracuse, NY 13204 • 518.817.2513 • djkelley@syr.edu

EDUCATION

Master of Arts in Geography 6/2018
Syracuse University, Syracuse, NY

Bachelor of Arts in Geography 12/2013
University at Albany, State University of New York, Albany, NY
Tau Sigma National Honor Society

Certificate in Geographic Information Systems 12/2013
University at Albany, State University of New York, Albany, NY

PROFESSIONAL EXPERIENCE

New York State –Department of Environmental Conservation Albany, NY
Environmental Engineering Technician 4/2015-9/2016

US Geological Survey Troy, NY
Soil and Water Analysis Intern 5/2013-4/2014

RESEARCH EXPERIENCE

Masters Thesis 8/2016-6/2018
Dirty snow: The impact of urban particulates on a mid-latitude seasonal snowpack
Syracuse University Department of Geography, Advisor: Dr. Susan Millar

Collaborative Research Seminar 8/2017-12/2017
Visualizing Indigenous Methodologies in Scientific Approaches to the Anthropocene
Syracuse University Department of Geography, Advisor: Dr. Susan Millar

Collaborative Research Seminar 1/2017-6/2018
Case Study: Riparian vegetation characteristics in a sporadically inundated flood plain
Syracuse University Department of Geography, Advisor: Dr. Jake Bendix

INTPART Arctic Summer Field School 5/2017-7/2017
UiT: The Arctic University of Norway
Centre for Integrated Remote Sensing and Forecasting for the Arctic

TEACHING EXPERIENCE

Teaching Assistantship 8/2016-6/2018
Course: The Natural Environment; Instructor: Dr. Jake Bendix
Department of Geography, Syracuse University

PRESENTATIONS

Dirty Snow – The Impact of Particulate Pollution on Seasonal Snowpack
Poster presentation at the American Association of Geographers Annual Meeting, New Orleans, LA, April 12, 2018

Visualizing Indigenous Methodologies in Scientific Approaches to the Anthropocene
Poster presentation at the American Association of Geographers Annual Meeting, New Orleans, LA, April 12, 2018

Grad School or Workplace: Experiences and Perceptions of Geography Graduate Students
Panel presentation to the Undergraduate Geography Senior Seminar, Syracuse, NY, October 31, 2017

From Lakes to the Arctic: Fieldwork experiences in Physical Geography
Paper presentation at GeoFest, Syracuse, NY, September 28, 2017

Harmful Algal Bloom (HABs) Surveillance and Sampling Training
Citizen science training series, Auburn, NY and Geneva, NY, June 2016

CERTIFICATIONS & TRAINING

FAA Airman Certificate (expected 8/2018)
Invasive Species Identification
CPR/AED
Wilderness First Aid
SKYWARN Weather Spotter
Boater Safety

PROFESSIONAL MEMBERSHIPS

Environmental and Engineering Geophysical Society
Geological Society of America
American Geophysical Union
American Association of Geographers
Association of Polar Early Career Scientists
Northeast Aquatic Plant Management Society

CONFERENCES, PROFESSIONAL MEETINGS & CONTINUING EDUCATION

Syracuse University Future Professorate Program	8/2016-6/2018
Geography Colloquia Series	8/2016-6/2018
Academic Program Senator	5/2017-6/2018
American Association of Geographers Annual Meeting	4/2018
Water and Photography panel discussion	11/2017
Snow Ice Rivers and Earthquakes – Himalayan Research and life in Nepal talk	4/2017
Restoring the Giant Tortoise Dynasties of Galapagos lecture	10/2016
Department of Environmental Conservation brown bag lunch series	5/2015-9/2016
New York State Federation of Lake Associations Annual Conference	5/2016
Northeast Aquatic Plant Management Society Annual Conference	1/2016
North American Lake Management Society Annual Conference	11/2015

SKILLS

GIS/Remote Sensing: ArcMap, ArcScene, Pix4D, CityEngine, Fusion, Idrisi, Erdas Imagine, ArcPad, GPS, Trimble, Aerial image interpretation

Field Research: Sample site selection and mapping, logistics, field technician instruction and oversight, sample collection and analysis, troubleshooting, equipment maintenance, data management,

UAS/UAV Operation: Litchi, mission planning, FAA regulation compliance

Geophotography: Composition and imaging tactics; Photoshop, Lightroom, Illustrator

MEMBERSHIP, VOLUNTEERISM, TRAVEL

Member: Adirondack Mountain Club, Adirondack Hiking Photography Club

Volunteerism: Rotary International, Saratoga Center for the Family; Relay for Life; Adirondack Mountain Club; New York State Office of Parks and Recreation, I Love My Park Day, National Trails Day; SU Wilderness Society

Travel: Iceland, Ireland, Australia, New Zealand, Peru, UK, France, Canada, Belgium, Netherlands, Italy, Norway, High-Latitude Arctic Ocean, 31 US States